Catalytic Removal of Tar and Hydrogen Production of Producer Gas by Gasification of Biomass

January 2018

ZHANG Ruiqin

Catalytic Removal of Tar and Hydrogen Production of Producer Gas by Gasification of Biomass

A Dissertation Submitted to
the Graduate School of Life and Environmental Sciences
the University of Tsukuba
in Partial Fulfillment of the Requirements
for the Degree of Doctor of Philosophy in Environmental Studies
(Doctoral Program in Sustainable Environmental Studies)

ZHANG Ruiqin

Abstract

With environmental issues of climate change and seriously environmental pollution associated with the use of fossil fuel as well as emphasis of resources utilization of biomass, the use of thermochemical processes to convert biomass into a useful fuel (H_2 or syngas) has received considerable attention and effort by businesses, governments, and the public since the 1970s. In particular, lingnocellulose (cellulose, hemcellulose and lignin), which is present in almost all agricultural and forest residues, potentially serves as an excellent feedstock for waste-to-energy conversion. Gasification along with pyrolysis is the most effective means to convert biomass into high energy content gases or liquids. Unfortunately, producer gas from gasification process usually contains unacceptable levels of tar with low H_2 content. Tar can cause operational problems in downstream processes. Most producer gas applications require removal of at least part of the dust and tar before the gas can be used.

In this study, two most important elements, tar removal and H_2 production, in gasification of biomass are evaluated. Catalytic conversion of tar is a straightforward approach at lower temperatures achieving the most effective efficiency of removing tars; the development of catalysts is essential. Ni-based catalysts have been extensively used in the petrochemical industry for naphtha and methane reforming. Also, olivine, a naturally occurring mineral, has been demonstrated for its effectiveness in tar reduction. Typically, Ni can be impregnated into olivine and the resultant Ni/olivine catalysts can enhance steam adsorption, facilitate the gasification of surface carbon and hence prevent carbon deposition. Furthermore, the use of promotor, such as Ce, has been successfully employed for tar reduction. In particular, the promoter Mg (in Ni/Al_2O_3) has been demonstrated for its effectiveness for exhibiting excellent catalytic activity, stability and sulphur tolerance in catalytic reforming of toluene and naphthalene. Also, enhanced H_2 production can be achieved through hot cleaning for tar removal as well as using the combining hot cleaning and water-gas shift system. Consequently, the current study was undertaken to utilize different techniques with Ni-based catalysts to remove tars and to enhance H_2 production.

The present study was divided into three tasks: Task (1) included catalytic steaming reforming for tar (toluene and benzene) removal using commercial Ni-based catalysts with olivine as a carrier. Three catalysts were prepared by wet impregnation in this task, yielding different compositions. Benzene was selected as a model tar compound. Catalytic steam reforming of benzene was performed in a bench scale fixed bed reactor at temperatures between 700 and 830 °C using a molar ratio of steam/carbon equal to 5. Task (2) utilized catalytic hot

cleaning in two-bed system (guard and catalytic reactor) from fluidized gasifier to remove tars. The system consisted of a guard bed and catalytic reactor to treat the producer gas from an air blown, fluidized bed biomass gasifier. A slipstream was drawn immediately downstream of the cyclone at a rate of 0.5–3.0 L min^{-1}. The guard bed used dolomite to crack the heavy tars. The catalytic reactor was used to evaluate three commercial steam reforming catalyst. Task (3) involved hydrogen production from combining hot cleaning and water-gas shift system (high temperature and low temperature bed). Since the conventional air-blown gasification of biomass in fluidized bed reactors produces relatively low concentrations of hydrogen (about 8 vol%), in order to produce high hydrogen concentration syngas, the four fixed-bed catalytic system including two water-gas shift reactors was set up in this task. The typical techniques were used for catalyst characterization including X-Ray diffraction, X-ray photoelectron spectroscopy, fourier transform infrared, scanning electron microscopy, BET, thermogravimetric and mercury porosimetry analysis, among others.

The results from Task (1) indicated that 3.0% NiO/olivine doped with 1.0% CeO_2 (prepared via wet impregnation) as the most promising catalyst based on catalytic activity and its resistance to coking. Cerium oxide is thought to promote the catalytic activity of nickel through a redox mechanism and resist the deposition of the carbon. In addition, the use of Mg promotor in Ni-Ce/olivine catalyst was evaluated and results indicates that Ni–Ce–Mg/olivine catalysts could improve the resistance to carbon deposition, enhance energy gas yield and resist 10 ppm H_2S poison at 100 mL min^{-1} for up to 400 min. As for the results from Task (2), the system was effective in eliminating heavy tars (> 99% destruction efficiency) and in increasing H_2 concentration by 6–11 vol%. Space velocity had little effect on gas composition while increasing temperature boosted hydrogen yield and reduced light hydrocarbons (CH_4 and C_2H_4), thus suggesting tar destruction is controlled by chemical kinetics. Lastly, the results from Task (3) indicated that steam reforming of tars and light hydrocarbons and reacting steam with carbon monoxide via the water–gas shift reaction could increase hydrogen content in the producer gas to 27-30 vol% through biomass gasification. In general, H_2 production as a function of temperature, space velocity and steam/gas ratio was quantified. The remarks in tar control with respect to end of pipe treatment and cleaner production are discussed.

Keywords: Biomass gasification; Tar removal; Syngas; Ni-based catalyst; Olivine; H_2 production

Contents

List of Tables

List of Figures

Chapter 1 Introduction

1.1 Overview

With environmental issues including climate change and serious environmental pollution associated with the use of fossil fuel, the use of thermochemical processes to convert biomass into a useful fuel (H_2 or syngas) has received considerable attention and effort by businesses, governments, and the public since the 1970s. In particular, lingnocellulose (cellulose, hemcellulose and lignin), which is present in almost all agricultural and forest residues, potentially serves as an excellent feedstock for waste-to-energy conversion. In addition, the use of the biomass as a feedstock is a carbon neutral process. In the United States, it is estimated that 1.3 x 10^{12} kg of biomass can be harvested for biofuel production (Perlack et al., 2005) – equivalent to the energy content of 4.6 x 10^{11} L petroleum oil (Gates et al., 2008). While in China, it is estimated that 1.4 x 10^{12} kg of biomass can be harvested and equivalent to the energy content of 4.9 x 10^{11} L petroleum oil. This clearly illustrates the need for using renewable biomass as an energy source.

Gasification along with pyrolysis is the most effective means to convert biomass into high energy content gases or liquids. Gasification process is conducted under O_2 deficient conditions at 800 to 900 ^oC that converts biomass into a combustible gas mixture (H_2, CH_4, and CO). This gas mixture can then be used in turbines and gas engines or as a raw material for industrial usage. In gasification, the use of catalysts is essential for completing thermal-chemical reactions. Unfortunately, catalyst deactivation is one of the major obstacles for utilization of this process in full-scale mass production. The deactivation of catalysts results in reduced energy yields and exerts significant costs to waste-to-energy operation; regeneration, replacement, and disposal of spent catalysts. In addition, disposal of spent catalysts can create environmental problems as they are typically classified as hazardous waste due to their heavy metal content.

In general, contaminants responsible for catalyst poisoning include all unavoidable reaction-induced byproducts [gases (e.g., HCl, H_2S, carbonyl sulfide), solid (e.g., tar), aerosols and liquid]. Their formation is typically related to the following parameters: feedstock, reactor configuration, operating conditions (feeding rate, temperature and Steam/Carbon (S/C) ratio), and type of catalysts. The adverse effects on catalysts may be reversible; however, some effects are irreversible (Hepola et al., 1994; Hepola and Simell, 1997a, 1997b) as in the case of bulk structure change (Forzatti and Lietti, 1999). Consequently, tar formation, prevention, and

removal remain a major challenge in the gasification field. Tar not only affects the performance of catalysts, but also affects downstream equipment. Thus, most producer gas applications require removal of at least part of the dust and tar before the gas can be used.

The formation of tar in the gasifier is affected by operating conditions (temperature, oxidizing agent quantity, feedstock rate, and type of catalyst, etc.) as well as reactor configuration. For example, updraft fixed bed gasifiers yield high amount of tar (up to 12 wt% of feed) due to lower temperature of exit gases, as compared to downdraft gasifier (> 1 wt%: Baker et al., 1988; Kumar et al., 2009). Typically, fluidized gasifiers (bubbling or circulating) have better capability to reduce tar content (e.g., Baker et al., 1988; Devi et al., 2003; ECN, 2004); its content depends on fuel properties and operating conditions (e.g., temperature and residence time).In general, higher S/C ratios (Devi et al., 2003) as well as higher temperatures (McKendry, 2002) can reduce tar content. A higher feed rate would yield high amounts of tar (Vreugdenhil and Zwart, 2009). Nonetheless, the addition of catalysts (e.g., olivine and dolomite) may catalyze tar destruction (Rapagna et al., 2000).

Catalyst plays an important role in tar removal. For example, in the reforming system, use of $Rh/CeO_2/SiO_2$ almost eliminates tar production (Dayton, 2002; Asadullah et al., 2002, 2003, 2004); $NiMo/Al_2O_3$ and dolomite reduce activation energy for toluene from 250-350 to 30-120 kJ mol^{-1} at 650-850 ^oC (Taralas and Kontominas, 2004). Huang et al. (2011) presented a novel gas purification technology based on catalytic hydrocracking with Pd catalysts in an updraft gasifier with most of the tar components converted and removed.

In this study, two most important elements, tar removal and H_2 production, in gasification of biomass are evaluated. There are some review papers covering catalytic hydrogen production from biomass (Ni et al., 2006; Tanksale et al., 2010) as well as numerous papers dealing with tar formation and removal.

The goals of this thesis are to (1) use synthesized catalysts to catalytically steam reforming of model tar compounds; (2) use commercial catalysts to test the hot cleaning system for reducing tar content; (3) enrich H_2 production through combination of hot cleaning system and water-gas shift reactors. The enhanced H_2 production in air-blown gasification of biomass such as switchgrass, agriculture waste straws and saw dusts in fluidized bed reactors could be realized through water-gas shift reaction using different catalysts. The catalytic tar removal could be achieved through a hot cleaning system, consisting of a guard bed and catalytic reactor by using commercial nickel based catalysts. In addition, the performance of steam reforming of benzene and toluene as model tar compound for the improvement of coke decomposition by

using synthesized catalysts was evaluated. The synthesized catalysts included Ni/olivine catalysts, Ni/olivine doped with CeO_2or even with promoter Mg. Olivine, a naturally occurring mineral [$(Mg,Fe)_2SiO_4$], has been demonstrated for its effectiveness in tar reduction (Devi et al., 2005d). Typically, Ni can be impregnated into olivine and the resultant Ni/olivine catalysts enhance steam adsorption, facilitate the gasification of surface carbon and hence prevent carbon deposition (Świerczyński et al., 2007). In addition, the use of promoters (e.g., Co, Ce, etc.) has been successfully employed for tar reduction, e.g., Ni–Co (or Fe)/dolomite (Chaiprasert and Vitidsant, 2009), Fe/olivine (Barisano et al., 2012) and Ni–Ce/olivine (Cheaha et al., 2013). In particular, the promoter Mg (in Ni/Al_2O_3) has been demonstrated for its effectiveness for exhibiting excellent catalytic activity, stability and sulphur tolerance in catalytic reforming of toluene and naphthalene (Yue et al., 2010) and $Ni–Mg/Al_2O_3$ over Ni/Al_2O_3 catalyst for biomass gasification (Garcia et al., 2002; Ozaki et al 2012). The $Ni–Ce/Al_2O_3$ has better resistance toward tar and coke formation as compared to Ni/Al_2O_3 due to strong interactions between Ni and CeO_2 (Tomishige et al., 2007). Also, Ni–Ce/zeolite exhibited better rate of cellulose gasification and partially inhibited carbon deposition, as compared to those without Ce promoter (Inaba et al., 2006). In addition, those obtained from manufacturers were also used in H_2 production including ICI 46-1 (Ni-based catalyst), a Fe–Cr-based LB catalyst, and Cu–Zn-based catalyst.

1.2 Biomass gasification process and derived products

1.2.1 Gasification process

Biomass contains varying amounts of cellulose, hemicellulose, lignin and a small amount of other biomass extracts (McKendry, 2002a). The abundance of elements in biomass follows the following order: C, O, H, N, Ca, K, Si, Mg, Al, S, Fe, P, Cl, Na, Mn, and Ti (Vassilev et al., 2010). The nitrogen content of biomass varies from 0.2% to more than 1%, while sulfur content is typically below 0.2%, with a few feedstocks having a sulfur content as high as 0.7% (DDG, 2012).The biomass feedstock needs to be first processed (e.g., size reduction, drying, etc.) before being fed to gasifiers for its conversion to energy-rich gas components. To further reduce impurities in the biomass to yield better gasification, biomass may be subject to fractionation and leaching (McKendry, 2002b).

Under partial oxidation conditions (approximately 25 to 40% of stoichiometric amount of combustion) with air, pure oxygen, steam or a mixture of these gases at appropriate

temperatures (800 to 900 ºC), the biomass feedstock is converted to producer gas mainly, tar and particulates with trace containments of NH_3, HCN, H_2S and HCl as illustrated in Fig. 1-1.

The organic carbon present in biomass undergoes a series of reactions in forming CO, H_2 CH_4, and CO_2 as follows (Huber et al., 2006; Kumar et al., 2009):

Partial oxidation reaction	$2C + O_2 = 2CO$	(1.1)
Complete oxidation reaction	$C + O_2 = CO_2$	(1.2)
Hydrogasification reaction	$C + 2H_2 = CH_4$	(1.3)
Water gas shift reaction	$CO + H_2O = CO_2 + H_2$	(1.4)
Steam reforming reaction	$CH_4 + H_2O = CO + 3H_2$	(1.5)
Water gas reaction	$C + H_2O = CO + H_2$	(1.6)
Boudourd reaction	$C + CO_2 = 2CO$	(1.7)

Since feedstock also contains trace amount of S, N, and Cl, the gas produced certainly contains H_2S, HCN and HCl, in addition to NH_3 due to an incomplete oxidation of N-containing feedstock. These undesirable gases along with tar generated significantly affect the performance of catalysts. The poly-aromatic $C_mH_nO_o$ and others (e.g., mixed oxygenates, heterocyclic ethers, etc.) are condensable after cooling and termed “tar-like compounds”. If not removed, they will significantly affect downstream equipment in terms of corrosion and blockage. The formation of unavoidable tar is the major bottleneck for the commercial application of biomass gasification.

In general, the fluidized systems yield less tar content (e.g., Baker et al., 1987; Devi et al., 2003). A co-current moving bed gasifier fed using wood chips with internal recycle and separate gas combustion produced a low tar content of < 0.1 g m^{-3} (Susanto and Beenackers, 1996). Another lab-scale fluidized bed system uses a unique design in which the biomass was initially pyrolyzed and the produced char was partially gasified in the upper reduction region of the reactor. The char residue was combusted at the bottom region of the reactor in an oxidization atmosphere (Cao et al., 2006).

Typically, gasifier operating conditions, such as temperature of air (or steam), residence time, and steam/carbon (S/C) ratios affect the amount of tar produced (Devi et al., 2003; Lucas et al., 2004; Umeki et al., 2010; Gröbl et al., 2012). The type of bed material also affects tar formation, e.g., calcined limestone proved to be most effective for tar adsorption (Weerachanchai et al., 2009; Pfeifer et al., 2011). In addition to the downstream process for tar removal (e.g., Pfeifer and Hofbauer, 2008; Gustam et al., 2009), catalysts may be directly used in the gasifier (in-bed catalyst) by impregnating them with the biomass to reduce tar content

and increase gas yield (e.g., Gil et al., 1999; Courson et al., 2000; Devi et al., 2003; Lv et al., 2004; Pfeifer et al., 2004; Devi et al., 2005a; de Andréset al., 2011). For example, use of dolomite in a gasifier could decrease the tar content of the outlet gas below 2 g m^{-3} (Corella et al., 1999a). Although the catalyst used (e.g., dolomite or olivine) is easily deactivated, the replacement in-bed catalyst may be less expensive (Sutton et al., 2001). The most effective catalyst is a nickel based one, such as Ni/olivine (Courson et al., 2000; Dayton, 2002). The use of Ni-based catalyst is effective not only for tar reduction, but also for decreasing the amount of ammonia formation (Devi et al., 2003).

A bundle of catalytic ceramic candles was placed in the gasifier freeboards (800-850°C) by using a catalytically active mineral substance for tar reforming and by optimizing the addition of sorbents into the bed for removal of detrimental trace elements (UNIQUE, 2012). In general, the above system could remove 58% of the tar produced (Rapagnà et al., 2009).

A multiple-stage system can be employed to reduce tar formation (Brandt et al., 2000; Henriksen et al., 2006). For example, Brandt et al. (2000) reported that the reduction in tar was achieved by the partial oxidation of the pyrolysis gas following multiple reactions on a charcoal bed in the char gasification unit; the tar content was decreased from 3000 to < 40 mg kg^{-1} woodchips. Also use of 2-stage gasification with secondary air injection in the gasifier can reduce tar formation (Devi et al., 2003). Asadullah et al. (2003) proposed a dual-bed gasifier consisting of a primary-bed section for pyrolysis of biomass as well as separation of pyrolyzed gas and tar and a secondary-catalytic tar reformer. The tar generated can be completely converted to a gas product. Recently, Galindo et al. (2012) used a 2-stage fixed bed downdraft gasifier with different air supply and found a better-quality gas (higher calorific content) with a lower tar content (reduction of gas tar content up to 87%). Another 2-stage system (fluidized bed zone and a tar cracking zone) loaded with activated carbon (AC) had a tar removal efficiency of up to 80% (Mun et al., 2009). In addition, the use of a simple guard bed with calcined dolomite to decrease the tar content at the inlet of the subsequent catalytic bed to a level below 2 g m^{-3} is effective (Corella et al., 1999b).

The alkali elements present in the biomass affect catalytic performance and the alkali compounds released in the reactor will condense on the fly ash particles or on the walls of the flue gas tube and also form aerosol particles in the flue gas (Glazer et al., 2005). During biomass gasification, gas-phase concentrations of K, Na and Ca typically exceed turbine fuel specifications with Si, Fe, P, and Cl also present in the gas phase (Turn et al., 1998). Thus, alkali content in the feedstock must be low or diluted with another feedstock. It has been demonstrated

that the alkali retention in the fluidized bed gasifier ranges from 4 to 12% while alkali separation in the cyclone could be as high as 70% (Gabra et al., 2001).

1.2.2 Cleaning treatment of the producer gas

The unwanted gases and incomplete byproducts will be subsequently subjected to multiple stages purification, further conversion of undesirable products and more importantly, upgrading product gas for use in gas turbines/engines or as raw materials for chemical production as shown in Fig. 1-2.

The particulate matter (PM) is removed via a series of cyclones and other devices (such as wet scrubbers, filters and electrostatic precipitators). The PM levels after purification should be significantly reduced. For example, $PM_{2.5}$ level in downstream filter purification outlet stream of 13 μg m^{-3} was significantly lower than the maximum level for catalyst protection of 500 μg m^{-3} (Wang et al., 2011b). For removal of large quantities of fly ash, use of a NiO-MgO/γ-Al_2O_3/cordierite monolithic catalyst exhibited excellent catalytic performance, operating stability, and little pressure buildup even with high fly ash content of 330 g m^{-3} in the raw fuel gas (Wang et al., 2011a; Qiu et al., 2012).

The scrubbing of gases consists of three approaches: hot gas cleanup, wet scrubbing and dry/wet-dry scrubbing. The product gas with high alkali content should be subjected to alkali removal for protecting downstream equipment. Increasing alkali retention/separation during the gasification process may lead to improved product gas quality. Research in this area, however, is limited (Kumar et al., 2009).

A simple way to reduce NH_3 content in gas produced is the use of catalysts in gasifiers typically with naturally occurring minerals, such as olivine, dolomite, and limestone (Hongrapipat et al., 2012), although ferrous materials and other commercial nickel catalyst proved to be the most efficient agents for decomposing NH_3 (Leppälahti et al., 1991).

Subsequently, the desulfurization and dechlorination processes may be used for the removal of H_2S, carbonyl sulfide (COS), HCN and HCl. The removal of H_2S can be accomplished with absorbents (Yumura and Furimsky, 1985; Fenouil and Lynn, 1995; Kwon et al., 2003; Atimtay, 2001; Ko et al., 2004, 2007; Kim et al., 2007; Li et al., 2008). As would be expected, different absorbents exhibit different absorption capacity towards H_2S. The use of zinc ferrite ($ZnOFe_2O_3$) for H_2S adsorption and subsequent regeneration can be described as (Kobayashi et al., 1997):

Reduction:

$$ZnFe_2O_4 + 1/3H_2 \rightarrow ZnO + 2/3Fe_3O_4 + 1/3H_2O \quad (1.8)$$

Sulfidation:

$$ZnO + H_2S \rightarrow ZnS + H_2O \quad (1.9)$$

$$2/3Fe_3O_4 + 2H_2S + 2/3H_2 \rightarrow 2FeS + 8/3H_2O \quad (1.10)$$

Regeneration:

$$ZnS + 2FeS + 5O_2 \rightarrow ZnFe_2O_4 + 3SO_2 \quad (1.11)$$

The catalysts composed of NiO, MoO_3 and Al_2O_3 were found to be able to remove COS and CS_2 by converting to H_2S (Dou et al., 2002); the same catalysts also simultaneously remove HCl, 1-methylnaphthalene (model tar) and NH_3.

A novel catalytic filter incorporating Ni/CaO catalyst was used to remove both tars and particles in the presence of H_2S at 900 ºC (Engelen et al., 2003); the nickel and calcium modified filter exhibited 67% conversion of tar model compound (benzene) at 900 °C with 100 ppm H_2S and 4 cm s^{-1} gas velocity (Draelants et al., 2000). Also, active carbon can be used for tar removal (Hu et al., 2007) as well as simultaneous removal of tar, particles, and sulfur compounds (Hanaoka et al., 2012).

The discharged gas stream is then delivered to a steam reforming reactor where tar and light hydrocarbons are further decomposed to CO, CO_2, CH_4, etc. along with NH_3 to N_2 and H_2. Typically, Ni based catalyst is employed in this process. Kawamoto et al. (2009) reported that nickel catalysts containing CaO exhibited superior catalytic performance, with the product gas having a maximum hydrogen content of 57 vol% and the lowest tar level converted from the wood material at 1023 K.

1.2.3 Enhanced hydrogen via catalytic tar conversion and water gas shift reaction

Tar formation, prevention, and removal remain a major challenge in the gasification field. Tar not only affects the performance of catalysts, but also affects downstream equipment. For example, the tolerance levels for tar have been suggested as 50 to 500, 5 to 100, and 5 mg Nm^{-3} for the use for compressors, internal combustion systems, and gas turbines, respectively (Milne et al., 1998). Its generation originates from the initial gasifier stage to subsequent reforming systems. The formation of tar in the gasifier is affected by operating conditions (temperature, oxidizing agent quantity, feedstock rate, and type of catalyst, etc.) as well as reactor configuration. Updraft fixed bed gasifiers yield high amount of tar (up to 12 wt% of

feed) due to lower temperature of exit gases, as compared to downdraft gasifier (> 1 wt%) (Baker et al., 1988; Kumar et al., 2009). In general, higher S/C ratios (Devi et al., 2003; see Eq. 1.13) as well as higher temperatures (McKendry, 2002b) reduce tar content. A higher feed rate (or lower residence time) would yield high amounts of tar (Vreugdenhil and Zwart, 2009). Nonetheless, the addition of catalysts (e.g., olivine and dolomite) may catalyze tar destruction (Rapagna et al., 2000).

Tar can be removed via several reactions of steam- (Eq. 1.12), dry- (Eq. 1.13), hydro-, thermal-reforming, cracking as (Devi et al., 2005b; Li and Suzuki, 2009: Xu et al., 2010):

Cracking: $C_nH_m \leftrightarrow nC + (m/2)H_2$ (1.12)

Hydro-cracking: $C_nH_m + (4n-m)/2)H_2 \leftrightarrow nCH_4$ (1.13)

Again, catalyst plays an important role in tar removal. For example, in the reforming system, use of $Rh/CeO_2/SiO_2$ almost eliminates tar production (Dayton, 2002; Asadullah et al., 2002, 2003, 2004); $NiMo/Al_2O_3$ and dolomite reduce activation energy for toluene from 250-350 to 30-120 kJ mol^{-1} at 650-850 ºC (Taralas and Kontominas, 2004). Huang et al. (2011) presented a novel gas purification technology based on catalytic hydrocracking with Pd catalysts in an updraft gasifier with most of the tar components converted and/or removed.

The short chain alkanes/alkenes (C1-C4) and large molecular weight compounds (aromatic $C_mH_mO_o$) formed in the gasifier undergo further reactions in the reformer reactors as (Mann, 1995; Sutton et al., 2001):

$C_mH_n + mH_2O \rightarrow mCO + (m + n/2)\ H_2$ (1.14)

$C_mH_n + mCO_2 \rightarrow 2mCO + (n/2)\ H_2$ (1.15)

The last stage is needed for further upgrading gases to H_2 via the water-gas shaft reaction in Eq. 1.4 (Choi and Stenger, 2003).

Again, catalyst plays an important role in tar removal. For example, in the reforming system, use of $Rh/CeO_2/SiO_2$ almost eliminates tar production (Dayton, 2002; Asadullah et al., 2002, 2003, 2004); $NiMo/Al_2O_3$ and dolomite reduce activation energy for toluene from 250-350 to 30-120 kJ mol^{-1} at 650-850 ºC (Taralas and Kontominas, 2004). Huang et al. (2011) presented a novel gas purification technology based on catalytic hydrocracking with Pd catalysts in an updraft gasifier with most of the tar components converted and removed.

1.3 Hot gas cleaning of tar by catalytic steam reforming

The technologies for removing tar from producer gas (raw syngas) mainly included physical method such as electrostatic capture, wet scrubber and adsorption and hot gas cleaning of catalytic steam reforming. Physical methods and cold gas cleanup use relatively mature techniques that are highly effective although they often generate wastewater streams and may suffer from energy inefficiencies. Hot gas cleaning of catalytic steam reforming of tar is attractive because it avoids cooling and reheating the gas stream and enhances production of syngas. Concerning the catalytic tar conversion, the catalyst takes an importance role so that catalyst properties ranging from types, catalyst characterization, mechanisms for catalyst deactivation, catalyst sensitivity to poisoning are described in details.

1.3.1 Tar from biomass gasification

Tars are a complex mixture of organic compounds resulting from biomass incomplete decomposition. Milne et al. (1998) classified tars in four different groups: “primary products” which are characterized by cellulose-, hemicellulose- and lignin-derived products; “secondary products” which mainly composed of phenolics and olefins; “alkyl tertiary products” which are mainly methyl derivatives of aromatic compounds; and “condensed tertiary products” which are polycyclic aromatic hydrocarbons (PAHs) without substituent groups. The primary and tertiary products are mutually exclusive, or the primary products are destroyed before the tertiary products are formed (Milne et al., 1998). In addition, tar species are classified into five classes as shown in Table 1-1.

Apart from their acute toxic and carcinogenic properties, tar species may condensate in cold environment and during gas compression. During condensation or resublimation the compounds agglomerate frequently with dust, which are entrained in the gas. Han and Kim (2008) reviewed the technologies for control technology of tar during biomass gasification/pyrolysis.

Tars are the most troublesome pollutants of producer gas and consist of a complex mixture of organic compounds (including aromatic and heteroaromatic species as well as PAHs) with high boiling points. The main technical problems caused by biomass gasification tars include tar condensation which causes plugging and fouling problems, tar polymerisation at high temperatures (which produces polycyclic compounds and even soot in extreme cases). The need for managing hazardous residual effluents derived from wet cleaning systems for tar removal, and catalyst deactivation due to tar deposition is apparent (Devi et al., 2003).

Tar is difficult to sample and analyze with the techniques that many research groups have developed their own protocols, which makes it difficult to compare results. To avoid this difficulty, in this study we employ the Provisional Protocol for the Sampling and Analysis of Tar and Particulates in the Gas from Large Scale Biomass Gasifiers (Version 1998) prepared by the Working Group of the Biomass Gasification Task of the IEA Bioenergy Agreement (Smeenk and Brown, 1998). Tars including heavy tar, light hydrocarbon and water soluble hydrocarbon will be measured by this Protocol. The detailed procedures can be found elsewhere (Smeenk and Brown, 1998).

1.3.2 Role of catalysts

There are numerous types of catalysts used in the gasification process for tar removal. Typically, domolite and olivine were used in gasifiers (Delgado et al., 1996; Gil et al., 1999; Devi et al., 2003; Pfeifer et al., 2004; de Andréset al., 2011) as well as in a subsequent separate unit (Rapagnàet al., 1998; Abu El-Rub et al., 2004; Gustam et al., 2009; Xu et al., 2010), and Ni or Ru-based catalysts with Al_2O_3 or SiO_2 support in reforming system for tar removal. Interestingly, the Co/MgO catalyst had higher activity than any other type of Ni/MgO catalysts at lower S/C ratio (0.6) and higher concentration of fed naphthalene of 3.5 mol% (Furusawa and Tsutsumi, 2005). The naturally occurring calcined dolomites, limestones, and magnesites (Delgado et al., 1996; Corella et al., 1999a; Dayton, 2002; Devi et al., 2005c) or Ni-based monoliths (Corella et al., 2004b) were used for cleaning raw hot gas from biomass gasifiers. Delgado et al. (1996) reported that not much catalyst deactivation was observed for tar concentrations with the raw gas below 48 g Nm^{-3}, particle diameters of less than 1.9 mm, temperatures above 800 °C, and space times above 0.13 kg h^{-1} Nm^{-3}. Abu El-Rub et al. (2008) used biomass chars for tar removal and found that char gave the highest naphthalene conversion among the low-cost catalysts used (calcined dolomite and olivine). As for the type of model tar compounds, the order of reactivity follows: benzene > anthracene > pyrene > toluene > naphthalene during purification of syngas (Coll et al., 2011) with the tendency towards coke formation growing as the molecular weight of the aromatics increased.

Typically, catalysts can be classified into 3 major source categories: (1) naturally occurring materials, e.g., domolite, olivine, calcite and alumina; (2) Ni based commercial catalysts; and (3) newly synthesized/developed catalysts to overcome particular problems. The domolites typically are composed of $MgCO_3$, $CaCO_3$ with small amounts of SiO_2, Fe_2O_3 and Al_2O_3

(Sutton et al., 2001), while olivine with $(Mg,Fe)SiO_4$ as the main phase plus small quantities of $MgSiO_3$, $MgFe_2O_4$ and α-F_2O_3 (Świerczyński et al., 2006). The exact crystal phase and catalytic activity as well as the extent of deactivation depend on the source of these minerals (Zhao et al, 2009; Buchireddy et al., 2010). Ni-based catalysts synthesized in the laboratory and commercially produced have been extensively studied. Although the yield performance is good, the deactivation of catalysts due to structure changes in Ni and carbon deposit is unfortunately unavoidable.

Ideally catalysts should have the following roles (Sutton et al., 2001): (1) effective in tar removal; (2) capable of achieving higher yield; and (3) providing suitable syngas ratio. The selection of catalysts is a function of cost, high activity, selectivity, resistant to deactivation, and ease of regeneration. Clearly no single catalyst can achieve and meet the above-mentioned goals and selection criteria. A particular catalyst may function well in one aspect (e.g., high catalytic activity), but suffer in another aspect (e.g., subject to deactivation). For example, K_2CO_3 supported on Al_2O_3 is more resistant to carbon deposition, but less active as compared to a Ni-based catalyst resulting in unsuitable application in hydrocarbon conversion (Sutton et al., 2001). A "in-bed catalyst", using dolomite yields only 60% of the tar content compared to olivine, but it generates 4 to 6 times more particulates and additional NH_3 (Corella et al., 2004a). Thus, the role of catalyst in enhancing H_2 production, prevention of tar formation and elimination of carbon deposition is different (Inaba et al., 2006). Also operating conditions for optimizing yield, gas composition and energy may be different for tar/carbon reduction/elimination. Therefore, the selection of the catalyst is goal- and selectivity-specific. Lastly, the selection of any catalysts should also consider cost, e.g., Ni-Ce/H-ZSM-5 catalyst may be selected for cellulose gasification over Rh-Ce/SiO_2 catalyst, since Ni-based catalysts are cheaper (Inaba et al., 2006). Also, under real conditions (e.g., presence of H_2S), the two natural materials, calcite and olivine, have clear advantages over perovskite-type oxides with respect to price, catalytic activity and oxygen capacity (Pecho et al., 2008). The bottom line is when evaluating catalysts, activity, stability, sensitivity, selectivity, reliability, durability and cost should be all considered to yield the so-called optimized conditions.

The preparation procedure of catalysts also affects catalytic activity (Bartholomew, 2001; Chen et al., 2005a). For example, the co-impregnation of Ni/CeO_2/Al_2O_3 catalyst is subject to less catalyst deactivation than sequential impregnation (Ni/Al_2O_3, Ni/CeO_2/Al_2O_3) (Kimura et al., 2006). The intimate interaction between Ni and CeO_2 on the Ni/CeO_2/Al_2O_3 catalyst by the co-impregnation method is responsible for the low yield of tar and coke as compared to

$Ni/CeO_2/Al_2O_3$ by a sequential impregnation method in steam gasification of biomass (Tomishige et al., 2007). Furthermore, the addition of 0.1% Pt to $Ni/CeO_2/Al_2O_3$ enhanced the performance compared to $Ni/CeO_2/Al_2O_3$ in terms of low tar yield and high gas yield, due to the formation of Pt–Ni alloy (Nishikawa et al., 2008). Seo et al. (2009) analyzed three methods (impregnation, co-precipitation, and sequential precipitation) for preparation of Ni/Al_2O_3 catalysts and found that the sequential precipitation method was the most effective for catalytic activity in suppressing the carbon deposition. This is because sequential precipitation yielded the highest Ni surface area, pore volume and better nickel dispersion. On the other hand, catalyst (Ni/domolite with promotor Pt, Co or Fe) preparation by the impregnation method had superior performance compared to co-precipitation (Chaiprasert and Vitidsant, 2009).

In addition, the support plays an important role in the overall catalytic performance as well as tar resistance (Wang and Lu, 1998; Inaba et al., 2006; Buchireddy et al., 2010). Clearly, support has an important function in the distribution and dispersion of an active metal catalyst. For example, Kong et al. (2011) employed MgO, carbon, α-Al_2O_3, γ-Al_2O_3, SiO_2 and ZrO_2 on Ni-based catalysts in CO_2 reforming of toluene in a fluidized bed reactor and observed that the Ni/MgO catalyst was the most effective due to the strong interaction between NiO and MgO via the formation of a Ni–Mg–O solid solution with the highest dispersion of Ni particle. In fact, anti-sintering and anti-carbon deposition properties of a NiO-MgO solid solution catalyst have been confirmed in reforming biomass fuel gas by Ni-MgO/γ-Al_2O_3 catalysts (Qiu et al., 2012). Also, Miyazawa et al. (2006) found that Ni/CeO_2 showed a lower amount of coke than other supports of Ni-based catalysts (Ni/Al_2O_3, Ni/ZrO_2, Ni/TiO_2, and Ni/MgO) in the steam reforming of tar derived from the pyrolysis of cedar wood. Tomishige et al. (2004) reported that gasification of cellulose over novel $Rh/CeO_2/SiO_2$ catalysts involved in the reforming of tar and the combustion of solid carbon. In addition, the impurities on the support surface can poison the catalyst (Wang and Lu, 1998). With the exception of nickel nitrate, all the Ni-precursors (chloride and sulfate) caused deactivation of the catalyst in the steam reforming of benzene (Park et al., 2010). The strong interactions between Cl inside the pores and the supports with chloride as a precursor and production of H_2S with sulfate precursors are the reasons for catalyst deactivation. However, the choice of a Ni-based precursor (NiO or Ni) demonstrated minimal influence on the catalytic activity and stability for naphthalene- and methane-steam reforming (Zhao et al, 2009).

In another study on Ni-based catalysis for cellulose gasification, Inaba et al. (2006) found that Ni/conventional metal oxide catalysts produced tar without carbon deposition, while most

Ni/zeolite catalysts could inhibit the formation of tar to some degree; however, carbon deposition still occurred. The Ni-Ce/zeolite support was able to enhance the rate of gasification due to inhibition of tar formation and carbon deposition (Inaba et al., 2006). Clearly the property of support (e.g., pore structure) and its interaction with metal catalyst are important (Wang and Lu, 1998). In fact, deterioration of support or change in support structure certainly leads to catalyst deactivation (McMinn et al., 2001; Klimova et al., 2003). Moreover the source or type of zeolite/olivine/domolite is also important; catalytic activity increases with an increase in the zeolite acidity (Buchireddy et al., 2010) and Washington olivine support (Ni based) demonstrates improved catalytic performance and stability compared to two other olivine supports (Austrian and North Carolina olivine) during reforming naphthalene (Zhao et al., 2009).

Ni−Al co-precipitated catalysts promoted with magnesium ($NiMgAl_2O_5$)showed the highest initial activity and stability compared to $NiAl_2O_4$ catalyst (Garcia et al., 2002). As for rare elements as a promotor, Ma et al. (1999) found that the catalytic activity of rare elements promoted to Ni-based catalysts decreased as: $CeO_2 > PrO_2 > Sm_2O_3$ in steaming reforming of methane, with CeO_2 exhibiting excellent anti-coking activity. Zhang et al. (2009) in their study of steam reforming of toluene also found the order of catalytic performance and carbon resistance as: Ni-Ce > Ni-La > Ni-Zr based on Ni/Mg(Al)O catalysts. The addition of mixed rare elements (La_2O_3, CeO_2, Pr_6O_{11}, Nd_2O_3, Sm_2O_3, Eu_2O_3, Gd_2O_3, Tb_2O_3, and Y_2O_3) onto Co/γ-Al_2O_3 catalysts exhibited good activity and stability with low carbon formation at 800 ºC for 320 h during CH_4/CO_2 reforming to syngas (Zeng et al., 2012). Also, the addition of promoters (Ce, La, Ca, K) to NiCoMn/ZrO_2 catalyst markedly improved CH_4 and CO_2 conversions as well as selectivities to H_2 and CO relative to the unprompted catalysts (Bhavani et al., 2012). The Ce and La were more effective than alkaline earth Ca and K, and exhibited higher activity and improved stability. However, coke deposition on the catalysts for the CO_2-reforming reaction was remarkably diminished with the addition of alkaline promoters such as K and Ca oxides. This was attributed to the formation of carbonate species on alkaline promoters, mainly Ca, which was located adjacent to Ni sites and to the dissociative adsorption of CO_2 on the Ni surface (Chang et al., 1996). In addition, the inclusion of some rare earth (La^{3+}) and alkaline earth oxides (Ba^{2+}) into a modified γ-alumina enhances sintering resistance (Church et al., 1994).The role of the promoter on Ni/dolomite apparently is different, e.g., platinum promoter enhances the reforming reaction, iron promotes a water-gas shift reaction, and the cobalt favors methanation reaction (Chaiprasert and Vitidsant, 2009).

The overall performance of catalysts is related to the content of metal loading as well as metal dispersion (Chen et al., 2005b), incorporation of other dopant metals/compounds (Bangala et al., 1998), type of impurity (Abu El-Rub et al., 2008), calcination temperature (Courson et al., 2000; Zhao et al., 2009) and time (Devi et al., 2005a), preparation method (Li et al., 2005), catalyst precursor (Park et al., 2010), type of supports (Breysse et al., 2003; Inaba et al., 2006; Kong et al., 2011; Xie et al., 2012), extent of "impurity" in support (Wang and Lu, 1998), operating temperature (Devi et al., 2003), among others.

In comparison of different Ni-based catalysts for coke resistance, Chen et al. (2005b) reported that a better resistance is due to smaller metallic Ni particle size through lowering Ni loading and in combination with the addition of B promoter with the decreasing order: 10 wt% Ni/AlO >1 wt% Ni/Ca-AlO > 1 wt% NiB/Ca-AlO >1 wt% Rh/AlO. The addition of other metal on a Ni-based catalyst may offer more sulfur resistance due to the adsorption of C_2H_4 and sulfur on Ni-Ru/Al_2O_3 on completely different sites (Rangan et al., 2012). This explains the observed phenomenon that this catalyst is more sulfur resistant than Ni/Al_2O_3. Also Ni/olivine (Świerczyński, et al., 2007, 2008) and Fe/olivine (Virginie et al., 2010) have been demonstrated to be effective for tar reduction with better product gas quality. The former is due to magnesium oxide enhanced steam adsorption, facilitating the gasification of surface carbon and Ni–Fe alloys prevent carbon deposition (Świerczyński, et al., 2007), and the latter due to the presence of metallic iron leading to C–C and C–H bonds breaking and a sufficient percentage of iron(II) available (Virginie et al., 2010). A zirconia-promoted Ni-based commercial catalyst (Katalco 46-6Q) showed 100% tar conversion efficiency even at a relatively low temperature of 600 °C (Yoon et al., 2010). The introduction of small amounts of molybdenum compounds (1 wt% of Mo) into the Ni-based catalysts greatly improved their resistance to coking during steam reforming of *n*-butane (Kepinski et al., 2000).

1.3.3 Newly developed catalysts

Because of some disadvantages associated with conventional catalysts, there are many newly developed catalysts to overcome the deactivation due to adverse effects caused by various factors. In fact, one of the research areas in the gasification field is to identify and synthesize catalysts for their use in enhancing both performance and resistance to poison and coke formation. Use of Ni-based monoliths has been found to be effective in hot gas cleaning, particularly in particle removal (Corella et al., 2004a). The addition of Rh, Pt, W or Ru to Ni-

based catalyst could result in less sulfur poison (Strohm et al., 2006; Wang et al., 2009; Ronkkonen et al., 2011a, 2011b). Examples of some newly developed catalysts are listed in Table 1-1. The table, by no means complete and only a fraction of literature data, illustrates the interest and improvement of new catalysts to overcome catalyst deactivation in the gasification process. Briefly, these catalysts shown in Table 1-2 indicate several important aspects: (1) use of noble metal catalysts (e.g., Rh, Pd) is extensive but may be expensive; (2) most Nickel based catalysts use a variety of supports (e.g., olivine, dolomite, Al_2O_3, SiO_2 and zeolite), and doped with various metals (e.g., Ce, Mg); (3) other transit metal catalysts (e.g., Fe, Co); and (4) char-based catalyst. Essentially Ni-based catalysts are widely used and improvements have been made to improve their catalytic capability and their resistance to deactivation.

1.3.4 Catalyst characterization and performance

Catalyst can be characterized via different techniques, including but not limited to: X-ray Diffraction (XRD), Field Emission Scanning Electron Microscopy (FESEM), X-ray Photoelectron Spectroscopy (XPS) and Mass Spectrometry (MS), Mossbauer Spectroscopy, Extended X-Ray Absorption Fine Structure (XAFES), Brunauer-Emmett-Teller (BET), UV-Vis Diffuse Reflectance Spectroscopy (UV-Vis DRS), Diffuse Reflectance Infrared Spectroscopy (DRIS), Scanning Electron Microscope/Microscopy (SEM), Transmission Electron Microscope/microscopy (TEM), Thermogravimetric Analysis (TGA), Temperature Programmed Desorption (TDP), Temperature Programmed Oxidation (TPO), Nuclear Magnetic Resonance Spectroscopy (NMR), and zeta potential meter, etc. In general, they determine physical properties (surface are, pore size, density, strength), fine structure (surface structure and topography), different phases, elemental composition, and chemical characterization or acid/base sites, and catalyst properties (measurements of activity parameters, selectivity, inhibition of the catalytic action, characterization of catalyst response to inhibitory substances, etc.) (Haber, 1999).

The characterization of catalysts may shed some light as to how are catalysts deactivated? Why are some less sensitive to poisoning? Which sites are affected? What mechanisms are involved? Where is competitive edge over other catalysts? For example, Orio et al. (1997) concluded that the order of activity of 4 different dolomite catalysts evaluated is primarily dependent on the content of measured Fe_2O_3. Based on EXAFS analysis, sulfur poisoning and

oxide formation, not carbon formation, nor changes in particle size and phosphorus poisoning, are responsible for deactivation of Ni-based (Mg and K) catalyst (Yung and Kuhn, 2010).

Typically, substances causing catalyst deactivation will initially undergo physical/chemical/thermal adsorption onto the surface of catalysts. The mechanisms for eventual catalyst deactivation are complex and the extent of catalyst deactivation depends on the type of substances, catalysts themselves, and operating conditions. Moulijn et al. (2001) outline deactivation in terms of length scale: nono scale (micropores); micro scale (macropore); macro scale (particles); and meter size (reactor). Deactivation can be classified into 6 types: (1) poisoning, (2) fouling, (3) thermal degradation, (4) vapor compound formation accompanied by transport, (5) vapor-solid and/or solid-solid reactions, and (6) attrition/crushing (Bartholomew, 2001), or 4 major elements: (1) fouling due to aggregation and polymerization of deposit resulting in structural changes; (2) poison; (3) catalyst sintering; and (4) catalyst/support degradation due to thermal erosion/attrition/abrasion (Forzatti and Lietti, 1999; Moulijn et al., 2001).

In order to better understand the mechanism(s) for catalyst deactivation, it is important to know how catalysts function. Essentially, it involves diffusion of reactants (step 1 and 2), adsorption (step 3), reaction (step 4), desorption of the products (step 5), and diffusion of products back into the bulk fluid (step 6 and 7) (Bartholomew and Farrauto, 2006). Any of these steps can be the limiting factor depending on the catalyst design, the reactor setup, and the reaction condition (Bartholomew and Farrauto, 2006; Lin and Huber, 2009).

For particles/aerosol, their direct deposition (blockage) on the surface of catalysts (Einvall et al., 2007) or pore (Rostrup-Nielsen and Trimm, 1977) is responsible for the decreased catalytic activity. Typically, the specific surface area and metal crystallite are decreased and changed after deactivation (Albertazzi et al., 2011). The formation of 27 to 36 wt% content of K_2O in Ni/monolith catalyst also causes its deactivation (Corella et al., 2005).

For hydrocarbons, the deposited carbon will undergo structural as well as morphological changes with formation of encapsulating, filamental and pyrotic carbons (Bartholomew, 1982; Xie et al., 2011). The formation of these carbons depends on temperature and they all exhibit catalyst deactivation. Xu and Saeys (2006) identified three types of chemisorbed carbon: on-surface carbon atoms, bulk carbon atoms, and extended graphene islands. They further reported that boron prefers to adsorb in the octahedral sites just below the surface, rather than in the Ni bulk phase; therefore, the addition of promotor B inhibited the formation of bulk carbide and

slowed the formation of graphene islands. This results in reducing coking of Ni-based catalyst. Fortunately, deposited carbon can be easily removed via steam reforming.

The deactivation problems are compounded by the fact that the presence of sulfur in steam reforming of liquid hydrocarbon significantly increases the carbon content on Ni/Rh-based catalysts supported by CeO_2-Al_2O_3 (Chen et al., 2010; Xie et al., 2011). The XANES analysis revealed that graphic carbon was dominant and Rh catalyst was less subject to the effects of sulfur as compared to Ni-based catalyst (Xie et al., 2011). Thus, the synergic effect of several substances is responsible for the eventual deactivation of the catalyst. For example, in a deactivation study of Ni-based catalyst during reforming of syngas, it was found that mechanisms consisted of physical deposition of fine particles, aerosol and carbon deposit and poisoning by sulfur (Albertazzi et al., 2011). Wambach et al. (2012) have recently reported that deactivation of Ru/C catalyst during gasification of aqueous organic feed is due to the complete disappearance of the spectral features in the valance band region. Coverage of the ruthenium clusters e.g., with a thin ‘carbonaceous' layer, or structural modifications of the ruthenium clusters may be the reason for deactivation of Ru/C catalyst.

For H_2S, direct adsorption of sulfur on the surface of Ni crystallites is responsible for the initial deactivation which in turn affects carbon gasification resulting in additional carbon deposit (Lakhapatri and Abraham, 2011). H_2S can directly react with Ni forming $NiSO_4$ (Li et al., 2010) and NiS (Hepola and Simell, 1997c; Koningen and Sjöström, 1998; Srinakruang et al., 2006a; Chen et al., 2010). There is a clear correlation between the H_2S concentration in gas (Alstrup et al., 1981), catalytic activity (Roberts et al., 1993) and the amount sulfur deposit on catalyst surface. Typically, the sulfur poison is reversible as (Srinakruang et al., 2006b):

$$NiS + H_2 \rightarrow Ni + H_2S \quad (1.17)$$

$$NiO + H_2 \rightarrow Ni + H_2O \quad (1.18)$$

In fact, after changing feed gas containing H_2S to H_2S-free feed, catalytic activity could be restored (Koningen and Sjöström, 1998; Ashrafi et al., 2008) due to self-regeneration Eq. (1.17).

Also, the presence of $FeSO_4$ may be the reason for the loss of activity based on XPS analysis of silica promoted ferric oxide based catalyst, compared to ferric oxides (Mashapa et al., 2007). For some catalysts, the formation of inorganic compound may be responsible for catalyst poisoning. For example, in the presence of NH_3 and H_2S, the formation of FeS on the catalyst (limonite) may cause catalyst deactivation, although it does not affect NH_3 conversion (Tsubouchi et al., 2008). On the other hand, the formation of NiO-MgO solid solution on the

olivine surface during calcinations and Ni-Fe during the reduction may increase carbon deposition resistance (Świerczyński et al., 2006).

The other route for catalyst deactivation is that toxic metals (e.g., Pb, Hg, Cd, etc.) may interact with catalysts by forming metal alloys. For HCl, the deactivation of Pt/γ-Al_2O_3 for steam reforming of trichloroethylene is due to chlorine poisoning, catalytic coke formation as well as support degradation (McMinn et al., 2001). For Ni/Mg/K/AD90 (90% α-Al_2O_3) catalyst, the loss of activity is due to the formation of a $NiAl_2O_4$ species that is not fully reduced under regeneration conditions, which in turn results in a decreased number of potential metallic nickel (NiO) sites needed for hydrocarbon steam reforming (Yung and Kuhn, 2010).

By performing kinetic studies of steam reforming of syngas using alkali-promoted Ni/Al_2O_3 catalyst, Bain et al. (2005) were able to model initial catalyst deactivation. The activated energy varies with the tar model compound, ranging from 16 kJ mol^{-1} for total tars to 74 kJ mol^{-1} for benzene and to 121 kJ mol^{-1} for tars and benzene. The formation of $NiAl_2O_4$ species during tar and methane reforming at 900 ^oC that is not fully reduced is responsible for the decreased number of potential metallic Ni sites resulting in deactivation of Ni-Mg-K/AD90 (Yung and Kuhn, 2010).

Waldner et al. (2007) evaluated catalyst stability and tolerance towards dissolved inorganics (Na_2SO_4) and found Ru/C to be more stable than Ni/C catalyst. However, Ru/C is deactivated over time due to irreversible sulfate bonding to Ru(III) which is formed in the redox cycle of biomass gasification. In wet feedstock gasification, inorganics also play an important role in catalyst deactivation, e.g., Ru catalyst pellets coated with magnesium phosphorus (with associated silicon) with some separate calcium-containing crystallites making Ru associated with sulfur (Elliott et al., 2004).

The sensitivity of catalyst towards fouling-causing substances is a function of type of catalyst as well as operating conditions. For example, it has been demonstrated that dolomite is easily deactivated in gasifiers (Simell et al., 1996; Sutton et al., 2001; Wang et al., 2008), and a Ni-based catalyst is more sulfur-sensitive than a Pt or Rh catalyst (Einvall et al., 2007; Xie et al., 2011). The addition of promoters (e.g., Li, K, Ca and Mg) could reduce carbon fouling and enhance the resistance of sulfur poisoning of Ni/alumina catalyst (Chen and Shiue, 1988; Draelants et al., 2001). For example, in a filter-Ni/CaO system to remove naphthalene in the presence of 100 ppm H_2S, the conversion of naphthalene at 2.5 cm s^{-1} could remain 98% over a period of 180 h (Engelen et al., 2003).

The inexpensive limonite catalyst is less susceptible to 100 ppm H_2S poison at 750 ºC (Tsubouchi et al., 2008), as compared to conventional and expensive Ni- and Ru-based catalyst at 50-500 ppm H_2S (800-950 ºC) (Simell et al., 1997). Tsubouchi et al. (2008) found that FeS may be responsible for enhancing NH_3 conversion as:

$$FeS + 2NH_3 \rightarrow N_2 + 2H_2 + H_2S \quad (1.19)$$

Both the type of metal and supports affect the sulfur tolerance and carbon resistance. The performance of CeO_2-supported Rh and Pt catalysts (compared to Tu and Pd on Al_2O_3, SiO_2 and MgO) was due to the promotion effect of CeO_2 on carbon gasification (Xie et al., 2012). The addition of CaO to the Ni-based catalyst on the filter discs resisted sulfur toxicity (Zhang et al., 2003), and yielded higher H_2 concentration level (57 vol%) with the lowest tar and H_2S concentrations for reforming wood at 750 ºC (Kawamoto et al., 2005).

1.4 Research objectives and thesis structure

1.4.1 Research objectives

As described above, biomass gasification is one of the most efficient route of biomass to energy conversion as well as hydrogen production. Unfortunately, the producer gas from this process usually contains unacceptable levels of tar. In terms of tar removal, it remains a major challenge since most producer gas applications require removal of at least part of the dust and tar before the gas can be used. Therefore, the main objectives of this study are three folds. Firstly, to synthesize suitable and efficient catalyst for tar conversion; olivine is used as a substrate for various catalyst formulations designed to steam reforming of tar to gas with nickel as active component and Ce and Mg as promoters. Benzene and toluene are selected as model tar compounds. Catalytic steam reforming of these compounds is performed in a bench scale fixed bed reactor. The effect of catalyst composition on tar conversion and yield of various product gases and coking tendencies are determined. Secondly, to investigate catalytic destruction of tar formed during gasification of biomass for improving the quality of the producer gas, a hot gas cleaning system consisting of a guard bed and catalytic reactor is designed to treat the producer gas from an air-blown, fluidized bed gasifier. The guard bed used dolomite to crack the heavy tars. The catalytic reactor was used to evaluate nickel based commercial steam reforming catalysts. Since air-blown gasification of biomass in fluidized bed reactors produces relatively low concentrations of hydrogen, the third goal is to increase hydrogen content in the producer gas from biomass gasification by steam reforming of tar and light hydrocarbons and reacting

steam with carbon monoxide via the water–gas shift reactions. The parameters evaluated included the temperature, space velocity, and steam/gas ratio to determine the effect of these variables on hydrogen production. The seed corn and switchgrass, a warm-season, perennial grass was used as gasification feedstock.

1.4.2 Thesis structure

The thesis is organized as below. Overview in Chapter 1.1 briefly covers gasification process in yielding biomass-derived energy. Chapter 1.2 reviews gasification process and derived products in rather details, including biomass feedstock, type of gasifiers, purification of undesirable compounds [particulate matter, inorganics (H_2S, NH_3, HCl) and organics hydrocarbons], tar formation and cleaning treatment of the producer gas as well as enhanced H_2 production via catalytic tar conversion and waster-gas shift reactions. Since catalyst plays an important role in gasification of biomass, the role of catalyst, particularly in hot gas cleaning of tar by catalytic steam reforming, is of importance and is thus also covered in Chapter 1.3. In particular, newly developed catalysts and catalyst characterization are reviewed. The end of Chapter 1.4 outlines research objectives and dissertation structure.

Figure 1-3 shows the methods, keys and goals of each chapter to better illustrate the content of the remaining three chapters (Chapter 2 to 5) which is divided into three main sections. Section (1) covers catalytic removal of tar with Ni/olivine along with different promotors (Ce and Mg) in Chapter 2 and 3. Section (2) describes catalytic removal of tar in two-bed systems (guard bed and catalytic reaction) in enhancing H_2 production in Chapter 4. Section (3) covers enhanced H_2 production in four fixed bed system including two water-gas shift reactors in Chapter 5. In short, the synthesized Ni/olivine catalyst is found to be useful for reforming the model compound toluene and benzene (Chapter 2 “Steam Reforming of Tar Compounds over Ni/olivine Catalysts Doped with CeO_2”). The addition of promoter Ce and Ce-Mg in Ni/olivine catalyst for reforming toluene is present in Chapter 3, entitled, “The related Ni/olivine catalyst in “Catalytic Reforming of Toluene as Tar Model Compound: Effect of Ce and Ce–Mg Promoter using Ni/olivine Catalyst”. The enhanced H_2 production with tar removal is in Chapter 4, entitled, “Catalytic Destruction of Tar in Biomass Derived Producer Gas”. Use of two different biomass feedstocks in enhancing H_2 production after hot cleaning tar is illustrated in Chapter 3 entitled, “Generation of Hydrogen from Switchgrass and Seed Corn from an Air-blown Fluidized Gasifier”.

Each chapter in these three sections is independent and has its own entirety with introduction in the beginning, following by methods, results/discussion and summary. For compliance with requirement, references for each chapter are provided at the end of this thesis.

The conclusions and future research direction are presented in the final chapter; improved gasification technologies, optimized operating conditions and innovative catalysts for enhancing H_2 production, end of pipe treatment of tar generated and source control to reduce tar formation. A large-scale pilot study and thermal and biochemical hybrid system of syngas fermentation are recommended.

Table 1-1. Five classes of tar (taken from Rabou et al., 2009)

Class	Name	Species
I	GC undetectable	very heavy (>7 rings)
II	heterocyclic	cyclic hydrocarbons with heteroatoms, (highly) water soluble (e.g., phenol, cresol, pyridine, thiophene)
III	light aromatic	1 ring compounds with low condensation temperatures (e.g., toluene, styrene, xylene)
IV	light polyaromatic	2-3 rings condensing at intermediate temperatures at high concentrations (e.g., naphthalene, phenanthrene, anthracene)
V	heavy polyaromatic	4-6 rings condensing at high temperatures at low concentrations (e.g., fluoranthene, pyrene)

Table 1-2. Newly developed catalysts enhancing performance and resistance to deactivation

Types of catalysts`	Catalysts	Function	Improvement	References
Noble metal based	Rh–$LaCoO_3/Al_2O_3$; $Rh/CeO_2/SiO_2$; Rh/Mg-Ce-Zr-O-based mixed oxides; Rh, Ni, Co, and their alloys; Rh/40Mg-20Ce-20Zr-20La-O	Reforming tar to syngas; Reforming of phenol	Unchanged catalytic properties upon 200 ppm H_2S, compared to $LaCoO_3/Al_2O_3$; High tar (biomass) removal to H_2 and CO; No effect with 280 ppm H_2S; Better than Ni catalyst in terms of tar reduction and coke formation; Reduce carbonaceous deposit; Synergy effects on metal-oxide and metal–metal	Ammendola et al., 2012; Li et al., 2015; Tomishige et al., 2005, 2007; Polychronopoulou et al., 2012
	Pt/Al_2O_3	Reforming of naphthalene/benzene	Steam reforming of naphthalene/benzene to produce H_2	Furusawa et al., 2013
Nickel based	Ni/olivine; Ni/olivine modified with Ca aluminate cement; Ni- cerium/olivine	Steam reforming of methylnaphthalene; enhancing gasification	Reforming of model tar and emphasized secondary reaction of water-gas shift; Tar removal efficiency of 98% with maximum hydrogen content of 34 vol%; Better activity and resistance to coking	Michel et al., 2013; Mun et al., 2014; Yang et al., 2010b; Cheah et al., 2013; Zhao et al., 2015
	NiO/MgO; NiO-MgO/ γ-Al_2O_3/cordierite monolithic	Reforming of benzene and naphthalene; CO_2 Reforming	Higher performance than Ni/Al_2O_3 and $Ni/CeO_2/Al_2O_3$ and provided lower yields of coke and tar, and higher yields of gaseous products; 35-95% ammonia removals, no deactivation of the catalyst at 50-150 ppm H_2S; No channel blocking	Furusawa et al., 2009; Kong et al., 2012; Wang et al., 2000, 2011a

Types of catalysts`	Catalysts	Function	Improvement	References
	Ni/MgO; Ni/MgO-Al_2O_3; Ni/MgO (Ni/(Ni + Mg) = 15) ; Ni/MgO-CaO doped with WO_3	Reforming of toluene and naphthalene with H_2S resistance; Particular removal; Reforming of tar; Reforming syngas	Excellent catalytic activity, stability and sulphur tolerance; Increase gas yield by 20% and converting 58% of the product tar; No carbon deposit for 100 h; Exhibited excellent activity, stability and resistance to carbon deposition; Higher naphthalene activity, resistant to coking and H_2S	Kong et al., 2012; Yue et al., 2010; Rapagnà et al., 2009; Wang et al., 2006; Yang et al., 2010a; Sato and Fujomoto, 2007
	Ni/zeolite; Ni/ Al_2O_3-ZrO_2; Ni/Al_2O_3 with dopant MnOx; nano-Ni–La–Fe/γ-Al_2O_3; NiO- MoO_3-Al_2O_3 NiO/Al_2O_3	Reforming of tar; Reforming of toluene; Enhancing H_2 yield; Removal of gaseous impurities	Better than Ni/Al_2O_3 or SiO_2; Naphthalene conversion 98% after 170 h, 99% benzene and 100% naphthalene conversion at 850 °C; Increased catalytic activity, suppression of coke deposition and the catalyst stability; Tar removal efficiency reached 99%; Simultaneous removal of organic sulfur, tar component, NH_3	Buchireddy et al., 2010; Ma and Baron, 2008; Koike et al., 2013; Li et al., 2009a; Dou et al., 2002; Ozaki et al., 2012
	Ni/CaO; Ni/(12CaO.7Al_2O_3); Ni/domolite with Fe_2O_3 powder; Ni/domolite WO3 doped; NiFe CaO-doped /FeO Al_2O_3	Reforming of wood tar and model tar	Reduce tar and enhance H_2 content (58 vol%); Excellent resistance to toluene coking with higher H_2 yield, higher CO selectivity; 98% tar (toluene) conversion with increased H_2 yield; Naphthalene conversion 98%; Superior resistance to coking as well as sulfur poisoning	Kawamoto et al., 2009; Taufiq-Yap et al., 2012; Di Carlo et al., 2015; Li et al., 2009b; Wang et al., 2005, 2012; Engelen et al., 2003 Sato and Fujimoto, 2007; Sato et al., 2007; Ashok and Kawi, 2015

Types of catalysts`	Catalysts	Function	Improvement	References
Other transition metal	Co(20%)/γ-Al_2O_3 catalyst promoted with rare earths; (Co/Mo) commercial catalyst	CH_4/CO_2 reforming; Water-gas shift reaction	Good activity and stability with low carbon formation for 320 h; Efficient tar removal and CO conversion close to 85%	Zeng et al., 2012; Chianese et al., 2016
	Fe/silicate	Reforming benzene	Benzene conversion and enhance syngas	Sarvaramini, and Larachi, 2012
	Fe_2O_3 dopant of CeO_2	Tar decomposition by both steam reforming and water gas shift reaction	Ceria promoted iron catalysts active for both hydrogen production and tar decomposition in steam gasification	Duman et al., 2014
	Fe/CaO	Enhanced gasification and conversion of tar	Enhanced biomass gasification, converted tar and enhanced hydrogen production.	Huang et al., 2012
	Fe (10%)/olivine	Tar conversion; Enhance hydrogen production	High conversion of tar	Rapagnà et al., 2002, 2011; Virginie et al., 2012
	$LaNi_{0.3}Fe_{0.7}O_3$; $FeTiO_3$; $LaNi_{0.3}Fe_{0.7}O_3$ and $LaNi_xCr_{1-x}O_3$	Tar conversion; Enhance hydrogen or syngas production; Tar Conversion	Increased gas yield by 40%, H_2 yield by 88%, reduced tar production per kg of dry ash free biomass by 46% compared to olivine alone; Convert about 90% of tar with no cake formation	Barisano et al., 2012; Virginie et al., 2012; Min et al., 2013; Grieco et al., 2013
	ZrO_2; $Y2O_3$–ZrO_2; ZrO_2/Al_2O_3	Reforming tar and NH_3 cleanup	Tar conversion and sulfur addition improved naphthalene and ammonia conversion; high toluene and ammonia	Ronkkonen et al., 2009; Ferella et al., 2013; Juutilainen et al., 2006; Viinikainen et al., 2013

Types of catalysts`	Catalysts	Function	Improvement	References
			conversions even below 600 °C; H_2S had little effect on the activity	
Char based	Biomass char; char-supported nickel-iron;	Tar conversion and adsorption of heavy metals and organic pollutants	Tar conversion; Biomass can directly adsorb heavy metal ions	Shen, 2015; Shen et al., 2015a, 2015b
	nano-nickel on char char supported nickel	Reforming of toluene	Higher removal efficiency of toluene, but decreased in the presence of naphthalene	Qian and Kumar, 2017

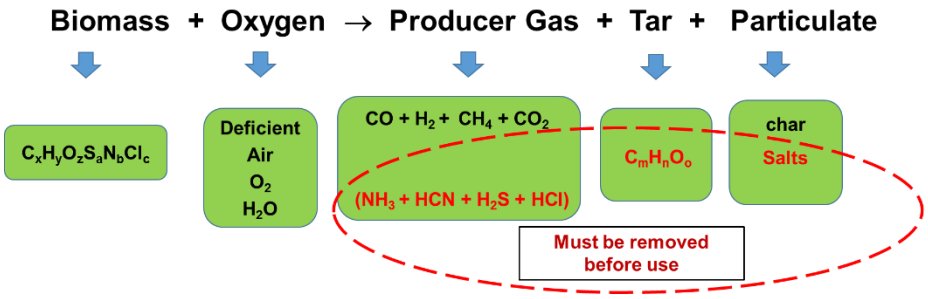

Figure 1-1. Schematic diagram of products by biomass gasification

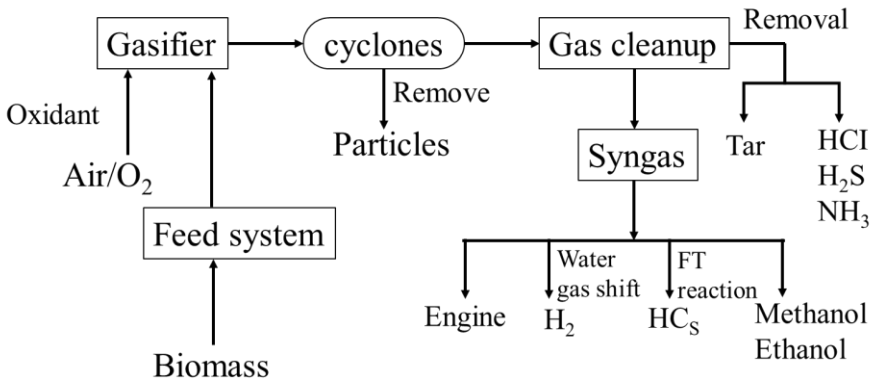

Figure 1-2. Schematic diagram for gasification process

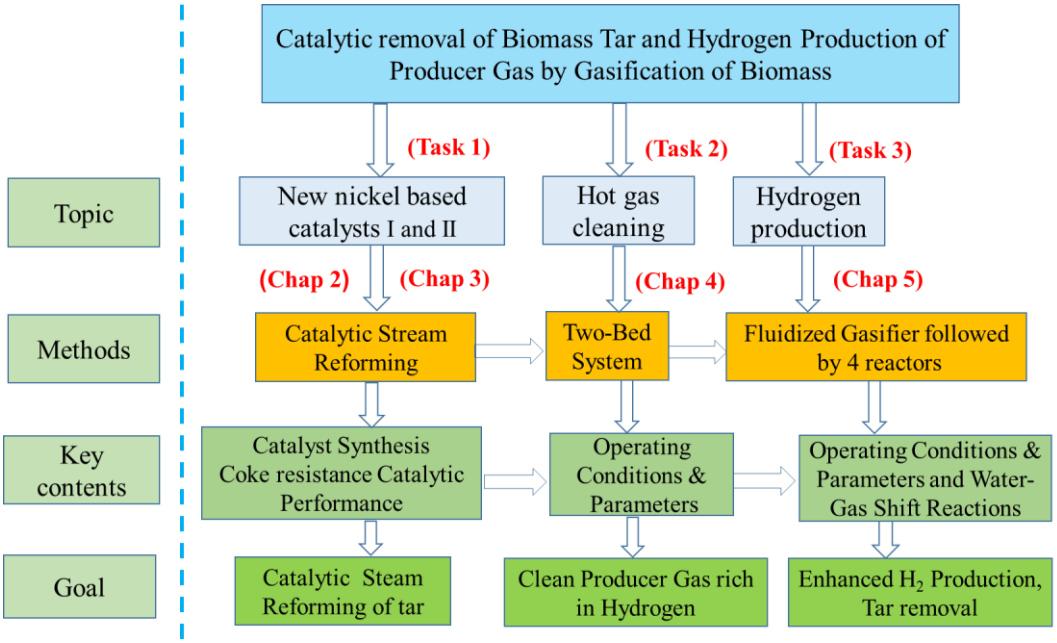

Figure 1-3. The thesis structure

Chapter 2 Steam Reforming of Tar Compounds over Ni/olivine Catalysts Doped with CeO_2

2.1 Introduction

Biomass as a source of renewable energy has several environmental advantages over fossil fuels. The main advantage is the lower net emission of greenhouse gases. Gasification of biomass produces a raw gas mixture composed of hydrogen (H_2), carbon monoxide (CO), carbon dioxide (CO_2), water (H_2O), methane (CH_4) and various light hydrocarbons. The producer gas also contains several undesirable constituents, including dust (ash and char), ammonia (NH_3), alkali (mostly potassium), sulfur, chlorine and tar. Tar is a complex mixture of aromatics including a significant fraction of polycyclic aromatic hydrocarbons. The concentrations of gas impurities are 5–30 g Nm^{-3} for particulate matter (Bridgwater, 1995) and 0.5–30 g Nm^{-3} for volatile alkali metals, depending on the type of gasifier and the characteristics of the feedstock. Tar content varies from 5 to 75 g Nm^{-3} for fluidized bed gasifiers (Kurkela and Sthalberg, 1992; Kinoshita et al., 1994; Narváez et al., 1997). This range is well above the maximum allowed for gas turbines and diesel engines (Milne et al., 1989; Bridgwater, 1995), so most power applications require substantial removal of tar before the gas can be used. Tar cracking and reforming increases the gas heating value and the overall efficiency of the biomass thermochemical conversion process. This approach is more desirable than water or oil scrubbing to remove tar, which poses environmental hazards not easily resolvable.

Both manufactured catalysts and naturally occurring minerals known to promote tar cracking and reforming have been investigated for potential incorporation in the gasification process (Sutton et al., 2001). Although the former is undoubtedly needed to reach very stringent specifications on gas purity, there is abundant experimental evidence that inexpensive and widely available basic oxide minerals are effective in drastically reducing the tar content of producer gas (Gil et al., 1999). In fact, simple mineral oxides are often suggested for initial gas conditioning followed by a secondary catalytic reactor in which the gas composition is further refined (Delgado et al., 1996).

It is well known that dolomite efficiently decomposes tar at the operating conditions usually employed in gasification processes (Ekstrom et al., 1985; Elliot and Baker, 1986). Dolomite has been utilized directly in fluidized bed gasifiers as well as in secondary reactors (Corella et al., 1996) in both demonstration units and industrial installations (Espenas et al.,

1998). The main problem with dolomite is its friability, which causes it to disintegrate into fines, which pose problems for the stable operation of the fluidized bed gasifier and its ancillary units.

For economic reasons, nickel catalyst is the most suitable choice among metals like cobalt (Co), iron (Fe), platinum (Pt), ruthenium (Ru) and rhodium (Rh). Several nickel (Ni) based catalysts have been investigated and found to be very effective in terms of tar removal (Arauzo et al., 1997; Corella et al., 1998; Devi et al., 2003). Ni based catalysts are also very effective for ammonia (NH_3) removal (Wang et al., 1999, 2000); The main limitation in using Ni based catalysts is severe deactivation of the catalyst. This deactivation occurs mainly when the catalyst is placed immediately after the gasifier where high tar levels cause coking and trace contaminants poison the catalyst. Steam reforming catalysts are useful for polishing purposes when very clean gas is needed in such operations as Fischer–Tropsch reactions.

Most commercially available Ni catalysts display moderate to rapid deactivation due to the buildup of surface carbon and "sintering" effects (Rostrup-Nielsen, 1984). This latter phenomenon occurs at high temperatures. When nickel is deposited on a support (usually alumina), the metallic particles tend to migrate and form larger aggregates, reducing the dispersion and consequently the catalyst activity. Sintering also encourages the formation of coke.

Olivine is a mineral containing magnesium oxide, iron oxide and silica. Olivine is resistant to attrition compared to dolomite. Investigations by Rapagna et al. (2000) showed that olivine's activity in steam reforming of tar was superior to that of calcined dolomite. The authors also performed experiments with olivine as bed material with lanthanum–nickel–iron (La–Ni–Fe) tri-metallic perovskite catalyst in a secondary reactor. The combined action of these materials was very promising; a gas with around 0.3 g m^{-3} of tar was obtained (Rapagna et al., 1998). Rose'n et al. (1997) reported success in using olivine as bed material for pressurized gasification (0.4–1.0 MPa) of birch. However, Abu El-Rub et al. (2002), using naphthalene as a model tar compound, observed no significant catalytic activity for olivine. Other researchers have proposed the use of olivine as a catalyst support (Courson et al., 2002; Devi et al., 2005).

Olivine contains iron, which helps stabilize nickel in the support structure (Petit et al., 1995; Provendier et al., 1999). The initial nickel–olivine interactions have to be strong enough to prevent nickel sintering and attrition of the active phase. Moreover, to be active for methane (CH_4) reforming, nickel particles must be accessible. Nickel strongly linked to the olivine support has previously been suggested for use with fluidized bed gasifiers (Courson et al., 2002). The results of previous research have revealed that the characteristics of natural olivine

(hardness, density and basicity) would be of particular interest in respect of this application. Active phase support interactions affect the dispersion of transition metals and the catalytic activity of the catalysts prepared from them (Tohji et al., 1984; Zou and Gonzalez, 1992). Che and Bonneviot (1988) have developed a two-step preparation method capable of controlling the particle size of Ni/SiO_2 catalyst. The nucleation step gave nickel oxide nuclei in strong interaction with the support; thereby the impregnation step effectively yielded a nickel reservoir (Yang et al., 1998). The effects of the active phase composition (Ni and/or NiO) are considered in relation to the catalytic properties in the dry reforming of methane ($CH_4 + CO_2$) (Courson et al., 2002).

Cerium oxide (CeO_2) has been used as a promoter in Ni based catalysts to enhance the resistance to coke formation since the $Ni–CeO_2$ system has strong metal support interaction (Wu et al., 1987). The role of CeO_x (x = 2 or 1.5) is to accelerate the reaction of steam with absorbed gaseous species on the nickel surface near the boundary area, so that carbon appearing on the surface can be quickly converted to gaseous products, preventing its accumulation. An attractive solution will be to associate nickel and olivine with cerium oxide as a promoter because olivine has an appropriate structure and mechanical strength. Moreover, olivine contains iron that can help stabilizing nickel in the structure (Petit et al., 1995; Provendier et al., 1999). Cerium oxide can improve catalytic activity and resistance to coking. The integration of small amounts of nickel into natural olivine could control the reducibility of nickel oxide and prevent carbon deposition on the catalyst during either dry or steam reforming of methane (Courson et al., 2000). This paper is an investigation of NiO/olivine and NiO/olivine doped with CeO_2. Benzene and toluene were used as model tar compounds to evaluate the catalytic quality and resistance to carbon deposition of the synthesized catalysts during steam reforming.

2.2 Experimental procedures

2.2.1 Micro-reaction system

A schematic of the experimental apparatus, which employs a WFS-3010 micro-reaction system manufactured by Xian Quan Science and Technology Ltd, Tianjin, China, is shown in Fig. 2-1. H_2 and N_2 were metered into a stainless steel vessel that served in these experiments to heat the gas mixture to 600 ℃. Mass flow meters adjusted the gas flow in the range of 10–200 mL min^{-1}. Liquid pumps were used to inject a model tar compound (benzene or toluene) and water into the gas flow, where they quickly evaporated at the elevated temperature, with metering accuracy better than 1.0%. Benzene and toluene injection rates were 1.7 and 1.8 mL

h^{-1}, respectively. The steam to carbon (S/C) ratio was maintained at 5.0. The hot gas mixture was admitted into a catalytic reactor constructed of a quartz tube with internal diameter of 8 mm and length of 280 mm. The catalytic reactor was mounted inside an electric furnace, which had a large homothermal area compared to the reactor dimensions. Temperatures were measured with two 1.0 mm OD thermocouples (type K), one placed at the center of the catalyst bed in the tubular reactor and the other placed against the outside surface of the tubular reactor wall. A pressure gage monitored the pressure drop across the catalyst bed during tests. Gases and vapors exiting the tubular reactor were passed through an ice water condenser where non-converted fractions of the model tar compounds were substantially condensed. Traces of steam and benzene were absorbed in a gas cleaner prior to analysis of the gas stream. A rotameter monitored the flow rate of product gas during a test, while a wet test meter monitored the cumulative volume of gas exiting the reactor.

The composition of the gas mixture at the reactor exit was determined by two on line Varian Model CP-3380 gas chromatographs (GC) with thermal conductivity detectors (TCD) with detection limits of 2 ppm and linear dynamic range of 104. One GC was equipped with a Molsieve 5A column and a thermal conductivity detector with argon as carrier gas to measure H_2, O_2, N_2, CH_4 and CO. The GC was equipped with a Porapak Q column and a thermal conductivity detector with helium as carrier gas to measure CO_2 and ethylene (C_2H_4). This system performed a complete gas analysis every 7 min. The duration of each test was 1 h with average gas composition calculated from the approximately eight measurements made during a test. The cumulative volume was monitored by a wet test meter so that the total volume of producer gas and the average volumetric flow rate at standard temperature and pressure could be calculated.

Conversion of model tar compounds to gaseous products (CO, CO_2 and CH_4) in the presence of the different catalysts was determined as a function of temperature (T), S/C, and space velocity (SV). Conversion efficiency, η, was calculated using the expression:

$$\eta = \frac{100\,Q\,(F_{CO} + F_{CO2} + F_{CH4})}{M\,N_c} \qquad (2.1)$$

where Q is the volumetric flow rate of gas (L h^{-1}); F_{CO} is the mole fraction of carbon monoxide in the gas products; F_{CO2} is the mole fraction of carbon dioxide in the gas products;

F_{CH4} is the mole fraction of methane in the gas products; N_C is the molar feed rate of carbon to the reactor (mol h^{-1}); and M is the molar density of the gas (22.4 L mol^{-1}).

2.2.2 Catalyst materials and preparation

The catalysts were prepared in the laboratory by wet impregnation. Preparation method, chemical composition and surface areas for the catalysts are listed in Table 2-1. The nickel and cerium contents are expressed as weight percent in the synthesized catalysts. Olivine supports were from Xixia Heqiang Company, China. The as received natural olivine was crushed and sieved to particle sizes between 20 and 30 mesh. $Ni(NO_3)3{\cdot}6H_2O$ and $Ce(NO_3)3{\cdot}6H_2O$ were dissolved in de-ionized water. Nickel and cerium were loaded onto supports by wet impregnation with $Ni(NO_3)_3$ and $Ce(NO_3)_3$ solutions, respectively, followed by drying in a vacuum at 105 ℃ for 8 h. After drying, the samples were calcined in air at a low heating rate until a final calcination temperature of 800 ℃ was achieved and maintained for 2 h. Three catalysts were obtained: 3.0% NiO/olivine, 3.0% NiO/olivine doped with 1.0% CeO_2 and 6.0% NiO/olivine, which are subsequently referred to as catalyst A, catalyst B and catalyst C, respectively.

2.2.3 Catalytic testing

The synthesized catalysts were sieved to particle sizes between 20 and 30 mesh in order to minimize internal mass transfer limitations (Kinoshita et al., 1994). Catalyst in the amount of 0.5 mL was loaded into the reactor for each test. A small plug of quartz wool at the bottom and top of the catalyst bed held the catalyst in place. A thermal couple placed at the center of the bed monitored reaction temperature. The gas preheater was heated to 600 ℃, and the catalyst bed was heated to 700 ℃ while passing 100 mL min^{-1} N_2 through it. Prior to starting a test, the catalyst was reduced at 700 ℃ by flowing a mixture of 50% H_2 and 50% N_2 through the reactor at a rate of 80 mL min^{-1} for 2.5 h. To commence a test, gas flow through the reactor was stopped and the catalyst bed was brought to the desired temperature. When the temperature stabilized, the model tar compound (either benzene or toluene) and steam were injected into the preheater where they were rapidly vaporized. The steam reforming of benzene and toluene were performed at the operating conditions specified for each test. Measurements included reactor pressure drop, volumetric flow rate and total gas volume exiting the reactor and gas composition (via the GC). During the steam reforming tests, space velocities (SV) were chosen high enough to minimize external mass transfer limitations while holding conversion efficiencies less than

80% (higher conversion efficiencies were not easily resolved in the present experimental system).

2.2.4 Catalyst characterization

Fresh and used catalysts were analyzed by powder X-ray diffraction (XRD), which was performed with a Japan D/Max-3B type diffractometer with a CuKα radiation source. Operating conditions were 2θ between 10° and 70°, current set to 30 mA and scan rate of 6° min^{-1}. The diffraction patterns were identified by comparing them with those listed in the Joint Committee of Powder Diffraction Standards (JCPDS) data base (JCPDS, 1984). Specific area and pore structure of the fresh and used catalysts were measured by BJH mode, which was performed with a US NOVA1000e Surface and Pore Analyzer. Scanning electron microscopy (SEM) was performed with a Japan Electronic JSM-5610LV SEM with accelerating voltage 0.5–30 kV and electron flow 1 pA to 1 μA and equipped with an energy spectrum analyzer.

2.3 Results and discussion

2.3.1 Catalyst for steam reforming

The baseline operating condition was initially selected to be the benzene injection rate of 3.6 mL h-1 (3.18 g h^{-1}), ICI steam reforming commercial catalyst volume 0.5 mL, S/C ratio equal to 5.0, SV equal to 1826 h^{-1} and reactor temperature equal to 750 ℃. However, within 115 min of starting tests under these conditions, the reactor became clogged by coke as indicated by a dramatic increase in pressure drop across the reactor. Thus, it was necessary to redefine the baseline test to be a benzene injection rate equal to 1.7 mL h^{-1} (1.5 g h^{-1}), catalyst volume equal to 0.5 mL, SV 862 h^{-1} and S/C 5. The baseline test for toluene had similar operating conditions except that the toluene injection rate was 1.8 mL h^{-1}. All subsequent catalysts tests were performed under these baseline conditions.

2.3.2 Performance of NiO/olivine catalysts

Tables 2-2 to 2-5 summarize the gas product compositions upon steam reforming of benzene and toluene for the three synthesized catalysts at 700 to 830 ℃. Generally, the gas products are 60–64 vol% H_2, 17–33 vol% CO, 4–18 vol% CO_2 and less than 0.2 vol% CH_4. All three impregnated catalysts of olivine catalyzed benzene steam reforming. The mechanism of steam reforming involves the absorption of the target molecules and water vapor on the catalyst

surface where they react until all carbon atoms are converted to CO or CO_2. Methane is not a reaction intermediate or primary product and is formed from CO through the methanation reaction. However, methanation is clearly unimportant as methane was less than 0.2% of the product gases.

Figure 2-2 plots H_2 concentration vs. benzene or toluene conversion for steam reforming by the synthesized catalysts at 700 to 830 ℃. As shown by the figures, catalyst A produced hydrogen to the same extent as catalyst C. Benzene or toluene conversions for catalyst C were slightly higher than the conversions for catalyst A at the four temperatures. This indicates that the catalytic activities of catalysts A and C were almost the same despite the 3.0%Ni difference in their catalyst compositions. Catalyst B produced more hydrogen than catalysts A and C.

Benzene or toluene conversions for catalyst B were much higher than the conversions for catalysts A and C at 700 ℃, 750 ℃ and 800 ℃, respectively. However, at the highest temperature tested (830 ℃), the differences in conversion were not obvious. Apparently, catalyst B, which was the CeO_2 doped 3.0% NiO/olivine, had better catalytic performance than catalyst A, the 3.0% NiO/olivine and catalyst C, the 6.0% NiO/olivine. In other words, the doped CeO_2 promoted the catalytic property of the NiO/olivine catalyst.

2.3.3 Comparison of NiO/olivine catalysts with NiO/olivine doped with CeO_2 catalyst

Benzene conversion was compared for 3.0%NiO/olivine (catalyst A), 3.0%NiO/olivine doped with CeO_2 (catalyst B) and 6.0%NiO/olivine (catalyst C).

Benzene steam reforming tests were performed at 700 ℃, 750 ℃, 800 ℃ and 830 ℃, respectively. Table 2-6 illustrates the effect of temperature on benzene conversion among the three catalysts. At 700 ℃, the benzene conversions by catalysts A, B and C were 5%, 34% and 13%, respectively. At 750 ℃, the benzene conversions by catalysts A, B and C were 41%, 61% and 41%, respectively. At 800 ℃, the benzene conversions by catalysts A, B and C were 52%, 69% and 62%, respectively. At the higher temperature 830 ℃, the benzene conversions by catalyst A, B and C were 70%, 70% and 71%, respectively. For all three catalysts, the benzene conversions increased with increased temperature. Benzene conversions by catalyst B were much higher than those by catalysts A and C at lower temperature. At the highest temperature (830 ℃), the difference was less than 0.5%. This clearly indicated the reaction was controlled by chemical equilibrium. NiO/olivine doped with CeO_2 had better catalytic activity than NiO/olivine for benzene steam reforming. Table 2-2 also illustrates that the catalysts produced CH_4 less than 0.04% at temperature 700 ℃ and about 0.01% at the temperature 700 ℃. At higher temperature, product CH_4 was so small as to be undetectable.

Table 2-7 illustrates the effect of temperature on toluene conversion among the three catalysts. Although the trend for these results is similar to those obtained for benzene, toluene conversion was higher than benzene conversion at comparable reaction conditions. This result is not surprising as benzene has a more stable chemical structure than toluene. For all three catalysts, toluene conversions increased with temperature increase. Toluene conversions by catalyst B were much higher than those of catalysts A and C at lower temperatures. At the higher temperature of 830 ℃, toluene conversions for catalyst A, B and C were 75%, 79% and 78%, respectively. The difference became smaller with temperature increase and was within 1.0% at the temperature of 830 ℃. This clearly indicates the reaction was controlled by chemical equilibrium at temperature 830 ℃. NiO/olivine doped with CeO_2 had better catalytic activity than NiO/olivine for toluene steam reforming. Table 2-3 also illustrates that the catalysts produced CH_4 of less than 0.3%, which was much higher than that from benzene steam reforming at the same reaction conditions.

Table 2-8 shows the carbon content by elemental analysis of the three expended catalysts. The amount of carbon found on catalysts A and C, on the order of 15 wt%, was much higher than the amount of carbon found on catalyst B, which was only about 3 wt%. These values indicated that doped CeO_2 could improve the resistance to carbon deposit on the Ni/olivine catalyst.

Figures 2-3a to 2-3c illustrate the crystal phases of the fresh, pre-reduced and expended catalysts A, B and C, respectively. The fresh NiO/olivine catalysts were composed of NiO, NiO, Mg_2SiO_4 and (Mg, Fe)SiO_3 according to the JCPDS file of the Mg_2SiO_4 (Efryushina et al., 1998; JCPDS, 1984). Besides the peaks of NiO/olivine catalyst, there was a very small CeO_2 peak in the NiO/olivine doped CeO_2 catalyst. In the reduced and expended samples, nickel appeared instead of NiO. Metallic nickel was an active component, while CeO_2 was a promoter for the steam reforming catalyst.

Figure 2-4 illustrates the SEM of the reduced catalysts and expended catalysts. The catalysts look similar before and after testing. This similarity suggests that the principal effect of the catalytic test is the reduction of nickel oxide particles to the metal along with an accompanying decrease in size. For the catalyst obtained via a two-step impregnation by nickel and cerium, the change consists of a less regular distribution of the metal upon the surface.

Data in Table 2-9 show the surface elemental compositions of reduced and expended catalysts A and B. Surface carbon content was much higher on the used NiO/olivine catalyst than on the used doped CeO_2 NiO/olivine catalyst. Surface oxygen content was much higher

on the used NiO/olivine catalyst than on the used doped CeO_2 NiO/olivine catalyst. Doped CeO_2 improved the properties and increased the crystal oxygen on the surface, which benefited the redox reaction during the steam reforming.

Carbon deposition on catalysts has been widely studied (Figueiredo, 1982; Vogt et al., 1987). The tendency of carbon to deposit depends upon the nature and fate of surface carbon species. The carbon species can either react with water or form products (hydrogen, carbon monoxide and carbon dioxide) or pass through a series of steps leading to carbon deposition. The carbon deposition process can be regarded as a competitive reaction with steam reforming. A general approach to preventing coke accumulation includes both reducing the deposition rate and increasing the rate of carbon gasification. Hydrocarbon steam reforming is an oxidative dehydrogenation process: the hydrocarbons are oxidized by steam to form carbon monoxide and carbon dioxide and simultaneously give up hydrogen. In the doped CeO_2NiO/olivine catalyst, some of the cerium might be in the state of Ce(III) during the steam reforming process. The cerium oxide promoting effect is assumed to be via a redox mechanism.

The lower valence state cerium might adsorb water and dissociate it, the resulting species –O or –OH transferring to nickel and reacting with surface carbon species to form CO, CO_2 and H_2.

2.4 Summary

Natural olivine showed good performance as a support for nickel catalysts. The hardness, density and basicity are compatible with the gasification environment. A proportion of nickel oxide is included in the olivine and maintains the level of reducible nickel oxide.

Steam reforming of benzene and toluene were investigated for Ni/olivine and Ni/olivine doped with CeO_2 catalysts. NiO/olivine doped with CeO_2 catalyst was particularly effective compared to the other two NiO/olivine formulations (catalysts A and C) in terms of both catalytic activity and coking resistance.

Cerium oxide is thought to promote the catalytic activity of nickel and resist the deposition of the carbon. CeO_x (x = 1.5 or 2) produced during the catalyst reduction, which also existed in the steam reforming environment. The promotion effect of cerium oxide on the nickel catalyst for steam reforming of benzene is probably through a redox mechanism. The lower valence state cerium might adsorb water and dissociate it, the resulting species –O or –OH transferring to the nickel and reacting with surface carbon species to form carbon monoxide, carbon dioxide and hydrogen.

Table 2-1. The chemical composition, preparation and surface areas for the catalysts

Catalyst	Preparation technique	Composition (wt%)	Specific area (m^2 g^{-1})	Pore radius (Å)
Olivine carrier	Natural mine	MgO 49.0, SiO_2 42.0 Fe_2O_3 8.0, Al_2O_3 0.5, CaO 0.5	4.6	21.2
A	One impregnation	NiO 3.0 on olivine carrier	1.3	68.2
B	Two impregnations	NiO 3.0 CeO_2 1.0 on olivine carrier	2.2	36.0
C	Two impregnations	NiO 6.0 on olivine carrier	2.3	52.8

A: 3.0% NiO/olivine

B: 3.0% NiO/olivine doped with 1.0% CeO_2

C: 6.0% NiO/olivine

Table 2-2. Gaseous products from steam reforming of benzene and toluene for three catalyst formulations (A, B and C) at 700 ℃ (catalyst volume of 0.5 mL; S/C ratio = 5.0; SV = 862 h^{-1})

Catalyst	Benzene steam reforming				Toluene steam reforming			
	H_2 (%)	CH_4 (%)	CO (%)	CO_2 (%)	H_2 (%)	CH_4 (%)	CO (%)	CO_2 (%)
A	62.3 ±0.1	0.02 ±0.01	32.3 ±0.3	5.3 ±0.3	63.4 ±0.4	0.1 ±0.0	24.4 ±1.7	12.1 ±1.7
B	64.0 ±0.3	0.02 ±0.01	23.9 ±0.9	12.1 ±1.2	64.8 ±0.6	0.1 ±0.0	16.6 ±0.9	18.5 ±1.3
C	63.6 ±0.1	0.04 ±0.01	31.7 ±0.3	4.7 ±0.3	63.9 ±1.1	0.2 ±0.0	23.6 ±1.5	12.3 ±0.3

Note: Uncertainty in tabulated values is expressed as 95% confidence intervals.

Table 2-3. Gaseous products from steam reforming of benzene or toluene for three catalyst formulations (A, B and C) at 750 ℃ (catalyst volume of 0.5 mL; S/C ratio = 5.0; SV = 862 h^{-1})

Catalyst	Benzene steam reforming				Toluene steam reforming			
	H_2 (%)	CH_4 (%)	CO (%)	CO_2 (%)	H_2 (%)	CH_4 (%)	CO (%)	CO_2 (%)
A	62.3 ±0.4	0.01 ±0.00	32.5 ±1.1	6.3 ±1.1	61.3 ±0.2	0.2 ±0.0	28.9 ±0.1	10.2 ±0.2
B	63.6 ±0.6	0.01 ±0.01	23.8 ±0.3	12.6 ±0.5	63.6 ±0.4	0.1 ±0.0	22.5 ±0.7	14.6 ±0.8
C	61.9 ±0.4	0.01 ±0.01	31.6 ±1.1	6.4 ±1.1	61.1 ±0.4	0.2 ±0.0	29.2 ±0.5	9.4 ±0.1

Note: Uncertainty in tabulated values is expressed as 95% confidence intervals.

Table 2-4. Gaseous products from steam reforming of benzene and toluene for three catalyst formulations (A, B and C) at 800 ℃ (catalyst volume of 0.5 mL; S/C ratio = 5.0; SV = 862 h^{-1})

Catalyst	Benzene steam reforming				Toluene steam reforming			
	H_2 (%)	CH_4 (%)	CO (%)	CO_2 (%)	H_2 (%)	CH_4 (%)	CO (%)	CO_2 (%)
A	61.6 ±0.4	0	32.3 ±0.2	4.8 ±0.3	58.1 ±1.7	0.2 ±0.0	31.2 ±1.2	10.5 ±0.5
B	62.5 ±0.4	0	27.6 ±0.5	9.0 ±0.5	61.8 ±0.4	0.2 ±0.0	23.4 ±0.4	15.6 ±0.3
C	61.7 ±0.2	0	29.8 ±0.2	7.3 ±0.3	58.9 ±0.3	0.2 ±0.0	31.6 ±0.2	9.3 ±0.2

Note: Uncertainty in tabulated values is expressed as 95% confidence intervals.

Table 2-5. Gaseous products from steam reforming of benzene and toluene for three catalyst formulations (A, B and C) at 830 ℃ (catalyst volume of 0.5 mL; S/C ratio = 5.0; SV = 862 h^{-1})

Catalyst	Benzene steam reforming				Toluene steam reforming			
	H_2 (%)	CH_4 (%)	CO (%)	CO_2 (%)	H_2 (%)	CH_4 (%)	CO (%)	CO_2 (%)
A	62.0 ±0.2	0	28.5 ±0.8	9.9 ±0.6	58.9 ±0.8	0.1 ±0.0	31.0 ±1.1	10.0 ±0.5
B	63.4 ±0.4	0	26.5 ±0.7	11.0 ±0.7	60.6 ±0.2	0.3 ±0.0	25.5 ±0.4	13.9 ±0.4
C	62.8 ±0.2	0	30.3 ±0.8	7.9 ±0.6	59.6 ±1.5	0.2 ±0.0	33.5 ±1.0	10.7 ±0.7

Note*:* Uncertainty in tabulated values is expressed as 95% confidence intervals.

Table 2-6. Benzene conversion and H_2 for steam reforming of benzene: comparison of synthetic catalysts A, B and C (CH_4 levels < 0.02%)

T (℃)	Benzene conversion (%)			H_2 (vol%)		
	A	B	C	A	B	C
700	5	34	13	62.4 ±0.1	64.0 ±0.3	63.6 ±0.1
750	41	61	41	61.3 ±0.4	63.6 ±0.6	61.9 ±0.4
800	52	69	62	62.0 ±0.2	63.4 ±0.4	62.8 ±0.2
830	70	70	71	61.6 ±0.4	62.5 ±0.4	61.7 ±0.4

Note: Uncertainty in tabulated values is expressed as 95% confidence intervals.

Table 2-7. Toluene conversion and H_2 concentrations for steam reforming of toluene: comparison of synthetic catalysts A, B and C

T (℃)	Toluene conversion (%)			H_2 (vol%)			CH_4 (vol%)		
	A	B	C	A	B	C	A	B	C
700	28.3	42.5	29.4	63.4	64.8	63.9	0.1	0.1	0.2
750	45.9	64.8	49.7	61.3	63.6	61.1	0.2	0.1	0.2
800	62.0	69.8	66.1	62.0	61.8	58.9	0.2	0.2	0.2
830	75.2	78.8	77.9	61.6	60.6	59.6	0.1	0.3	0.2

Note: Uncertainty in tabulated values is expressed as 95% confidence intervals.

Table 2-8. Carbon content of three expended catalysts

Catalyst	A		B		C	
	Carbon Content (wt%)	On stream (h)	Carbon content (wt%)	On stream (h)	Carbon content (wt%)	On Stream (h)
Sample 1[a]	13.8 ±3.1	10	2.4 ±0.7	10	15.2 ±3.3	10
Sample 2[b]	14.6 ±2.8	8	3.2 ±0.8	10	18.0 ±3.4	8

Note: Uncertainty in tabulated values is expressed as 95% confidence intervals.

[a] Used for benzene steam reforming

[b] Used for toluene steam reforming

Table 2-9. Surface composition of catalysts

Catalyst	Elemental composition (wt%)						
	Mg	Si	Fe	O	Ni	Ce	C
Reduced A	8.3 ±4.2	4.4 ±2.2	3.1 ±1.6	5.5 ±2.8	70.7 ±35.4	0	8.0 ±4.0
Used A	5.9 ±3.0	5.5 ±2.8	1.2 ±0.6	6.8 ±3.4	11.1 ±5.6	0	69.5 ±24.8
Reduced B	10.1 ±5.1	6.3 ±3.2	4.6 ±2.3	5.9 ±3.0	50 ±25.0	16.1 ±8.1	7.0 ±3.0
Used B	8.9 ±4.5	11.9 ±6.0	1.9 ±1.0	14 ±7.0	32.4 ±16.2	4.7 ±2.4	26.2 ±13.1

Note: Uncertainty in tabulated values is expressed as 95% confidence intervals.

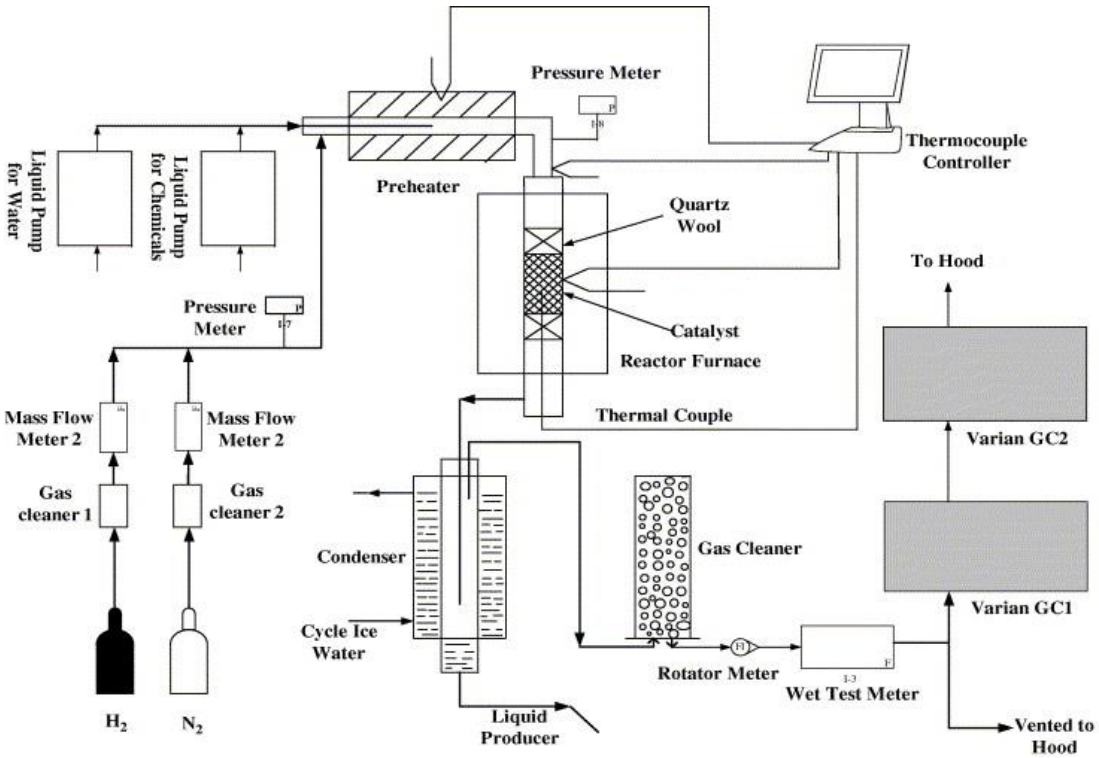

Figure 2-1. The schematic diagram of the reaction system.

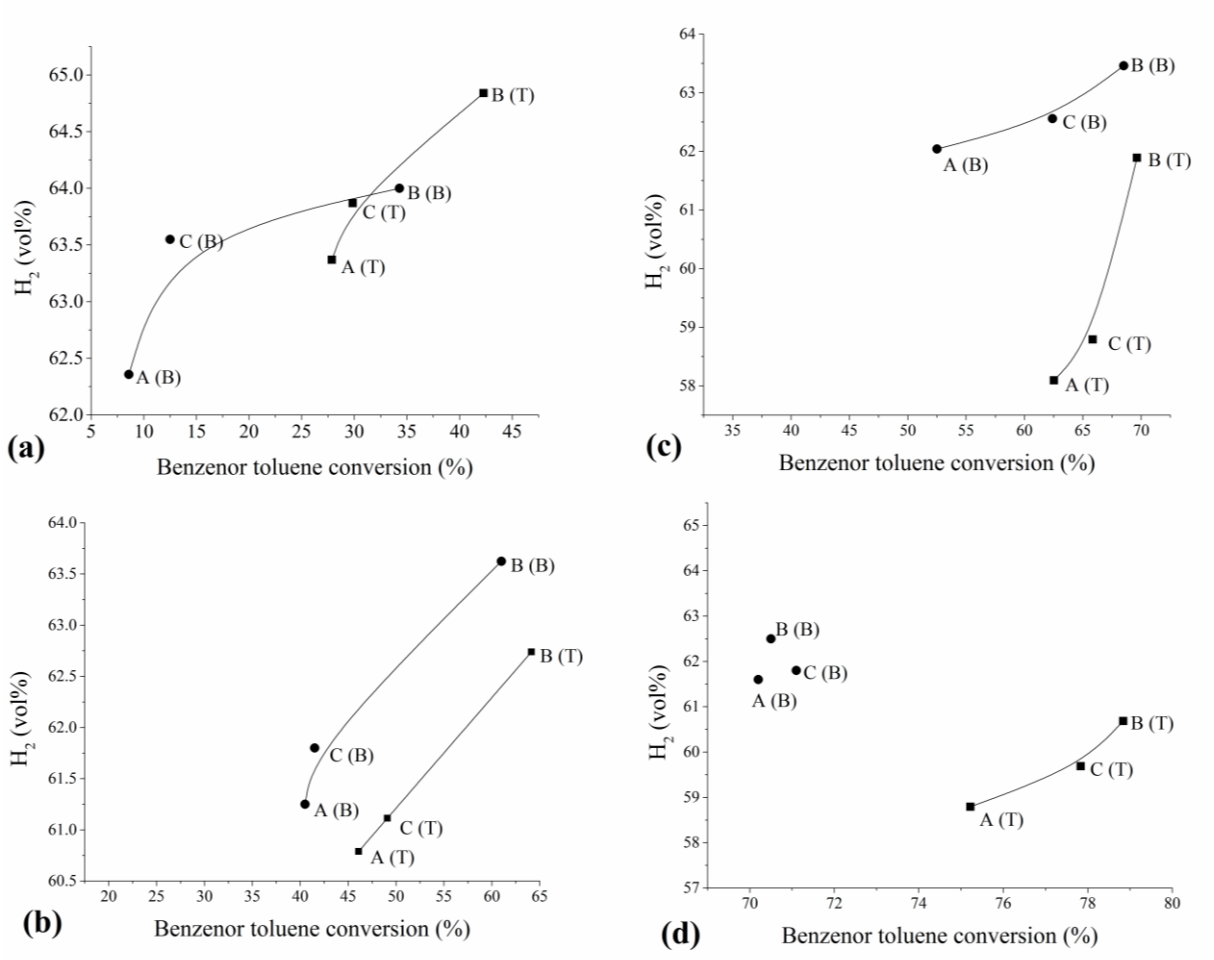

Figure 2-2. H_2 concentration vs. benzene (B) or toluene (T) conversion for steam reforming of benzene using three catalyst formulations (A, B and C). Conditions were: catalyst volume of 0.5 mL; S/C ratio = 5.0; SV = 862 h^{-1}; reaction temperature (a) 700 ℃; (b) 750 ℃; (c) 800 ℃; (d) 830 ℃.

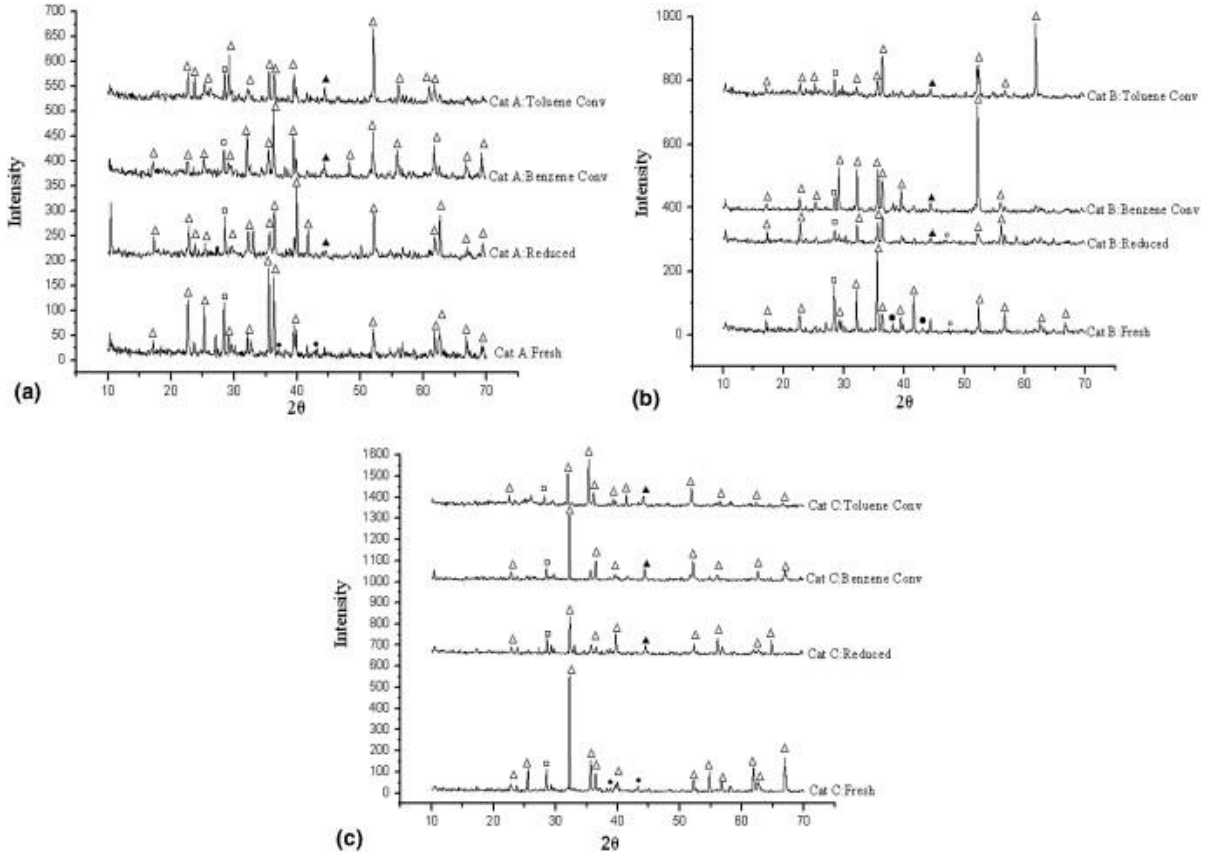

Figure 2-3. X-ray diffraction (XRD) of synthesized catalysts. (a) Catalyst A, (b) catalyst B and (c) catalyst C (peaks: ▲ – Ni, ● – NiO, ○ – CeO_2, △ – Mg_2SiO_4, □ – (Mg, Fe)SiO_3).

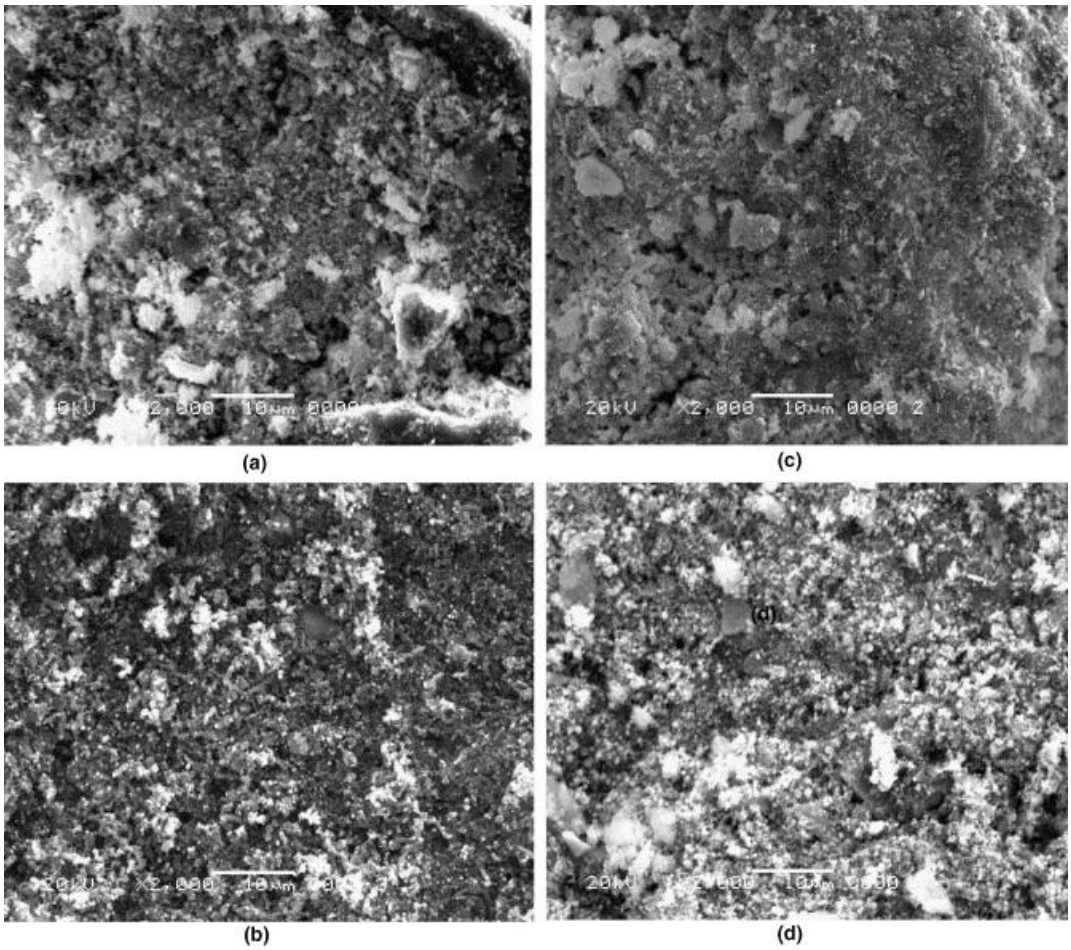

Figure 2-4. Scanning electron micrographs of catalysts: (a) Reduced 3.0% Ni/olivine, (b) used 3.0% Ni/olivine, (c) reduced and (d) used 3.0% Ni/olivine doped with 1.0% Ce.

Chapter 3 Catalytic Reforming of Toluene as Tar Model Compound: Effect of Ce and Ce–Mg Promoter using Ni/olivine Catalyst

3.1 Introduction

Due to the depletion of fossil fuels, environmental problems associated with these resources, along with high energy demand worldwide, renewable energy resources are attaining increasing attention (Demirbas, 2001). Among renewable energy resources, biomass is considered as a potential substitute for fossil fuels. Further, the use of biomass is a carbon neutral process. Among all biomass conversion processes, gasification is one of the promising ones (Garcia et al., 1999). However, this process is always accompanied by the formation of tar (Sutton et al., 2001). The "tar-like" compounds are a complex mixture of condensable hydrocarbons, which includes single to multiple ring aromatic compounds along with other oxygen containing hydrocarbons and complex polycyclic aromatic hydrocarbons (Devi et al., 2005a). The presence of tar is undesirable because of various problems associated with condensation, formation of tar aerosols and polymerization to form more complex structures, which cause catalyst deactivation and present problems in the process equipment including the engines and turbines used in application of the producer gas (Bui et al., 1994).

The reduction of tar content is the major challenge for successful operation of gasification. There are many factors associated with its formation (Milne et al., 1998) and different processes for its removal (Aub Ei-Rub et al., 2004). Catalytic reforming is considered to be the most potential method of reducing tar (Anis and Zainal, 2011).

The exploration of effective catalyst is vital for reducing tar in the biomass gasification process. Both synthesized catalysts and naturally occurring minerals known to promote tar cracking and reforming have been investigated in the gasification process (Sutton et al., 2001). Calcined dolomite is a porous catalyst, and its high surface area and the presence of oxides in its matrix (CaO, MgO) make it an active catalyst for tar reduction (Devi et al., 2005b). However, the main problem with dolomite is its softness, especially at high temperature (Gil et al., 1999). Olivine, a naturally occurring mineral [$(Mg,Fe)_2SiO_4$], has been demonstrated for its effectiveness in tar reduction (Devi et al., 2005a). Typically, Ni can be impregnated into olivine and the resultant Ni/olivine catalysts enhance steam adsorption, facilitate the gasification of surface carbon and hence prevent carbon deposition (Świerczyński et al., 2007).

The use of promoters (e.g., Co, Ce, etc.) has been successfully employed for tar reduction, e.g., Ni–Co (or Fe)/dolomite (Chaiprasert and Vitidsant, 2009) and Ni–Ce/olivine (Zhang et al.,

2007). In particular, the promoter Mg (in Ni/Al_2O_3) has been demonstrated for its effectiveness for exhibiting excellent catalytic activity, stability and sulphur tolerance in catalytic reforming of toluene and naphthalene (Yue et al., 2010) and $Ni–Mg/Al_2O_3$ over Ni/Al_2O_3 catalyst for biomass gasification (Garcia et al., 2002). The $Ni–Ce/Al_2O_3$ has better resistance toward tar and coke formation as compared to Ni/Al_2O_3 due to strong interactions between Ni and CeO_2 (Tomishige et al., 2007). Also, Ni–Ce/zeolite exhibited better rate of cellulose gasification and partially inhibited carbon deposition, as compared to those without Ce promoter (Inaba et al., 2006). Based on our previous study (Zhang et al., 2007) as well as others (e.g. Carlos et al., 2011), it appears that Ce promoter incorporated into Ni/olivine should be an effective catalyst.

Further, the use of more promoters may exhibit better catalytic activity and prolong catalyst life duration, e.g., $Ni–Ce–Fe/Al_2O_3$over $Ni–Ce/Al_2O_3$ in reforming ethanol for hydrogen production (Huang et al., 2009) and $Ni–Cr/Al_20_3$ ŀMgO ŁLa_2O_3 over Ni/Al_2O_3alone in steam reforming of naphthalene (Bangala et al., 1998). Unfortunately, a systematic evaluation of Ni/olivine with one and two promoters has not been performed before. Consequently, the present study was undertaken to synthesize different Ni/olivine catalysts to see their activity towards toluene as a model compound for tar reduction, since toluene is the major part of tar, e.g., 20% of tar (Coll et al., 2001). Initially, we tried different concentrations of Ni/Ce impregnating onto olivine (Ni–Ce/olivine) to select the optimum Ni/Ce content for toluene conversion. Thereafter, the selected Ni–Ce catalyst was then modified with the addition of MgO (Ni–Ce–Mg/olivine) to see its impact on overall catalyst activity.

The effect of Ce and Mg promoter on the reaction activity and the resistant ability to carbon deposition were investigated by powder X-ray diffraction (XRD), Fourier Transform Infrared (FTIR) and thermogravimetric (TG) analysis.

3.2 Methods

3.2.1 Preparation of catalysts

Natural olivine obtained from Xixia Heqiang Minerals, China was sieved through 20 and 30 mesh (0.60–0.85 mm). The catalyst was prepared by impregnating different amounts of aqueous solution of $Ni(NO_3)2·6H_2O$ and $Ce(NO_3)_3·6H_2O$ into sieved olivine, calcined at 800 ℃ for 2 h, and then dried at 105 ℃ for 2 h. A total of 9 catalysts with different Ni/Ce ratios were synthesized and it was found that the composition of 3% Ni/1% Ce yielded the highest

toluene conversion (88%). Consequently, this catalyst was chosen with addition of promoter [$Mg(NO_3)_2$]. The preparation method, procedure and composition of catalysts are shown in Table 3-1.

3.2.2 Catalytic tests

Activity tests were carried out in an atmospheric fixed-bed micro-reaction apparatus WFS-3010 (Fig. 3-1). The reaction temperature in the quartz tube reactor was controlled between 730 and 790 ℃ by programmed heating apparatus and measured by a thermocouple. The catalysts (0.5 mL; 0.8 g) were placed into quartz tube and heated to 730 ℃ for 3 h in the mixed gas of 50 vol% N_2 and 50 vol% H_2. The total flow rate of the mixed gas was 100 mL min^{-1}. The toluene was fed by pump (SZB-1A) at 1.7 mL h^{-1} with a gas volumetric space velocity (SV) loading of 782 h^{-1}. The test lasted for about 440 min for catalyst durability test.

One major factor, steam/carbon (S/C, from 3.5 to 6.5), was evaluated for toluene conversion and gas composition with different catalysts. All other conditions were maintained constant: catalyst loading 0.5 mL, toluene feed 1.7 mL h^{-1} and SV at 782 h^{-1}. The toluene conversion efficiency (η), was determined as:

$$\eta = \frac{100Q(F_{CO} + F_{CO2} + F_{CH4})}{M N_c} \quad (3.1)$$

Where Q is the volumetric off-gas rate (L h^{-1}), F_{CO}, F_{CO2}, and F_{CH4} is the molar fraction of CO, CO_2 and CH_4, respectively, N_C is the molar feed rate of carbon to the reactor (mol h^{-1}); and M is the molar density of the gas (22.4 L mol^{-1}). Similarly, energy gas yield (Y, mol gas mol^{-1} toluene) was determined with the above equation where the numerator was replaced by useful gases (F_{CO} + F_{H2} + F_{CH4}) as:

$$Y = \frac{100Q(F_{CO} + F_{H2} + F_{CH4})}{M N_c} \quad (3.2)$$

The specific energy yield (mol mol^{-1} g^{-1}) was then determined by dividing energy yield with the amount of catalysts.

To further compare the capability of various catalysts, we have defined a new term, called specific toluene loading rate which is determined as total toluene molar loading rate divided by the amount of catalyst, or toluene mol h^{-1} kg^{-1} catalyst.

3.2.3 Gas analysis

Product gas was measured by a wet meter and analyzed simultaneously with two on-line gas chromatographs (GC). The first GC (CP-3380, Varian, USA) was equipped with a 5A

molecular sieve and a thermal conductivity detector (TCD) for the measurement of CH_4, CO, H_2, O_2, and N_2. The injector, oven and detector temperatures were kept at 50, 80 and 130 C, respectively. Argon (99.9999%) was used as the carrier gas at flow rate 30 L min^{-1}. The second GC (CP-3800) equipped with a Propack Q column with another TCD was used for measuring CO_2roduction. He gas was used as carrier gas at flow rate 30 mL min^{-1} and the oven temperature was kept at 80 ℃ for 13 min. Both Instruments were calibrated by calibration gas for quantification of all gas components. The reported gas composition was the average of at least 3 measurements over the duration of 2 h.

3.2.4 Characterization of catalysts

The crystal phases of catalysts were detected by XRD on a Rigaku D/Max-3B diffractometer (Tokyo, Japan) using Cu Kα radiation with voltage 35 V and current 30 A. The samples were detected in the range of 2θ between 10 °and 90 °with scanning velocity of 6 min^{-1}. The crystal profiles were identified by JCPDS database.

FTIR analysis was performed using a Tensor 27 (Bruker Optics) spectrometer. The spectra were recorded within the region from 4000 to 400 cm^{-1}. The FTIR sample was mixed with KBr and pressed into pellets, then placed into the plate which was cleaned with acetone twice. The amounts of coke formed on the spent catalysts were determined by TG analysis in air. The experiments were carried out in the temperature range from ambient temperature to 973 K at a heating rate of 10 K min^{-1} in an air flow of 60 mL min^{-1}.

3.3 Results and discussion

3.3.1 Catalyst activity

(1) Effects of Ni and Ce content

The activity of the catalysts at T = 790 ℃ and SV = 782 h^{-1} at constant S/C ratio of 5 is related to the content of Ni in olivine as shown in Fig. 3-2a. The conversion efficiency initially increased slightly with the increase of Ni content (from 1% to 2%), reached the highest at Ni = 3% and then decreased with further increases in Ni content. With the lower Ni content, the active sites may not be adequate while higher Ni contents may form agglomerated crystals (Bangala et al., 1998) – all these phenomena result in lower efficiency. Courson et al. (2000) also reported that 2.8% Ni/olivine yielded the best performance in terms of syngas yield and stability for reforming of CO_2/CH_4.

In general, the addition of a dopant can improve the dispersion of the active phase, increase the thermal stability of support, and resist sintering of the active phase in which Ce is most effective (Wenge et al., 2012). Therefore, the next step was to find the optimum Ce content in 3% Ni/olivine for toluene reforming. Similar to Ni pattern, there exist an optimum Ce content (1%) for yielding the highest toluene conversion as shown in Fig. 3-2a. The toluene conversion has been remarkably increased, or from 59% to 88% in the presence of 1% Ce in 3% Ni–Ce/olivine catalyst. There is a strong interaction between Ni and CeO_2 by the formation of Ni–CeO_2 nanocomposite structure (Li et al., 2012). Therefore, the catalyst of 3% Ni/1% Ce was subsequently used for incorporating Mg to see its impact on overall performance.

(2) Effects of promoter MgO

The 3% Ni-1%Ce-1% Mg/olivine catalyst was used for determining the effects of S/C ratio on toluene reforming with the results shown in Fig. 3-2b. Clearly, the addition of Mg improved toluene conversion up to 93% at the lowest S/C ratio of 3.5. With increased S/C ratios, activity decreased for all three catalysts, as high steam exhibited a negative impact on Ni. It is believed that the addition of promoters may lead to better Ni dispersion and higher interaction with nickel-support resulting in increasing catalytic activity and reducing carbon formation (Zhang et al., 2007). In fact, highly dispersed and well-stabilized Ni particles have been found with NiO–MgO solid solutions (Choudhary et al., 1997).

It must be noted that the toluene conversion is remarkably high considering the fact that pure toluene solution was used at concentration almost 50 wt%. For comparison, in other studies, gaseous toluene feed was only 0.7 vol% (Świerczyński et al., 2007), 2000 ppm (Li et al., 2009), and 2.0 vol% (Yue et al., 2010) as shown in Table 3-2. The specific toluene loading rate (mol toluene h^{-1} kg^{-1} catalyst) shown in Table 3-2 indicates a much high value in the present study as compared to other studies (e.g., 20 mol toluene h^{-1} kg^{-1} in the present study as compared to 3–7 mol toluene h^{-1} kg^{-1} by others).

(3) Gas composition

The composition of the gases produced from catalytic steam reforming of toluene by these three catalysts as function of S/C ratio is shown in Table 3-3. In general, all three catalysts yield higher amount of H_2 with content 57–66% (Eq. 3.3). The product gas flow rate depends on the type of catalysts and to some extent, S/C ratio. The introduction of Ce or Ce–Mg promoter enhances the overall gas production rate and yields higher H2concentration. For example, at S/C = 3.5, gas production conversion was 56%, 75% and 93% for Ni/olivine, Ni–Ce/olivine

and Ni–Ce–Mg/olivine catalyst, respectively. In general, CH_4 content with Ni-Ce/olivine and Ni–Ce–Mg/olivine catalysts was slightly decreased. The profiles of CO for two modified N/olivine catalysts were completely different. For Ni–Ce catalysts, the CO content was significantly reduced (almost 50%), resulting in high levels of CO_2 concentration. On the other hand, CO level was slightly increased for Ni–Ce–Mg catalyst. Also, the specific energy yield reached the highest value of 20 mol gas mol^{-1} toluene g^{-1} catalyst. In short, the addition of Mg promoter to Ni–Ce/olivine clearly enhances toluene conversion and energy yield, especially at lower S/C ratio. It is noted that despite higher toluene conversion for Ni–Ce/olivine, the selectively of this catalyst is poor (high CO_2 formation) resulting in lower specific energy yield; clearly, the Ni–Ce/olivine catalyst favors the water shift reaction Eq. (3.4):

Steam reforming $C_7H_8 + 7H_2O = 7CO + 11H_2$ (3.3)

Water-gas shitng $CO + H_2O = CO_2 + H_2$ (3.4)

(4) Durability and sensitivity of the catalysts

Figure 3-3 shows the toluene conversion efficiency and corresponding pressure buildup over three catalysts at two S/C ratios. Clearly, the Ni–Ce–Mg/olivine has the highest toluene conversion and exhibits a steady performance up to 400 min at lower S/C ratio of 3.5 (Fig. 3-3a), and the performance remains the same up to 300 min at higher S/C ratio of 5 (Fig. 3-3b). Thus the addition of Mg has a profound impact on the Ni–Ce catalysts. The reason for longer catalytic activity is due to less tar deposit as reflected by the observed pressure buildup (Fig. 3-3c and 3-3d). For example, pressure started to build up at 150 min for both Ni/olivine and Ni–Ce/olivine whereas it remained essentially the same for Ni–Ce–Mg/olivine catalyst until 400 min (Fig. 3-3c).

Since there will be a small amount of H_2S produced during biomass gasification process, three different catalysts were further subject to H_2S test with the results shown in Fig. 3-4. In general, the initial toluene conversion is similar in the presence of H_2S for all catalysts as in the cases of without H_2S (Fig. 3-3a and 3-3c). But the toluene conversion dropped significantly with prolonged time for those catalysts without Mg or Ce promotor (Fig. 3-4a and 3-4c). For example, at S/C = 5.0, toluene efficiency for Ne/olivine catalyst started to decrease at ca 75 min while other two catalysts could maintain the relatively constant efficiency until 150 min (Fig. 3-4c). At lower S/C = 3.5, the Ni–Ce–Mg/olivine could maintain the same conversion efficiency (90%) up to 400 min. The corresponding pressure plots essentially confirm the sensitivity of these three catalysts (Fig. 3-4b and 3-4d). In order to see whether Ni–Ce–

Mg/olivine catalyst can withstand a higher H_2S mass loading, the H_2S injection flow rate is doubled to 200 mL min^{-1}. The results indicate that activity can be maintained up to 300 min (Fig. 3-5). Clearly, the addition of Mg helps improve the sulfur resistance of the catalyst.

3.3.2 Characterization of carbon deposition on catalyst

(1) Characterization of coke by FTIR and XRD

The surface functional groups of the used catalyst were analyzed by FTIR spectrometer shown in Fig. 3-6. There are no peaks in the region of 1400–1600 and 690–860 cm^{-1} which indicates aromatic rings. It means that coke formation on the used catalysts probably is graphite or graphite precursor. Figure 3-7 shows the XRD patterns for the used catalysts. The peak at 2θ = 26.6 ° (PDF 75–1621) corresponds to graphitic carbon. The peak of 26.6 ° (0 0 2) almost disappears after Ce and Mg doped in Ni/olivine. It is suggested that CeO_2 and MgO can inhibit the growth of graphite. In addition, the peak at 35.7 ° was assigned to SiC (PDF 22–1273, Du et al., 2011). As in the case of graphite peak, the SiC peak is significantly reduced for Ni–Ce–Mg/olivine catalyst. The spent Ni–Ce–Mg/olivine catalyst shows no such graphite and SiC peaks indicating its resistance to carbon deposit.

(2) Kinetic characteristics of coke by TG

To further determine the type and amount of coke present in the used catalysts, TG analysis was performed. There is no significant mass reduction before 550 ℃ (Fig. 3-8), or no decomposition and phase transformation occurs before 550 ℃ in an air atmosphere. The reduction of three catalysts at 790 ℃ was 29%, 8% and 3% for Ni/olivine, Ni–Ce/olivine, and Ni–Ce–Mg/olivine, respectively. In other words, the carbon deposition on Ni/olivine is the most, and significantly reduced with Ce dopant and almost insignificant for Ni–Ce–Mg/olivine after 7 h reaction.

According to the results of previous studies (Belgued et al., 1991; Świerczyński et al., 2007), there are three carbon combustion temperature ranges under air atmosphere and heating rate 10 K min^{-1}. The carbide is more likely to be converted due to its high activity and can be burned at 250 ℃. The amorphous carbon with its lower activity is burned at 400 ℃.

The carbon burning at 550–700 ℃ is graphite carbon or its precursor. As seen from Fig. 3.9, the catalyst after the reaction loses weight from 570 ℃, and reaches a maximum rate at 666 ℃ which may indicate that the above catalyst carbon is present in the form of graphite or graphite precursor.

As discussed above, the TG diagrams have shown that coke can be decomposed through burning with air at high temperatures. In general, the activity of coked catalysts can be partly restored after the coke was treated with oxygen-containing mixtures to increase the catalyst lifetime. So, the investigation of coke burning kinetic parameters will contribute to the regeneration study of catalyst on the basis of TG results.

According to the TG curves, the kinetics equation of coke burning reaction can be described as follows (Yang et al., 2013):

$$\ln\left(\frac{-\ln x}{T^2}\right) = \ln\frac{AR}{\beta E} - \frac{E}{RT} \qquad (3.5)$$

where x is the mass percentage of the unburned coke, A is the pre-exponential factor, E is the activation energy, R is the gas constant, T is the temperature, and $\beta = dT/dt$.

According to the results of TG analysis, a straight line can be obtained corresponding to each catalyst as shown in Fig. 3-10. The slopes and intercepts of these lines were calculated by linear regression to obtain the coke burning E and A for different catalysts as shown in Table 3-4.

It is obvious that the E of Ni/olivine is higher than those of Ni–Ce/olivine and Ni–Ce–Mg/olivine (lowest 126 kJ mol^{-1}). It illustrates that the coke deposition on Ni/olivine without promoter is the most difficult to be removed. The addition of Ce relatively increases the regeneration ability of deactivated catalysts and then incorporating Mg further increases the regeneration capability. Yang et al. (2013) also reported that the E for 3.9% Ni/olivine was 180 kJ mol^{-1}, which is similar to the value determined in the present study.

3.4 Summary

The efficiency of the Ni–Ce/olivine catalyst in tar removal was high in steam reforming of toluene. The addition of Ce can reduce the coking formation on the catalyst and increase toluene conversion. 1% Ce impregnation into 3% Ni/olivine effectively increases the toluene conversion yield from 59% to 88%. Further addition of 1% Mg to 3% Ni–1%Ce/olivine also increases reaction activity (toluene conversion up to 93%), prevents coke deposition and is resistant to H_2S poison. In short, Ce and Mg promoters enhance Ni/olivine catalysts in toluene conversion; Ni–Ce–Mg/olivine exhibits the highest toluene conversion and energy yield; Ni–Ce–Mg/olivine is resistant to 10 ppm H_2S poison; and Ni–Ce–Mg/olivine is resistant to deactivation.

FTIR and XRD analyses indicate that the deposition of graphite-like compound on the surface of the three catalysts. XRD shows that an addition of Ce or Mg can inhibit carbon from depositing on the catalyst surfaces. TG analyses show that Ce and Mg promoters decrease the coke deposition on Ni/olivine. The activation energy of coke burning of Ni/olivine decreases from 165 to 126 kJ mol^{-1} after adding Ce and Mg.

The more complex compounds, e.g., naphthalene, will be selected as a model compound in the future study to see the effectiveness of developed Ni–Ce–Mg/olivine in reforming complex compounds. If successful, the use of catalysts can be extended to actual biomass gasification.

Table 3-1. Preparation method, composition, carrier of three catalysts

Name	Preparation method	Composition (wt%)	Carrier	Impregnating order
Ni/olivine	Impregnation preparation	3 Ni	Olivine	Ni
Ni/Ce/olivine	Two-step preparation	3 Ni and 1 Ce	Olivine	Ce-Ni
Ni/Ce/Mg/olivine	Three-step preparation	3 Ni, 1 Ce and 1 Mg	Olivine	Mg-Ce-Ni

Table 3-2. Comparison of toluene conversion using Ni-based catalysts

catalyst	Condition* S/C	mol toluene h^{-1} kg^{-1}	toluene conversion (%)	References
Ni/olivine	2.3	4.5	98	Swierczynski et al., 2007, 2008
Katalco 46-6Q	2.2	6.5	100	Yoon et al., 2010
Ni-CeO_2 SBA-15	3	2.6	95	Tao et al., 2013
Ni/MgO-Al_2O_3	0.28	5.4	100	Yue et al., 2010
Ni/mayenite	2.1	4.6	100	Li et al., 2009
Ni-Ce/olivine	5	20	70	Zhang et al., 2007
Ni-Ce-Mg/olivine	3.5	20	93	this study

Note: All at 800 ℃

Table 3-3. Gas production, toluene conversion and specific energy yield as the function of S/C ratio.

Catalyst	S/C	H_2 (mol%)	CH_4 (mol%)	CO (mol%)	CO_2 (mol%)	Volume (L h^{-1})	Conversion (%)	SY[a] (g^{-1} cat)
Ni/olivine	6.5	64.3	0.13	27.4	6.0	2.4	34	8.1
	5	60.4	0.12	23.4	9.2	4.3	59	13.1
	3.5	58.3	0.08	23.2	8.0	4.1	56	11.9
Ni/Ce/olivine	6.5	66.2	0.04	12.2	21.9	5.4	80	15.6
	5	65.8	0.03	13.5	21.5	5.8	88	16.9
	3.5	64.6	0.13	18.1	15.7	5.1	75	15.6
Ni/Ce/Mg/olivine	6.5	62.6	0.08	28.0	8.5	5.2	81	17.5
	5	62.6	0.08	26.5	10.2	5.5	89	19.4
	3.5	61.8	0.09	27.3	9.6	6.2	93	20.0

[a] SY, the specific energy gas yield (mol gas mol^{-1} toluene g^{-1} catalyst).

Table 3-4. Kinetics parameters of coke burning of catalysts

Catalyst	Temp. range (K)	E (kJ mol^{-1})	A (s^{-1})	Correlation coefficient
Ni/olivine	850-970	165	9.1×10^{5}	0.9949
Ni-Ce/olivine	850-970	152	4.0×10^{4}	0.9907
Ni-Ce-Mg/olivine	850-970	126	5.7×10^{2}	0.9862

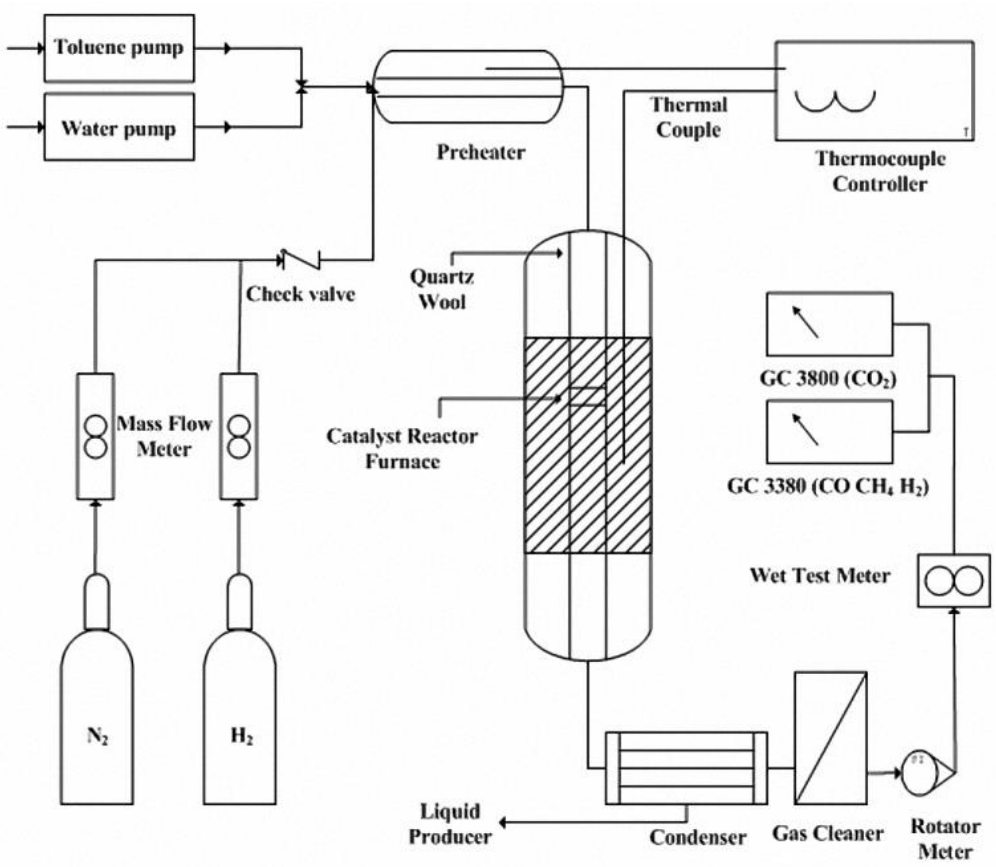

Figure 3-1. Schematic diagram of the reaction system.

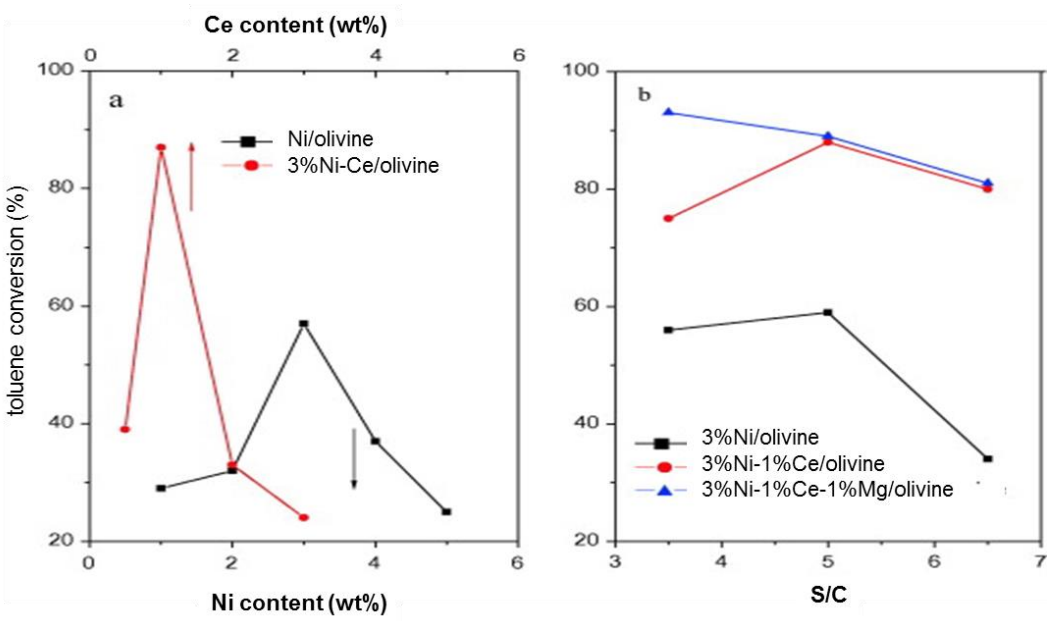

Figure 3-2. Toluene conversion of the catalysts. (a) Ni/olivine with different nickel content and 3% Ni–Ce/olivine with different cerium content at S/C = 5; (b) three catalysts at different S/C ratios. Reaction condition: 790 ℃; SV, 782 h^{-1}; time, 2 h.

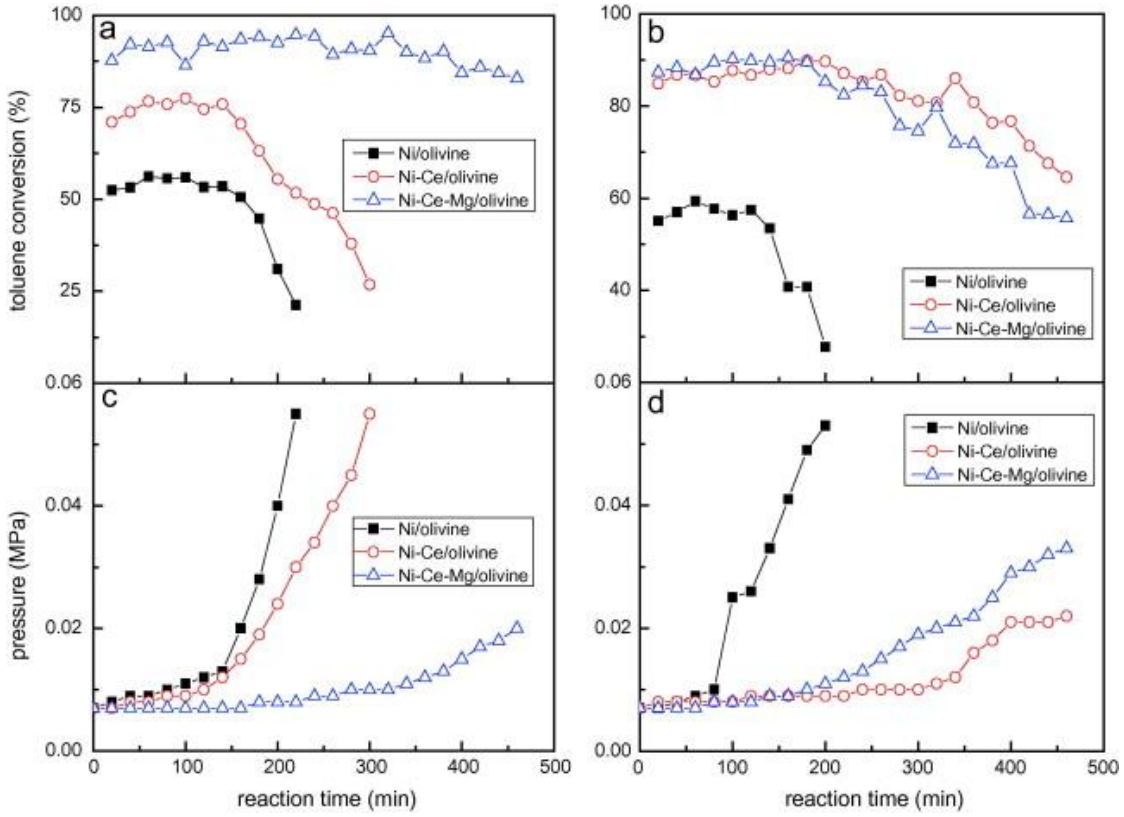

Figure 3-3. Durability test in steam reforming of toluene. Reaction condition: 790 ℃; SV, 782 h^{-1}; time, 7 h. (a) S/C 3.5, (b) S/C 5. (c) Pressure buildup corresponding to (a), (d) Pressure buildup corresponding to (b).

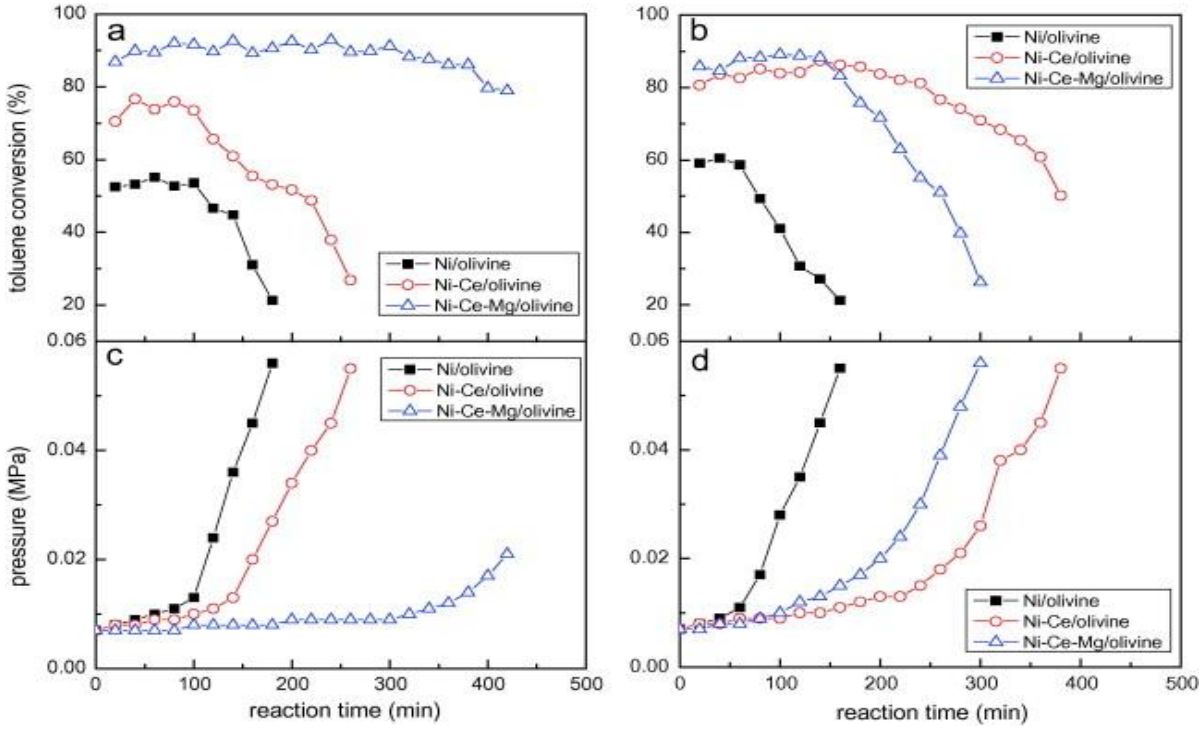

Figure 3-4. Effect of H_2S in steam reforming of toluene. Reaction condition: 790 ℃; SV, 782 h^{-1}; time, 7 h. H_2S: 10 ppm, 50 mL min^{-1}. (a) S/C 3.5, (b) S/C 5, (c) pressure buildup corresponding to (a), (d) pressure buildup corresponding to (b).

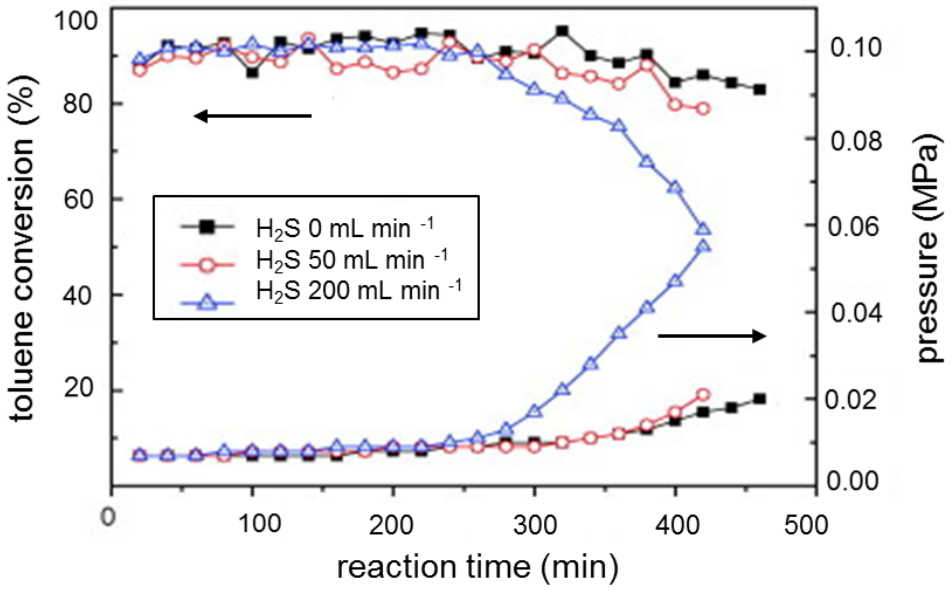

Figure 3-5. Effect of H_2S in steam reforming of toluene at different inject rate with Ni–Ce–Mg/olivine catalyst. Reaction condition: 790 ℃; S/C, 3.5; SV, 782 h^{-1}; time, 7 h; H_2S, 10 ppm.

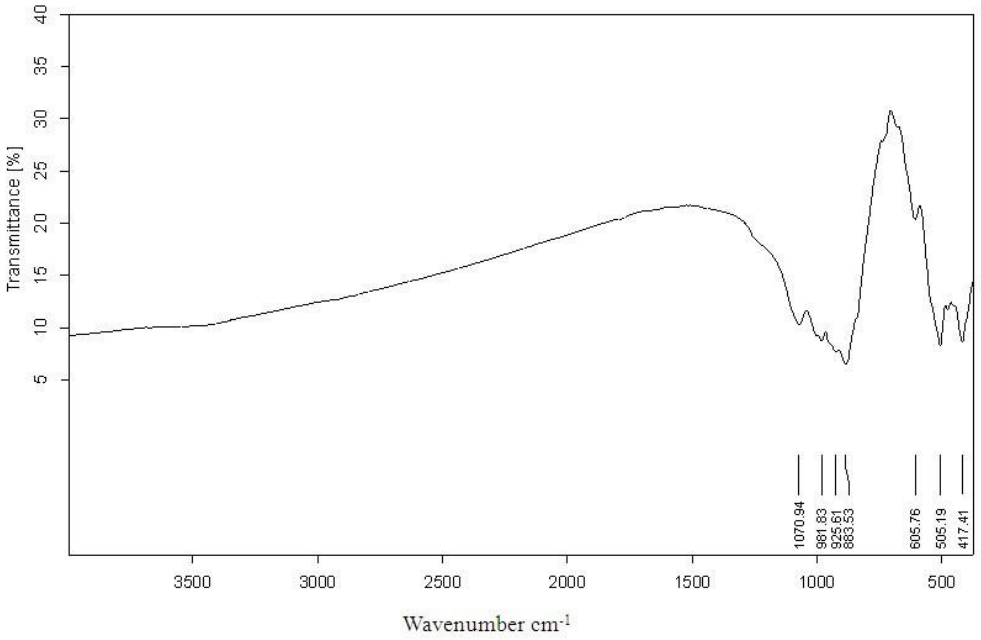

Figure 3-6. FTIR profiles of the Ni-Ce-Mg/olivine catalyst after reaction. Reaction condition: 790 ℃; S/C, 3.5; SV, 782 h^{-1}.

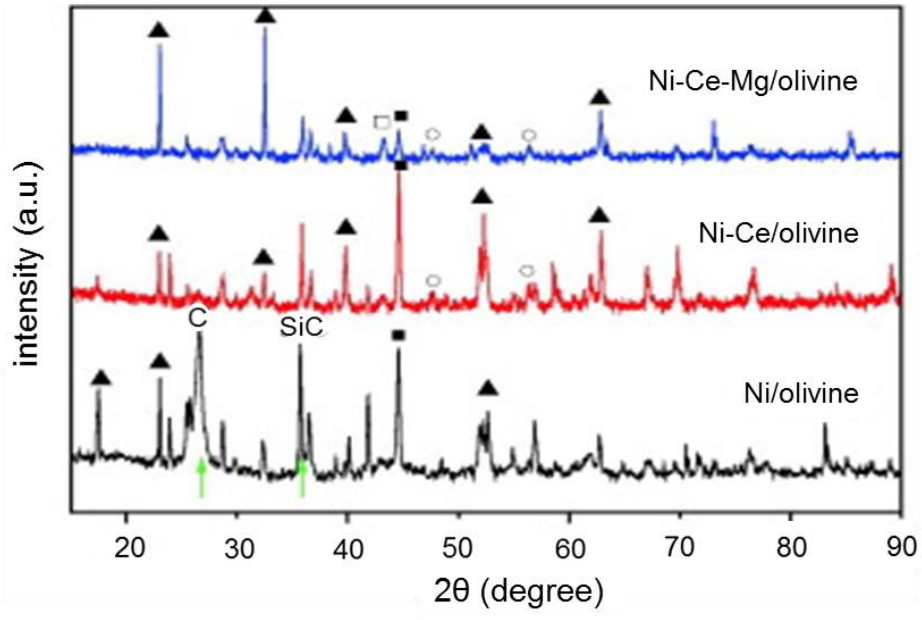

Figure 3-7. X-ray diffraction (XRD) patterns of the spent catalysts. Reaction condition: 790 ℃; SV, 782 h^{-1}; time, 2 h.

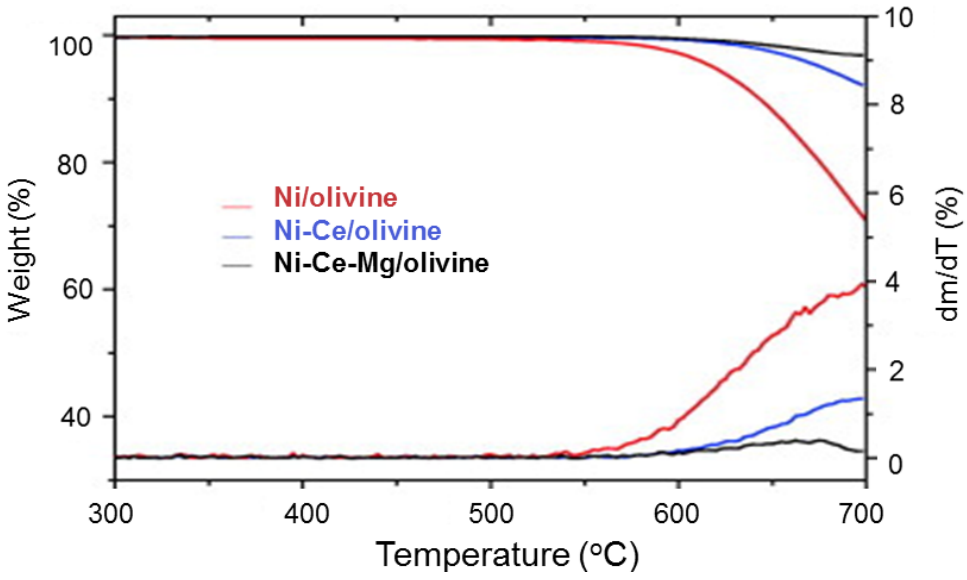

Figure 3-8. Thermogravimetric profiles of the catalysts after reaction. Reaction condition: 790 ℃; S/C = 3.5; SV, 782 h^{-1}. TG condition: air atmosphere, 10 K min^{-1}

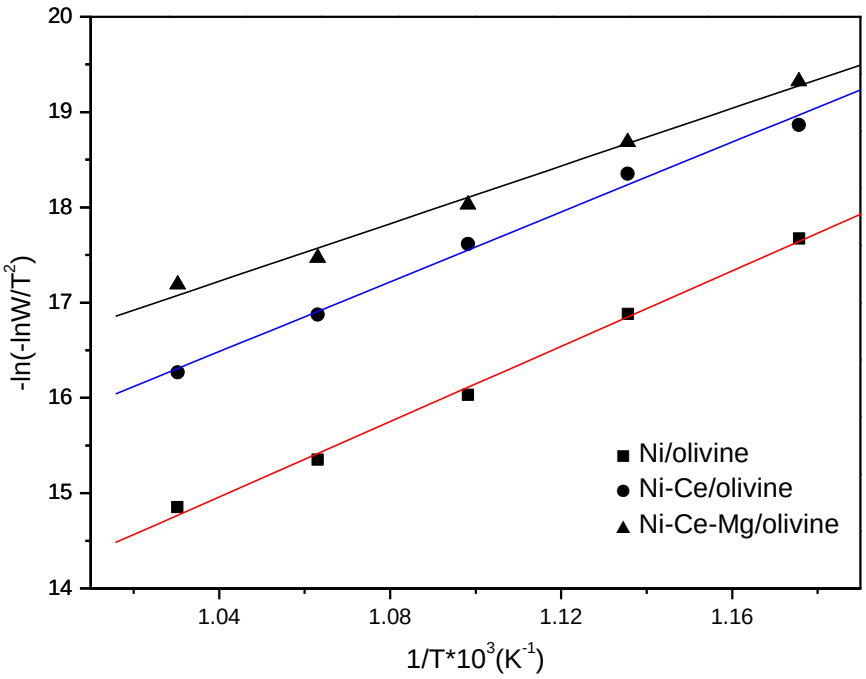

Figure 3-9. Kinetic curves of coke burning for the catalysts after reaction

Chapter 4 Catalytic Destruction of Tar in Biomass Derived Producer Gas

4.1 Introduction

Gasification of biomass produces a dirty raw gas mixture composed of hydrogen (H_2), carbon monoxide (CO), carbon dioxide (CO_2), water (H_2O), methane (CH_4) and various light hydrocarbons along with undesirable dust (ash and char), tar, ammonia (NH_3), alkali (mostly potassium) and some other trace contaminants. Most applications require removal of at least part of the dust and tar before the gas can be used.

It is widely recognized that tar in the producer gas presents a significant impediment to the use of biomass gasification systems. Tar can deposit on surfaces in filters, heat exchangers and engines where they reduce component performance and increase maintenance requirements. These effects must be mitigated if biomass gasification is to become a viable option for energy producers.

The purpose of this study is to investigate catalytic destruction of the tar formed during gasification of biomass. This work focuses on nickel based catalysts treated with alkali in an effort to promote steam gasification of the coke that deposits on the catalyst surface. Three metal catalysts were tested: ICI46-1, Z409 and RZ409.

Methods to remove tars from producer gas can generally be classified into one of three categories: physical processes, thermal processes or catalytic processes. Physical processes, such as filters or wet scrubbers, remove the tar from the producer gas through gas/solid or gas/liquid interactions. While these methods are effective and relatively easy to maintain, they do not truly alleviate the problem, as the tar is not destroyed and environmentally responsible disposal of the resulting tar laden filter material is difficult.

Thermal processes raise the temperature of the producer gas to levels that “crack” the heavy aromatic tar species into lighter and less problematic species, such as hydrogen, carbon monoxide and methane. For thermal cracking of tars, it is suggested that temperatures exceed 1000 ℃ (Milne et al., 1998) in order to reduce tars effectively. High temperatures require the cracking system be constructed of expensive alloys.

Catalytic processes can operate at much lower temperatures (600–800 ℃) than thermal processes, alleviating the need for expensive alloys for reactor construction. Depending on the catalytic process, this temperature range may eliminate the need to heat and/or cool the producer

gas as it leaves the gasifier. Most physical processes usually require the producer gas temperature to be lowered to 150 ℃ or less. Gas cooling substantially reduces the thermodynamic efficiency of the gasification process, impairing the performance as well as the economics of the system. Also, unlike physical processes, catalytic cleaning destroys the tar, eliminating waste disposal problems. Potentially, catalytic cracking processes provide the simplest and most effective means of removing tars while retaining the sensible heat required for efficient use of the producer gas in close coupled applications.

A number of catalytic processes have been previously investigated. Early on, it was discovered that in situ catalysis, in which the catalysts are placed directly in the gasification reactor, is not effective. Nickel based catalysts showed rapid deactivation when employed in fluidized bed gasifiers (Baker et al., 1985). In tests with non-metallic catalysts, the catalysts eroded and were elutriated from the bed (Corella, 1988, 1996). Tar destruction was verified for each type of catalyst, but the short lifetimes of these catalysts precluded the continued use of in situ catalysts.

Adding steam and/or oxygen to the catalytic reactor can enhance catalytic tar conversion. The addition of oxygen at 600–700 ℃ accelerates the destruction of primary products and inhibits the formation of aromatics. However, once benzene rings, the primary component of aromatics, are formed, they cannot be easily destroyed by oxygen. The addition of steam has been reported to produce fewer refractory tars, enhance phenol formation, reduce the concentration of other oxygenates, convert few of the aromatics and produce tars that are easier to reform catalytically (Milne et al., 1998). The addition of steam also facilitates the water/gas shift reaction:

$$CO + H_2O \rightarrow CO_2 + H_2 \qquad (4.1)$$

As greater amounts of steam are introduced into the system, the $H_2$and CO_2 concentrations increase, while the CO concentration decreases (Zhou et al., 1999). This reaction is extremely beneficial for methanol production applications, as methanol production occurs most efficiently when the H_2/CO ratio is 2. The H_2/CO ratio for unprocessed producer gas is usually less than 1, and steam addition to a catalytic tar conversion system has demonstrated the ability to adjust the H_2/CO ratio to levels as high as 13 (Gebhard et al., 1995).

The use of a catalytic reactor downstream of the gasification reactor has proven to be an effective approach to catalytic tar destruction (Kurkela et al., 1993). A variety of catalysts have shown significant ability to destroy tar in gasifier streams. These catalysts include dolomite (Alden et all., 1988; Simell and Bredenburg, 1990), nickel and alumina based catalysts (Hepola,

1993; Wiant et al., 1994) and various proprietary catalysts (Gebhard et al., 1995; Bain and Overend, 1996; Paisley, 1997). System variables, such as biomass composition, residence time and reactor temperature, play important roles in the successful application of these catalysts.

The use of a guard bed of inexpensive catalytic material upstream of a metallic catalyst bed has been demonstrated to improve the life of the metallic catalysts (Narvaez et al., 1997). The inexpensive mineral catalyst converts many of the heavy tars, while the metallic catalysts serve to "polish" the gas stream, reducing tar concentrations to very low levels. Lifetime tests have not been reported for catalysts protected by guard beds, but Milne et al. (1998) recommend this approach to catalytic tar destruction.

Nickel based catalysts almost completely remove the tar, but they are gradually deactivated by the deposition of coke on the catalysts. Coke formation on nickel results from a balance between coke formation and gasification. In industrial operations, coke gasification is accelerated by the use of alkali or alkali containing supports. Magnesium and potassium based materials are mainly used (Rostrup-Nielsen, 1984; Ross, 1975; Twigg, 1994). A complex of potassium alumina silicate and calcium magnesia silicate is used in the ICI nickel based catalyst. The potassium is liberated slowly as non-volatile K_2CO_3, which is hydrolyzed to the hydroxide. Mobility on the surface ensures good coke-alkali contact and rapid gasification (Twigg, 1994). Recent research results (Brown et al., 2000; Snoeck and Froment, 2002) also verify that alkali, by itself or added to commercial catalysts, promotes carbon or coke gasification.

4.2 Methods

4.2.1 Gasifier

Tests were conducted at the Biomass Energy Conversion Facility (BECON) in Nevada, IA, which is operated by the Iowa Energy Center. A pilot scale fluidized bed reactor was used to perform the experiments. The system was rated 800 kW thermal input, which corresponds to an average throughput of 180 kg h^{-1} of solid biomass fuel at a heating value of 16,000 kJ kg^{-1}. The major components of the plant include the fluidized bed reactor, fluidization gas system, fuel delivery system, data acquisition system and gas sampling system.

The current experiments employed discard seed corn as fuel. The proximate and ultimate analyses of the waste seed corn are given in Table 4-1. A variable speed auger metered the fuel into a rotary airlock where it fell into a constant speed injection auger. The high speed auger injected the fuel into the bottom of the fluidized bed. A small amount of air, introduced immediately below the airlock, prevented backflow of the fuel gas into the fuel hopper.

The diameter of the steel fluidized reactor was 46 cm standing 2.44 m tall. The reactor wall was lined with castable ceramic to insulate the vessel. Fluidization air entered the reactor through an array of perforated pipes that evenly distributed the air to the bottom of the bed. The bed media were sand mixed with a small quantity of limestone, making up about 5% of the total bed weight, to prevent agglomeration of the bed material arising from alkali in the biomass feed. The particulate laden fuel gas exited the reactor through the freeboard and passed through a cyclone that removed much of the particulate matter larger than 10 μm in size. Details on the operation of the biomass gasifier can be found in Simell et al. (2000).

The gasifier was fluidized with air at an equivalence ratio between 0.25 and 0.35, which maintained the reactor in the temperature range of 700–760 ℃. The feed rate of seed corn during these trials was in the range of 160 -200 kg h^{-1}. The overall experimental apparatus is illustrated in Fig. 4-1.

4.2.2 Catalytic tar conversion system

The catalytic tar conversion system is illustrated schematically in Fig. 4-2. A slipstream was drawn immediately downstream of the cyclone at a rate of 0.5–3.0 L min^{-1}. The slipstream passed through a heated particulate filter before entering the tar conversion system. Both the slipstream line and the particulate filter were maintained at 450 ℃ to prevent condensation of the tars.

The tar conversion system consisted of a guard bed reactor of dolomite stone in series with a tar-cracking reactor containing a metallic catalyst. The guard bed was designed to capture fine particulates as well as steam reform the heavy tars and absorb hydrogen sulfide. The metallic catalyst bed, which is susceptible to coking during destruction of the heavy tars and poisoning by hydrogen sulfide, was designed to convert the lighter tars into carbon monoxide and hydrogen. The two reactors, which were identical in construction, were operated as fixed beds.

The more complex compounds, e.g., naphthalene, will be selected as a model compound in the future study to see the effectiveness of developed Ni–Ce–Mg/olivine in reforming complex compounds. If successful, the use of catalysts can be extended to actual biomass gasification. Fig. 4-2 illustrates the reactor setup. They have internal diameters of 22 mm and can be filled to various depths to give space velocities between 1500 and 6000 h^{-1}. Each was installed in an electrically heated oven to maintain the desired temperature for each experiment. Each reactor had two thermocouples, as indicated in Fig. 4-2: one at the center of the fixed bed,

which was moveable for obtaining longitudinal temperature profiles and the other at the perimeter of the bed.

The catalysts evaluated in our tests included three kinds of commercial steam reforming Ni based catalysts: ICI46-1 was produced by the Imperial Chemical Industry, while Z409 and RZ409 are products of Qilu Petrochemical Corp., P.R. China. The compositions of the catalysts are listed in Table 4-2. All three catalysts contained alkali additives, such as potassium, calcium and magnesium oxides, which promote the elimination of coke formed on the catalyst by reactions of the type:

$$C + H_2O \rightarrow CO + H_2 \qquad (4.2)$$

Although the potassium promoter might be expected to diffuse readily out of the catalyst, it is in the form of potassium aluminosilicate, which releases the potassium very slowly, resulting in long service life.

Catalysts are usually activated before use by exposure to a reducing environment, typically a mixture of N_2 and H_2 at 750–850 ℃ for several hours. However, in our experiments, we tested ICI46-1 and Z409 without reduction. RZ409 is a reduced form of Z409 prepared by the manufacturer. The as-received catalysts were in the form of 15 mm rings. For use in our reactor, these rings were crushed and sifted to obtain 0.9–2.0 mm diameter particles. The pore size distributions of the crushed and sieved catalyst particles were obtained by mercury porosimetry. Typical characteristics for catalysts used in steam reforming are: specific surface area of 16–23 $m^2\ g^{-1}$, total pore volume of 0.14–0.18 $cm^3\ g^{-1}$ and average pore diameter of 200–500 Å.

The operating conditions for the catalysts are given in Table 4-3. In addition to the type of catalyst, operating variables include temperature of the guard bed (TGB), temperature of the catalytic bed (TCR), space velocity (SV) calculated on a dry gas basis and the ratio of steam to total organic carbon ratio (steam/TOC). TOC represents the amount of carbon in the organic compounds that are susceptible to steam reforming.

4.2.3 Sampling and analysis of gas and tar

Tar is a very difficult substance to sample and analyze with the result that many research groups have developed their own protocols, which makes it difficult to compare results. To avoid this difficulty, we employed the Provisional Protocol for the Sampling and Analysis of Tar and Particulates in the Gas from Large Scale Biomass Gasifiers (Version 1998) prepared by the Working Group of the Biomass Gasification Task of the IEA Bioenergy Agreement

(Smeenk and Brown, 1998). We only briefly outline this procedure; details can be found in the literature.

Gas drawn from the slipstream is passed through a heated particulate filter followed by a series of six impinger bottles placed in cooling baths (Fig. 4-1). The first four bottles were immersed in an ice bath while the last two bottles were immersed in an acetone/dry ice bath. The first and sixth bottles were filled with glass beads, while the second, third and fourth bottles were filled with dichloromethane (DCM). The fifth bottle was filled with both glass beads and DCM. Gas leaving the impinger train is passed through a vacuum pump before exiting through a wet test meter to determine accurately the total (dry) gas volume sampled.

Gas samples were taken before the guard bed and after the catalytic reactor to provide information about overall system performance. Gas sampling was done every half hour after steady operation of the gasifier and catalytic reactors. Gas samples were analyzed off line by gas chromatography using a Varian Micro-GC CP-2003 Quad equipped with Molsieve 5A BF, Poroplot Q and CP-Sils CB columns and a thermal conductivity detector with argon as carrier gas for the first column and helium as carrier gas for the second and third columns. The first column gave H_2, O_2, N_2, CH_4 and CO concentrations, while the second and third columns yielded CO_2, C_2H_4 and some light hydrocarbons.

At the completion of a test, DCM was rinsed through gas lines connected to the impingers to remove any tar condensed in them. This rinse liquid and impinger liquid were combined and refrigerated until the tar analysis was performed.

Two types of analysis were performed on these tar samples: evaporation at 105 ℃ and distillation at 75 ℃. In either case, analysis began by filtering out solids from the sample mixture and decanting the water from it. Evaporative analysis was the simpler of the two analyses performed and yielded tar values in good agreement with traditional methods of measuring “heavy tar” (Milne et al., 1998). This analysis consists of pouring 50 mL of DCM/tar mixture in a ceramic dish, letting it stand in a fume hood overnight, moving it to a heating chamber at 105 ℃ for 1 h and recording the weight of the remaining residue. From knowledge of the total gas flow through the sampling system, the tar concentration in the producer gas can be obtained, which we shall refer to as “heavy tar.”

The second method of analysis is based on distilling 50 mL of the DCM/tar mixture in a water bath maintained at 75 ℃ for 30 min. This distillation produces two fractions of hydrocarbons: light hydrocarbons (still dissolved in the distilled DCM and the distillation residue. In addition, the decanted water contains a third fraction of dissolved hydrocarbons

referred to as water soluble hydrocarbons. These three fractions were sent out for TOC analysis, which is useful in estimating the amount of steam required to convert the hydrocarbons in the tar to carbon monoxide and hydrogen.

4.3 Results and discussion

4.3.1 Properties of raw producer gas

When operating in the equivalence ratio range of 0.25–0.35 and at gasification temperature of 700–760 ℃, the average composition of the producer gas was (dry, volumetric basis): 51.2% nitrogen, 15.7% carbon monoxide, 14.2% carbon dioxide, 6.5% hydrogen, 4.8% methane and 4% higher hydrocarbons. The concentration of tar determined from evaporation at 105 ℃ was 10.4 g Nm^{-3}.

From the TOC analysis of the three tar sampling fractions, the carbon concentrations associated with hydrocarbons recovered in the tar impinger train are: 27.8 g Nm^{-3} from the distillation residue, 13.6 g Nm^{-3} from the light hydrocarbons and 5.7 g Nm^{-1} from the water-soluble hydrocarbons. Thus, the TOC concentration arising from hydrocarbons recovered from the impinger train was 47.1 g Nm^{-1}. The carbon concentration arising from CH_4 and C_2H_4 in the producer gas (that is, hydrocarbons not recovered in the impinger train) was 58.9 g Nm^{-1}. Taken together, the steam/TOC ratio in the producer gas is estimated to be 2.8.

4.3.2 Tar destruction

For all catalysts and operating conditions tested, no visible tar was observed in the lines after the catalytic reactor or in the impingers. The DCM mixtures recovered after these tests were clear with no hint of color. Analysis by evaporation at 105 ℃ found no detectable tar at the exit of the catalytic reactor for any of the tests, indicating heavy tar reduction in excess of 99%. Analysis by distillation at 75 ℃ was performed for only one test: the ICI46-1 catalyst operated at 800 ℃ with a SV of 3000 h^{-1} and a steam/TOC ratio of 2.8. Carbon from the light hydrocarbon fraction was present in the amount of 5.8 g Nm^{-3}, while carbon in the form of soluble hydrocarbons was 0.6 g Nm^{-3}. Although 6.4 g Nm^{-3} of carbon associated with hydrocarbons recovered in the impinger train may appear to be a relatively large concentration, it includes organic compounds that are not considered “tar” in many applications since they would not normally condense out. Nevertheless, it represents a carbon conversion efficiency of 86% for hydrocarbons collected from the raw gas by the impinger train operated at −70 °C.

4.3.3 Effect of catalytic reactor operating conditions on gas composition

The effects of space velocity, catalytic bed temperature, and steam/C ratio on gas composition (H_2, CO, CO_2, CH_4 and C_2H_4) for each of the three catalysts are presented in Fig. 4-3 to 4-5. In these figures, "GB Inlet" refers to the concentration of a gas species at the guard bed inlet (upstream of the tar destruction system), and "CR Outlet" refers to the concentration of a gas species at the catalytic reactor outlet (downstream of the tar destruction system). In general, H_2 and CO_2 increase, while CO decreases in the producer gas as it passes through the tar destruction system, as expected for steam reforming reactions acting in tandem with the water–gas shift reaction. Concentrations of CH_4 and C_2H_4 decrease in the producer gas. The decrease in CH_4 was about 0.2–1.0 vol%, while the decrease in C_2H_4 was about 0.5–1.5%. Although these low molecular weight hydrocarbons can be products of steam reforming of tar, they are also susceptible to further steam reforming to CO and H_2. The ICI46-1 catalyst showed no deactivation during 12 h of testing, while the Z409 and RZ409 catalysts showed no deactivation during 18 h of testing.

The effect of space velocity on hydrogen concentration in the producer gas is illustrated in the left column of Fig. 4-3 for catalysts ICI46-1, Z409 and RZ409 (TCR = 800 ℃; Steam/TOC = 2.8). There was little evidence that decreasing SV significantly increased hydrogen production (observed variations were within the uncertainty of hydrogen measurements). The effects of SV on CO and CO_2 concentrations in the producer gas are illustrated in the middle column of Fig. 4-3 for catalysts ICI46-1, Z409 and RZ409. For SVs less than 4500 h^{-1} there is no effect (in excess of uncertainty) on CO concentration. The concentration of CO2 is not substantially influenced by SV in the range of 1500–6000 h^{-1}. The effects of SV on CH_4 and C_2H_4 concentrations in the producer gas are illustrated in the right column of Fig. 4-3 for catalysts ICI46-1, Z409 and RZ409. No definitive trends (in excess of uncertainty) are evident for CH_4, while C_2H_4 clearly decreases as SV decreases. These observations indicate that tar destruction is not mass transfer limited in the present experimental system.

The effect of catalytic bed temperature on hydrogen concentration in the producer gas is illustrated in the left column of Fig. 4-4 for catalysts ICI46-1, Z409 and RZ409 (SV = 3000 h^{-1}; Steam/TOC = 2.8). As expected, hydrogen production increases with increasing reaction temperature although the increase is less than 25% from 740 to 820 ℃. The effect of catalytic bed temperature on CO and CO_2 concentrations in the producer gas are illustrated in the middle column of Fig. 4-4 for catalysts ICI46-1, Z409 and RZ409. Carbon monoxide increases, while CO_2 decreases with increasing temperature. The strongest effect is observed for catalyst Z409

(CO increases 40% from 740 to 820 ℃) and weakest for ICI46-1. The effects of catalytic bed temperature on CH_4 and C_2H_4 concentrations in the producer gas are illustrated in the right column of Fig. 4-4 for catalysts ICI46-1, Z409 and RZ409. No definitive trends (in excess of uncertainty) are evident for CH_4, while C_2H_4 clearly decreases, especially for the Z409 and RZ409 catalyst (reduction greater than 85% from 740 to 820 ℃). These observations indicate that the rate of tar destruction is controlled by chemical kinetics.

The effect of steam/TOC ratio on hydrogen concentration in the producer gas is illustrated in in the left column of Fig. 4-5 for catalysts Z409 and RZ409 (TCR = 800 ℃; SV = 3000 h^{-1}). As expected, hydrogen production increases with increasing steam/TOC ratio, although the increase is less than 30% in going from a steam/TOC ratio of 2.8–6.5. The effects of steam/TOC ratio on CO and CO_2 concentrations in the producer gas are illustrated in in the middle column of Fig. 4-5 for catalysts Z409 and RZ409. Carbon monoxide decreases by 50%, while CO2increases by 50% in going from a steam/TOC ratio of 2.8–6.5 for both catalysts, indicating a strong water–gas shift reaction. The effects of steam/TOC ratio on CH4 and C2H4 concentrations in the producer gas are illustrated in in the right column of Fig. 4-5 for catalysts Z409 and RZ409. No definitive trends are evident for either CH_4 or C_2H_4.

One reason for evaluating both the Z409 and RZ409 catalysts was to determine whether reducing the catalyst prior to use on gasification streams was important to catalytic activity (RZ409 catalyst is pre-reduced Z409). During the tests, we observed that hydrogen concentrations exiting the tar destruction system were 2.0–3.0 vol% higher for RZ409 than for Z409 during the first 2–3 h. However, for longer times, the difference between them disappeared. Thus, it appears that the producer gas is able to quickly reduce the metallic catalysts, making unnecessary a separate reducing step before using the catalyst.

4.3.4 Mercury porosimetry analysis

The catalysts were analyzed by mercury porosimetry to compare surface areas, pore sizes and pore size distributions before and after use in the tar destruction system (fresh and used catalyst, respectively). The results are shown in Table 4-4. In all cases, the pore structure of the used catalysts changed.

The ICI46-1 catalyst showed an insignificant change in surface area while the Z409 and RZ409 catalysts showed surface area reductions of 30–35%. Furthermore, all three catalysts showed shifts away from small pores (R < 100 Å) and micro-pores (100–500 Å) to medium pores (500–2000 Å) and large pores (R > 2000 Å). Although this could result from coke

blocking the smaller pores, the fact that pore volume increased suggests the conversion of small pores and micro-pores into larger pores during high temperature operation. If this transformation were to continue, the catalytic activity would eventually degrade

4.3.5 Carbon and sulfur analysis of catalysts and dolomite

Carbon and sulfur analyses were performed on each of the three metallic catalysts and the dolomite catalyst both before and after the catalysis tests. Since all of the catalysts are inorganic, the appearance of carbon is an indication of coking. Likewise, the accumulation of sulfur on the metal catalyst indicates the breakthrough of hydrogen sulfide from the guard bed. The results are listed in Table 4-5.

Although the metallic catalysts were selected for their high resistance to carbon deposition, both the metallic and mineral catalysts accumulated carbon. However, the accumulation on the dolomite bed was 6–20 times greater than on the metallic catalysts, suggesting that the guard bed was doing its job of cracking the heaviest tar compounds, which are most likely to produce coking.

Steam/TOC ratios of 4–6 are typically used in Ni based catalytic steam reforming of naphtha. In our tests, the first several hours of testing for all the catalysts were performed without steam injection, that is, only steam arising from biomass gasification was present. This resulted in steam/TOC ratios of only 2.8. In an effort to remove coke accumulated after 18 h of testing, the steam/TOC ratio of the producer gas was increased to 4–6 for the last 6 h of testing of the Z409 and RZ409 catalysts. Although higher steam levels may enhance destruction of hydrocarbons absorbed on the catalysts, we saw no evidence that coke already deposited was readily removed by the steam/carbon reaction of Eq. 4.2.

We hoped that the calcined dolomite in the guard bed would absorb most of the hydrogen sulfide existing in the producer gas. However, the appearance of sulfur in all the samples of used metallic catalysts and the relatively low concentration of sulfur in the used dolomite indicates significant breakthrough of hydrogen sulfide from the guard bed. In fact, the high concentration of sulfur in the used ICI46-1 catalyst (0.4 wt% after 12 h without steam injection) indicates a very serious problem. However, relatively little sulfur accumulated on the used Z409 and RZ409 catalysts, which were subjected to steam injection for the last 6 h of testing. This observation suggests that steam injection can regenerate metallic catalysts that have been poisoned by sulfur. The regenerative process may consist of the following three reactions:

$$NiS + H_2O \rightarrow NiO + H_2S \quad (4.3)$$

$$NiO + H_2 \rightarrow Ni + H_2O \quad (4.4)$$

$$NiO + CO \rightarrow Ni + CO_2 \quad (4.5)$$

After as little as 6–8 h of testing, a white powder was found in the tar sampling line after the catalytic reactor. This proved that dolomite had attrite in the guard bed and blown through the slipstream line. Clearly, the strength of catalytic material for the guard bed needs to be improved.

4.4 Summary

A tar conversion system consisting of a guard bed and catalytic reactor was designed for the purpose of improving the quality of producer gas from an air blown, fluidized bed biomass gasifier. All three metal catalysts (ICI46-1, Z409 and RZ409) proved effective in eliminating heavy tars (> 99% destruction efficiency) and in increasing hydrogen concentration by 6–11 vol% (dry basis). Space velocity had little effect on gas composition while increasing temperature boosted hydrogen yield and reduced light hydrocarbons (CH_4 and C_2H_4), thus suggesting tar destruction is controlled by chemical kinetics.

Although the reactivity of the tar conversion system did not diminish during the 12–18 h of testing, measurements of surface area and pore size distribution indicated the conversion of small pores into larger pores during high temperature operation. If this transformation were to continue, the catalytic activity would eventually degrade. Furthermore, coke accumulated on both the dolomite and metallic catalysts, although this might have been mitigated if higher steam/TOC ratios had been employed from the beginning of the tests.

Significant breakthrough of hydrogen sulfide from the guard bed occurred. However, relatively little sulfur accumulated on the Z409 and RZ409 catalysts, which were subjected to steam injection for the last 6 h of testing. This observation suggests that steam injection can regenerate metallic catalysts that have been poisoned by sulfur.

Table 4-1. Chemical characterization of obsolete seed corn used as fuel

	Proximate analysis				Ultimate analysis[a]				
Seed corn	Moisture	Volatile matter	Fixed carbon	Ash	C	H	N	S	O[a]
As Received.	9.0	77.9	11.7	1.4	41.7	6.4	1.1	0.1	49.2
Dry	0.0	85.6	12.9	1.5	45.8	6.0	1.2	0.1	45.4

[a] oxygen determined by difference.

Table 4-2. Chemical composition of tested catalysts

Catalyst	Active component	Promoter	Carrier	Preparation
ICI46-1	NiO	CaO, K_2O	SiO_2, Al_2O_3	Not reduced
Z409	NiO	MgO, K_2O, FeO*x*	SiO_2, Al_2O_3	Not reduced
RZ409	NiO	MgO, K_2O, FeO*x*	SiO_2, Al_2O_3	Reduced

Table 4-3. Operating parameters for catalytic reactors

Parameter	ICI46-1	Z409	RZ409
Amount of calcined dolomite (guard bed reactor)	120 mL (132.16 g)	120 mL (132.10 g)	120 mL (132.10 g)
Amount of Ni based catalyst (metal catalyst reactor)	20 mL (22.30 g)	20 mL (23.24 g)	20 mL (23.10 g)
Amount of inert material (metal catalyst reactor)	20 mL (15.30 g)	20 mL (15.20 g)	20 mL (15.40 g)
Pretreatment of catalyst	No reduction	No reduction	Pre-reduced by manufacturer
Guard bed temperature, T_{GB} (±5 ℃)	650	650	650
Catalytic reactor temperature, T_{CR} (±3 ℃)	740 - 820	740 - 820	740 - 820
Space velocity—dry gas basis (h^{-1})	1500 to 6000	1500 to 6000	1500 to 6000
Operating time without steam injection (h)	12 (S/C = 2.8)	12 (S/C = 2.8)	12 (S/C = 2.8)
Operating time with steam injection (h)	0	6 (S/C = 4.5, 5.5, 6.5)	6 (S/C = 4.5, 5.5, 6.5)

Table 4-4. Pore volume, specific surface and pore size distribution of catalyst samples (by mercury porosimetry)

Sample no.	Pore volume ($cm^3 g^{-1}$)	Specific surface ($m^2 g^{-1}$)	Distribution of pore radius (%)			
			R < 100 Å	100–500 Å	500–2000 Å	R > 2000 Å
Fresh ICI46-1	0.17	16.5	13	32	26	29
Used ICI46-1	0.21	16.2	10	18	37	35
Fresh Z409	0.14	22.9	34	38	22	6
Used Z409	0.23	16.0	9	28	49	14
Fresh RZ409	0.18	23.3	28	34	34	4
Used RZ409	0.21	14.8	11	24	43	22

Table 4-5. Carbon and sulfur analysis of metallic catalysts and dolomite

Sample	S (wt%)	C (wt%)	Condition
Fresh ICI46-1	0.016	~0	Fresh
Used ICI46-1	0.4	0.36	12 h run (no injected steam)
Fresh Z409	0.013	~0	Fresh catalyst
Used Z409	0.021	0.80	18 + 6 h with injected steam
Fresh RZ409	0.018	~0	Fresh catalyst
Used RZ409	0.019	1.04	18 + 6 h with injected steam
Fresh dolomite	0.0084	~0	Fresh
Used dolomite 1	0.014	7.26	12 h (no injected steam)
Used dolomite 2	0.012	6.46	18 h (no injected steam)
Used dolomite 3	0.013	6.76	18 h (no injected steam)

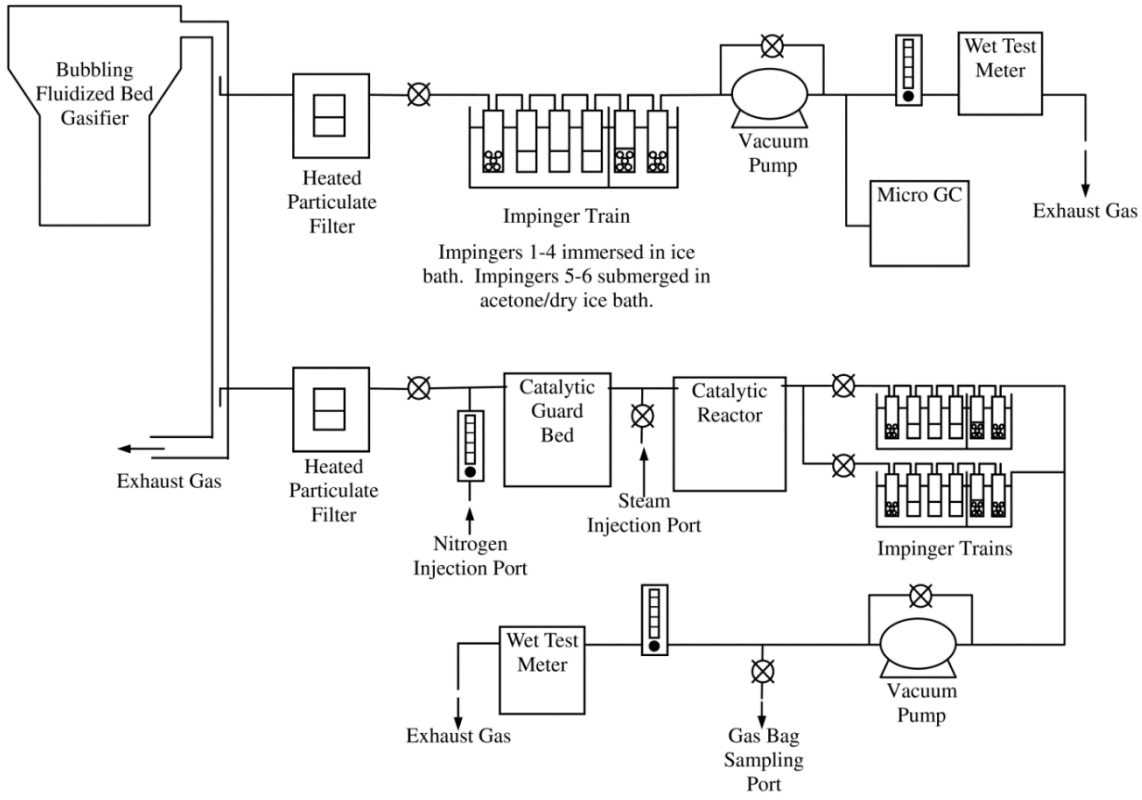

Figure 4-1. Schematic of overall experimental apparatus

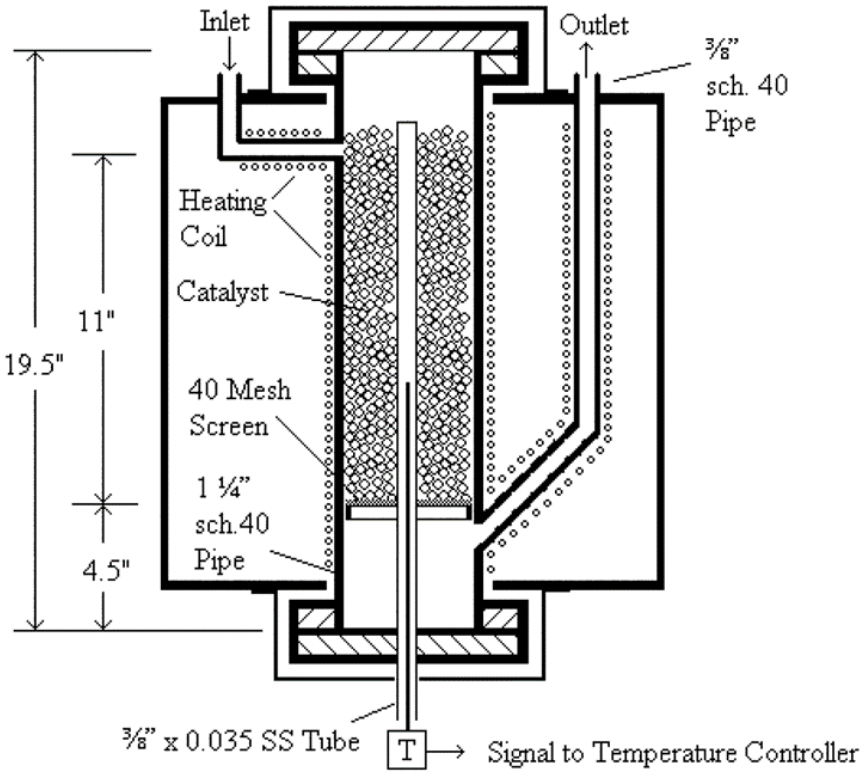

Figure 4-2. Catalytic reactor

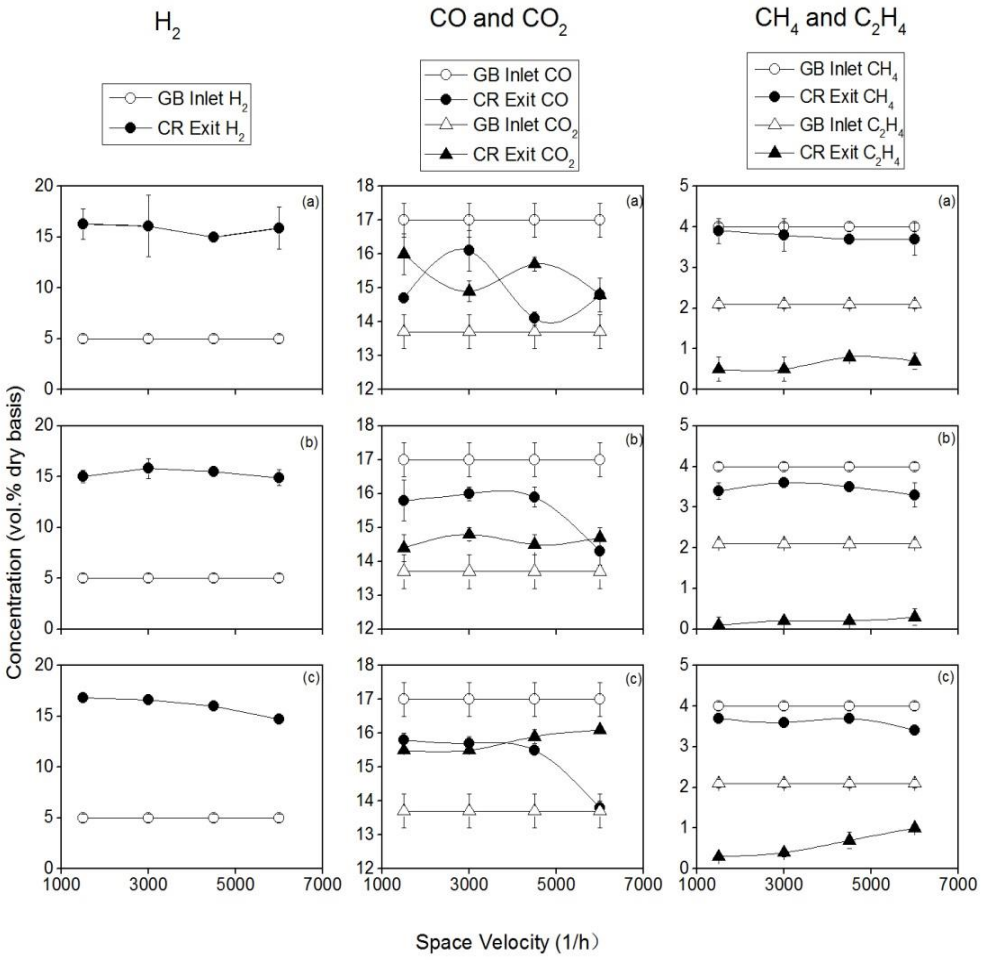

Figure 4-3. Concentrations in producer gas at the inlet of the guard bed and the exit of catalytic bed as a function of space velocity: TGB = 650 ℃; TCR = 800 ℃; steam/TOC = 2.8. (a) ICI46-1, (b) Z409, (c) RZ409

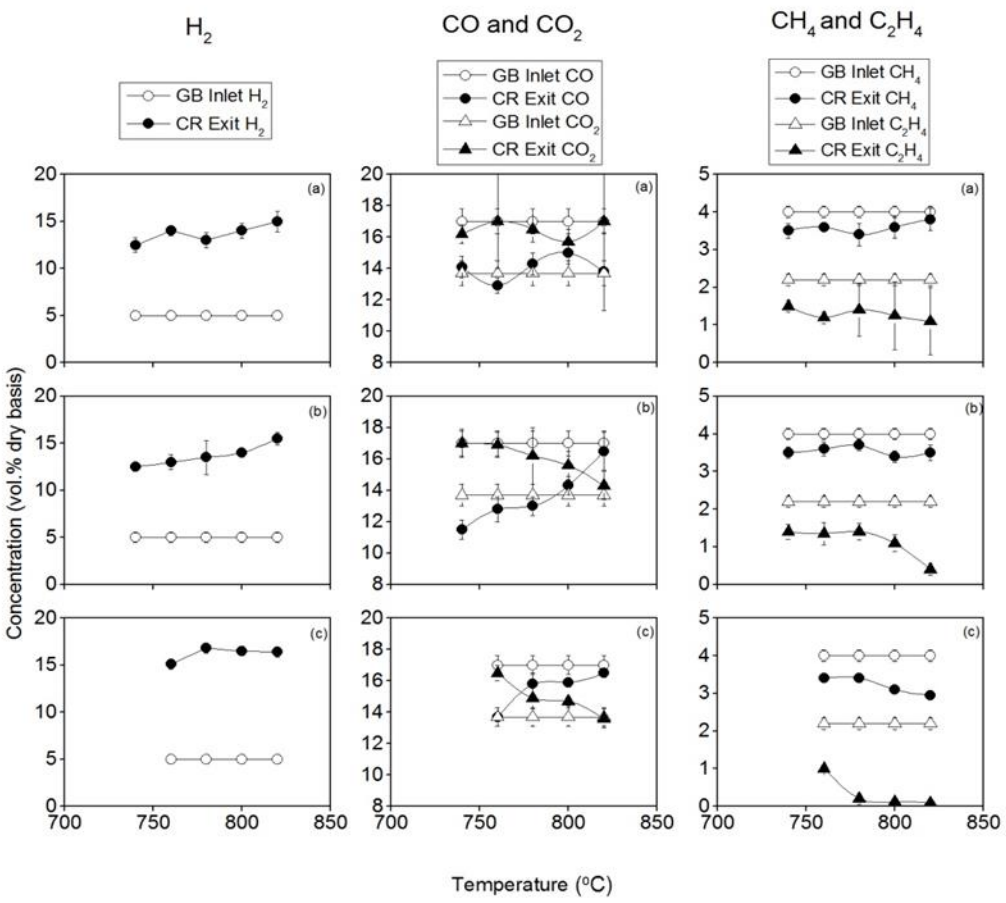

Figure 4-4. Concentration in the producer gas at the inlet of the guard bed and the exit of catalytic bed as a function of catalytic bed temperature: TGB = 650 ℃; SV = 3000 h^{-1}; steam/TOC = 2.8. (a) ICI46-1, (b) Z409, (c) RZ409

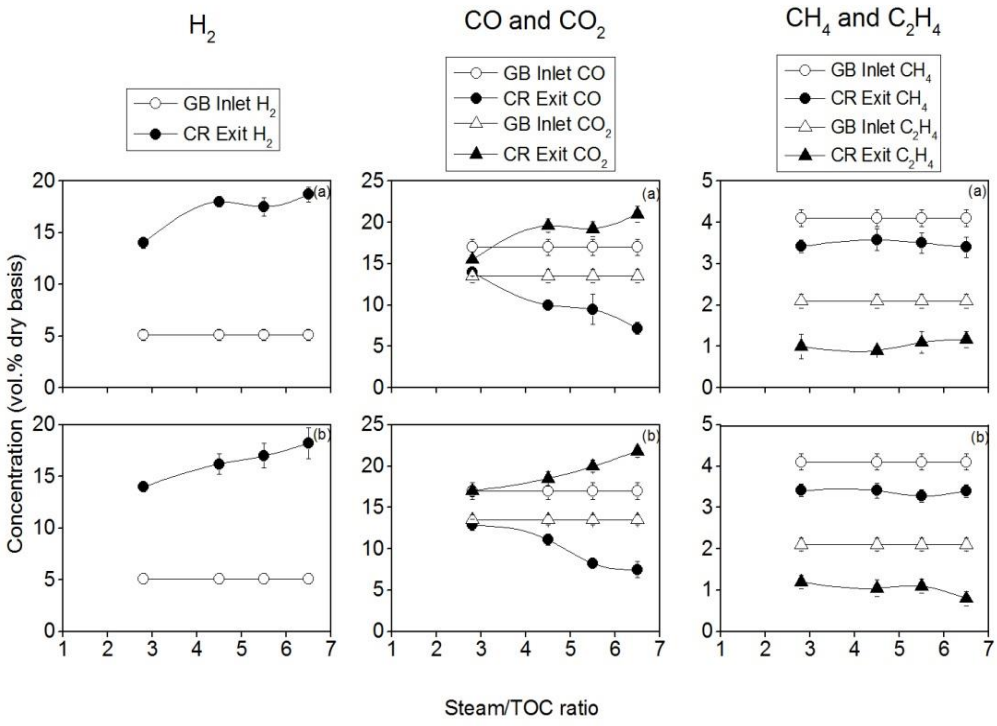

Figure 4-5. H_2 concentration in producer gas at the inlet of the guard bed and the exit of catalytic bed as a function of steam/TOC ratio: TGB = 650 ℃; TCR = 800 ℃; SV = 3000 h^{-1}. (a) Z409, (b) RZ409

Chapter 5 Generation of Hydrogen from Switchgrass and Seed Corn from an Air-blown Fluidized Gasifier

5.1 Introduction

The gasification of renewable materials provides one of the most cost-competitive means of obtaining hydrogen gas from renewable resources (Milne et al., 1998). Because it is produced thermochemically, it offers good prospects for market integration with conventional petrochemical industries (Baker et al., 1985).

A hydrogen economy will most likely be based on fuel cells, which requires high-purity hydrogen for their reliable operation. Gasification of biomass produces a number of contaminants including tars and trace levels of nitrogen, sulfur, and chlorine compounds that must be removed, not only for end use applications, but to prevent poisoning of catalysts used in steam reforming, water–gas shift reactions, and gas separation. Gas cleaning technologies are under development for removing dust, absorbing trace contaminants, and converting the condensable tar to low molecular weight gases to render the gas acceptable for fuel cells.

The traditional method of gas cleaning by means of wet scrubbing not only wastes the chemical energy of the tar but also poses environmental pollution problems that are not easily resolvable. In the previous work (Baker et al., 1985), a tar cracking system consisting of a guard bed and reforming catalytic reactor was designed for the purpose of improving the quality of producer gas from an air-blown, fluidized bed biomass gasifier. Steam reforming of tar increases both the hydrogen (H_2) and carbon monoxide (CO) content of the producer gas.

Further increases in hydrogen content can be achieved via the water–gas shift reaction:

$$CO + H_2O \leftrightarrow CO_2 + H_2 \qquad \Delta H = -41.1 \text{ kJ mol}^{-1} \qquad (5.1)$$

This reaction is widely used to adjust the CO/H_2 ratio of producer gas prior to the manufacture of ammonia and methanol. Water–gas shift catalysts have been commercially developed for use by the petrochemical industry (Corella, 1996; Zhou et al., 1999).

Presently, there is renewed interest in the water–gas shift reaction because of its importance in reforming fuels to hydrogen for use in fuel cells. Since biomass gasification yields relatively high CO/H_2 ratios, higher H_2 contents can be achieved by using commercial CO shift catalysts in two fixed bed reactors operated in series: a high-temperature shift (HTS) reactor for rapid reaction and a low-temperature shift reactor to shift thermodynamic equilibrium to very low levels of CO. The high-temperature shift reaction takes advantage of faster kinetics at elevated temperatures to convert about 75% of the CO into H_2. Conversion is,

however, limited by thermodynamic equilibrium, which favors hydrogen formation at low temperatures. Accordingly, the gas is slightly cooled and passed through a second, low-temperature shift reactor to convert most of the remaining CO to H_2.

The goal of this research is to increase the concentration of hydrogen in producer gas that has been obtained from air-blown gasification of biomass. The steam reforming system evaluated in a previous study (Corella, 1988) is combined with a water–gas shift system to maximize hydrogen production. The effects of temperature, steam/gas ratio, and space velocity on hydrogen production are evaluated. At the completion of these tests, the deposition of carbon, chlorine, and sulfur on the catalysts was investigated.

5.2 Experimental apparatus and methodology

Tests were conducted in a pilot-scale fluidized bed reactor located at the Biomass Energy Conversion Facility (BECON) in Nevada, IA, which is operated by the Iowa Energy Center. The system is rated 800 kW thermal input, which corresponds to an average throughput of 180 kg h^{-1} of solid biomass fuel at a heating value of 16,000 kJ kg^{-1}. The major components of the plant include the fluidized bed reactor, fluidization gas system, fuel delivery system, data acquisition system, and gas sampling system. Details on the operation of the biomass gasifier can be found in Smeenk and Brown (1998). The fuel for these tests was discard seed corn or switchgrass. The composition is given in Table 5-1. It was gasified in air at an equivalence ratio between 0.25 and 0.35, which maintained the reactor in the temperature range of 700 to 760 ℃. The feed rate of seed corn during these tests was in the range of 160-200 kg h^{-1}.

A 5 L min^{-1} slipstream from the gasification stream, illustrated in Fig. 5-1, was used to evaluate gas cleaning and hydrogen enhancement. This catalytic reaction system includes a guard bed, a tar (steam reforming) reactor, and high- and low-temperature catalytic water–gas shift reactors. A series of gasification trials was performed to evaluate the efficiency of hydrogen production and CO conversion.

The four fixed bed reactors were of identical construction, fabricated from 22-mm ID stainless steel. Each was mounted in an electrically heated oven to maintain desired temperatures for each experiment. Each reactor had two thermocouples: one at the center of the fixed bed, which was moveable for obtaining longitudinal temperature profiles, and the other fixed at the center of catalytic bed, which was used for temperature control. The catalysts used in the reactors were sandwiched between layers of inert alumni spheres (4-mm diameter). Table

5-2 details operating conditions of the reactor, as well as the amount of inert material added above and below the catalyst in the reactor.

Water was fed by means of a micropump into a stainless-steel pipe heated to 150–240 ℃ for the purpose of generating steam to mix with the producer gas just prior to its entry into the steam reformer. Gas composition both upstream and downstream of the gas conditioning system was periodically analyzed by online gas chromatography using a Varian Micro-GC CP-2003 Quad equipped with Molsieve 5A BF, Poroplot Q, and CP-Sils CB columns, and a thermal conductivity detector with argon as carrier gas for the first column and helium as carrier gas for the second and third columns. The first column gave H_2, O_2, N_2, CH_4, and CO concentrations; the second and third columns yielded CO_2, C_2H_4, and some light hydrocarbons. Continuous monitoring of exit gases was achieved with non-dispersive infrared analyzers for CO and CO_2, a Nova thermal conductivity analyzer for H_2, and a California Analytic electrochemical sensor for O_2. The reliability of the analyzers was checked periodically using calibration gas. The volumetric flow rate of the dry gas exiting the gas conditioning system was measured by means of a wet test meter and converted to normal conditions. Since the focus of this work was the water–gas shift reactors, direct measurements of tar content in the producer gas were not performed, although previous work indicated that heavy tar in the raw producer gas was on the order of 20 g m^{-1} and steam reforming was able to reduce heavy tar to undetectable levels.

Analysis of the extent of conversion of CO by the water–gas shift reaction requires careful consideration of changes in mole fractions of the reacting gases. Although the water–gas shift reaction is an equal molar reaction, resulting in no net volume change, one must account for the fact that gas analysis is performed on a dry gas basis.

Let χ be defined as the molar conversion of CO:

$$\chi = \frac{n_{CO_{inlet}} - n_{CO_{outlet}}}{n_{CO_{inlet}}} \tag{5.1}$$

where n designates the number of moles of CO at the inlet or outlet of the reactor as appropriate. Since the water–gas shift reaction is equimolar, the total number of moles at the inlet and outlet of the reactor are equal, and it follows that:

$$\chi = \frac{X_{CO_{inlet}} - X_{CO_{outlet}}}{X_{CO_{inlet}}} \tag{5.2}$$

where X designates mole fractions based on water vapor being one of the constituents of the gas mixture. In practice, gas analysis is performed on dry gas, the water vapor having been removed from the gas mixture before analysis; thus, it is convenient to define mole fractions that are based on moles of dry gas:

$$\chi'_{CO} = \frac{n_{CO}}{n_{DG}} \tag{5.3}$$

where n_{DG} is the total moles of dry gas. Solving Eq. (5.3) for n_{CO}, substituting this expression into Eq. (5.1), and recognizing that the change in moles of dry gas through the reactor is equal to the change in moles of CO through the reactor, it can be shown that the molar conversion of CO expressed in terms of X_{CO} is:

$$\chi = \frac{X'_{CO_{inlet}} - X'_{CO_{outlet}}}{X'_{CO_{inlet}}(1 + X'_{CO_{outlet}})} \tag{5.4}$$

This formula was used to calculate CO conversions presented in the results.

The guard bed was designed to capture fine particulate, absorb hydrogen sulfide, and steam-reform some of the heavy tars in the producer gas. It plays an important role in protecting the nickel catalyst in the steam-reforming reactor, which is susceptible to coking by heavy tars and poisoning by hydrogen sulfide. Calcined dolomite was used in the guard bed reactor.

The tar reactor converts light tars into carbon monoxide and hydrogen. ICI 46-1, a Ni-based catalyst produced by Imperial Chemical Industry, was used in the steaming reforming tar reactor. A Fe–Cr-based LB catalyst, synthesized according to China National Patent No. ZL 96102477.1 (Zhang and Ma, 2000) was used in the high-temperature water–gas shift reactor. A Cu–Zn-based catalyst was used in the low-temperature shift reactor. The chemical compositions of the shift catalysts are given in Table 5-3.

All three catalysts were reduced prior to evaluation of catalytic activity. This was done by treating them with producer gas in the amount of 1 L min^{-1} along with steam injected at a steam/gas ratio of 0.8. The Ni-based ICI-46 catalyst in the tar reactor was reduced at a temperature of 700 ℃, while the Fe–Cr-based catalyst in the high-temperature shift reactor was reduced at 250 ℃, and the Cu–Zn-based catalyst in the low-temperature shift reactor was reduced at 180 ℃. Judging from the hydrogen content exiting the reactors, the Fe–Cr-based catalyst was substantially reduced after 20 min, while the Cu–Zn-based catalyst required 45 min. Reduction was assumed complete when the hydrogen concentration exiting the reactor stopped increasing and reached a steady-state concentration. The catalysts were readily reduced by producer gas without requiring the addition of hydrogen as a reducing agent.

Both fresh and spent catalysts were characterized by BET specific surface and porosity and by X-ray photoelectron spectroscopy (XPS). Analysis by XPS was performed to check for coking and poisoning of the catalysts by chlorine and sulfur. Specific surface area and porosity were tested using ASAP 2010 with analysis adsorptive N_2 at 77.35 K.

Analysis by XPS was performed using a Physical Electronics 5500 Multitechnique system with monochromatic Al and standard Mg/Al sources using sample sizes of less than 2 ×2 cm.

5.3. Results and discussion

5.3.1 Seed corn

Producer gas was passed through the gas conditioning system at flow rates of 3–5 L min^{-1}, with steam added to achieve steam/gas ratios between 0.6 and 1.1. The raw producer gas entering the system had nominal composition as follows: H_2 at 5–9 vol%, CO at 13–16 vol%, CO_2 at 14–17 vol%, CH_4 at 4 vol%, and C_2H_4 at less than 2.0 vol%. The guard bed was operated at a temperature TGB equal to 650 ℃, while the steam reformer (tar reactor) was operated at a temperature TTR equal to 800 ℃. Exiting the tar reactor, typical gas compositions were H_2 at 17–21 vol%, CO at 6–13 vol%, CO_2 at 17–21 vol%, CH_4 at 3.5 vol%, and C_2H_4 at less than 0.6 vol%, which were dependent on the steam/gas ratio. The combination of guard bed and tar reactor was effective in boosting hydrogen and substantially reducing CO, CH_4, and C_2H_4. Producer gas exiting the tar reactor entered sequentially the high-temperature and low-temperature water–gas reactors, where the effects of volumetric flow rate, steam/gas ratio, and reactor temperature were evaluated.

The effect of space velocity on performance of the high-temperature shift (HTS) reactor was investigated for baseline conditions of TTR = 800 ℃, THTS = 350 ℃, and steam gas ratio S/G = 0.9. Three flow rates were tested: 2.6, 3.8, and 4.6 L min^{-1}, which represent space velocity varying from 1350 to 2300 h^{-1}. As shown in Table 5-4, CO content was reduced from 6.7 vol% to less than 2.7 vol%, while H_2 increased from 17.8 vol% to as high as 28.1 vol%. CH_4 and C_2H_4 had almost no concentration change through the high-temperature reactor.

The effect of temperature on performance of the high-temperature shift reactor was conducted for baseline conditions of TTR = 800 ℃, S/G = 0.7, SV = 1950 h^{-1}. Four temperatures were investigated: 360, 380, 420, and 440 ℃. As shown in Table 5-5, CO content was reduced from 8.4 vol% to less than 2.6 vol%. The extent of CO conversion was around 80% independent of temperature. Hydrogen content increased from 20 to 28 vol%.

The effect of steam/gas ratio on performance of the high-temperature shift reactor was conducted under baseline conditions of TTR = 800 ℃, THTS = 400 ℃, SV = 1950 h^{-1}. Four steam/gas ratios were evaluated: 1.09, 0.73, 0.67, and 0.6. Since both injected steam and steam generated from gasification of biomass contributed to the total steam, the steam/gas ratio was determined from the amount of steam condensed from the gas exiting the water–gas shift reactor system. As shown in Table 5-6, CO content was reduced at the outlets of both the tar reactor and the high-temperature shift reactor as a result of steam addition. Carbon monoxide in the raw producer gas was reduced from 13.3 vol% to as little as 1.0 vol% by the combined action of the tar reactor and the high-temperature shift reactor, with about 60% of this change arising from the tar reactor. CO conversions were more than 75%. High levels of steam clearly enhanced the water–gas shift reaction. Steam levels had little effect on CH_4 and C_2H_4 concentrations.

The effect of space velocity on performance of the low-temperature shift reactor was conducted under baseline conditions of TTR = 800 ℃, THTS = 400 ℃, TLTS = 210 ℃, and S/G = 0.8. The effect of volumetric flow rates was determined for flows of 2.0, 3.0, and 4.0 L min^{-1}, representing a range of space velocities between 800 to 1600 h^{-1}. As shown in Fig. 5-2, CO concentration dropped dramatically between the exit of the tar reactor and the exit of the low-temperature water–gas shift reactor. However, space velocity had negligible effect on the CO concentration exiting the low-temperature water–gas shift reactor.

The effect of temperature on performance of the low-temperature shift reactor was conducted under baseline conditions of TTR = 800 ℃, THTS = 400 ℃, S/G = 0.8, SV = 1200 h^{-1}. Four reactor temperatures were evaluated: 180, 200, 220, and 240 ℃. As shown in Table 5-8, CO concentration exiting the low-temperature water–gas shift reactor was as low as 0.20 vol% at 180 ℃ increasing to 0.46 vol% as the temperature was raised to 240 ℃, a result in accordance with an exothermic reaction. Overall, CO conversion of 95% is possible, and H2 concentrations in air-blown producer gas can reach 29.5 vol%.

The effect of steam/gas ratio on performance of the low-temperature shift reactor was conducted under baseline conditions of TTR = 800 ℃, THTS = 400 ℃, TLTS = 210 ℃, SV = 1200 h^{-1}. Four steam/gas ratios were evaluated: 1.20, 0.85, 0.54, and 0.32. As shown in Table 5-9, the performance of the low-temperature shift reactor in reducing CO in the producer gas was strongly dependent on steam/gas ratio, reaching 0.19 vol% CO for S/G of 1.2.

Atomic concentrations (mol%) of carbon, oxygen, sulfur, chlorine, and metals found on fresh and spent catalysts as determined by XPS are summarized in Table 5-10. Figures 5-2 to

5-4 illustrate the XPS of carbon, sulfur, and chlorine for the Ni catalyst, Fe–Cr catalyst, and Cu–Zn catalyst, respectively.

Comparison of fresh and spent catalysts indicates that carbon accumulated on all three kinds of catalysts to some extent. Coking was most serious on the Cu–Zn catalyst, where the relative amount of carbon almost doubled during the gasification test (Fig. 5-4). Coking on the Ni catalyst was also serious, with carbon content increasing by nearly 30%. Accumulation of sulfur of atomic concentration on the catalysts was less than 0.5 mol%, while chlorine accumulation represented 1.0 to 2.0 mol%. Clearly, some hydrogen chloride and hydrogen sulfide in the raw producer gas broke through the guard bed and deposited on the catalysts. Although the reactors did not show any evidence of catalyst deactivation, the design of the guard bed needs to be improved to protect the metal catalysts from these trace contaminants.

Table 5-11 summarizes the specific surface and average pore diameters of catalysts as determined by BET analysis. In all cases, specific surface area of spent catalysts greatly decreased compared to fresh catalysts. The average pore diameter of Ni-based catalyst decreased while it increased for the other two catalysts shown in Fig. 5-5 and Fig. 5-6, respectively. Figure 5-8 plots pore volume distributions for the three catalysts as determined by BJH adsorption (Barret et al., 1951), illustrating that pore volumes changed greatly during the tests. Generally, the micropores and mesopores decreased, while macropores remained relatively unchanged. These changes are probably the result of both the reduction of catalysts prior to tests, as well as from coking, which blocks pores with carbon.

5.3.2 Switchgrass

Table 5-12 presents gas composition at different points in the gas conditioning system. The raw producer gas entering the system contained 8.6 vol% H_2, 14.3 vol% CO, 18.0 vol% CO_2, 4.5 vol% CH_4, and 1.5 vol% C_2H_4. The producer gas contained about 19.5 g Nm^{-3} heavy tar with the average gas composition of 19.4 vol% H_2, 9.0 vol% CO, 20.5 vol% CO_2, 3.36 vol% CH_4, and 0.28 vol% C_2H_4. No condensable (heavy) tar was detectable at the exit of the steam reformer. As might be expected, the reaction between steam and tar increased the hydrogen content of the producer gas. Although steam reforming might also be expected to produce CO, this gas actually decreased 5.3 vol%, indicating that the water-gas shift reaction is occurring even at the elevated temperature of the steam reformer. The steam reformer substantially reduced the concentration of C_2H_4, but only moderately reduced CH_4. Although CH_4 is expected to be more resistant to catalytic cracking than C_2H_4, the most probable reason for its persistence arises from thermodynamic equilibrium of the steam reforming reaction for methane:

$$CH_4 + 2H_2O \rightarrow CO_2 + 4H_2 \quad (5.5)$$

This reaction is strongly endothermic and highly reversible. Thus, complete reaction favors high temperatures and low partial pressures of CO_2. At the operating conditions of the tar reactor in this study (750−850 °C, 20.5 vol% CO_2) a few percent of CH_4 in the product gas is not surprising. Temperatures approaching 1000 °C would be required to substantially reduce methane.

Exiting the high-temperature shift reactor, the average gas composition was 23.7 vol% H_2, 1.4 vol% CO, 26.8 vol% CO_2, 3.1 vol% CH_4, and 0.08 vol% C_2H_4. The high-temperature shift reactor reduced CO content by 7.6 vol%, representing 83% conversion. The concentration of CH_4 is essentially unchanged through the high-temperature shift reactor, while the concentration of C_2H_4 decreases substantially. The fact that CH_4 is essentially unchanged gives some confidence that the high-temperature shift reactor was operated with adequate steam. Otherwise, the Fe−Cr-based catalyst has a tendency to be over-reduced by H_2 and CO to form metallic iron, which catalyzes the methanation reaction:

$$CO + 3H_2 \rightarrow CH_4 + H_2O \quad (5.6)$$

Exiting the low-temperature shift reactor, the average gas composition was: 26.7 vol% H_2, 0.11 vol% CO, 27.4 vol% CO_2, 1.9 vol% CH_4, and 0.13 vol% C_2H_4. The total decrease in CO content through the shift-reactor system of 8.9 vol% represents an overall CO conversion of 99%. The overall increase in H_2 due to the combined action of the steam reforming and shift reactors is 18 vol%. Within the uncertainty of the measurements, the concentrations of CH_4 and C_2H_4 were not significantly affected through the low-temperature shift reactor.

Table 5-13 summarizes the atomic concentrations (mol%) of carbon, oxygen, sulfur, chlorine, and metals found on fresh and spent catalysts as determined by XPS. Comparison of fresh (Figs. 5-2 to 5-4) and spent catalysts indicates that carbon accumulated on all three kinds of catalysts to some extent. Coking was most serious on the Cu−Zn catalyst where the relative amount of carbon almost doubled during the gasification test. Coking on the Ni catalyst was also serious, with carbon content increasing by nearly 40%. Accumulation of sulfur of atomic concentration on the catalysts was less than 0.2 mol% while chlorine accumulation represented about 1.0 to 2.5 mol%. Clearly, some hydrogen chloride and hydrogen sulfide in the raw producer gas broke through the guard bed and deposited on the catalysts. Although the reactors did not show any evidence of catalyst deactivation, the design of the guard bed needs to be improved to protect the metal catalysts from these trace contaminants.

In all cases, the specific surface area of spent catalyst greatly decreased compared to fresh catalyst (Table 5-11). The average pore diameter of Ni-based catalyst decreased while it increased for the other two catalysts. Figures 5-5 to 5-7 plot pore volume distributions for the three catalysts as determined by BJH adsorption, illustrating that pore volumes changed greatly during the tests. Generally, the micropores and mesopores decreased while macropores remained relatively unchanged. These changes are probably the result of both the reduction of catalysts prior to tests and from coking, which blocks pores with carbon.

5.4 Summary

A catalytic reactor system was successfully tested with biomass-derived producer gas to determine its ability to steam reform tar and water–gas shift CO and steam to CO_2 and H_2. The catalytic tar reactor in combination with high-temperature and low-temperature water–gas shift reactors upgraded hydrogen in the raw gas from 5.8–8.8 vol% to as high as 27–29 vol%. Carbon monoxide concentration of 13–15 vol% in the raw gas was reduced to less than 0.5 vol%. The conversion of carbon monoxide in the high-temperature water–gas shift reached 75% to 80%, while CO conversion by the combination of high-temperature and low-temperature water–gas shift reactors exceeded 95%. The tar reactor did not significantly reform either CH_4 or C_2H_4. Hydrogen production in the steam reformer favored high steam-to-gas ratios and high temperatures but appeared to be independent of low space velocities. Hydrogen production in the high-temperature shift reactor favored high steam-to-gas ratios, high temperatures, and low space velocities. The highest H_2concentrations and the lowest CO concentrations exiting the low-temperature water–gas shift reactor occurred at the lowest reactor temperature, the lowest space velocity, and at a steam–gas ratio of 0.85.

Characterization of the catalysts by XPS showed that coke and small quantities of sulfur and chloride deposited on the catalysts. BET analysis revealed losses in micropores and mesopores. Although no sign of catalytic deactivation was evident during the tests, these changes indicate the need for improvements in the design of the guard bed.

Table 5-1. Chemical characterization of seed corn and switchgrass used as feedstock (in %)

	Proximate analysis				Ultimate analysis[a]				
Seed corn	Moisture	Volatile matter	Fixed carbon	Ash	C	H	N	S	O
As rec.	9.0	77.9	11.7	1.4	41.7	6.4	1.1	0.1	49.2
Dry	0.0	85.6	12.9	1.5	45.8	6.0	1.2	0.1	45.4
Switchgrass									
As rec.	3.2	79.9	13.3	3.6	42.4	5.3	0.6	0.1	48.1
Dry	0.0	82.6	13.8	3.6	43.8	5.1	0.6	0.1	46.7

[a] Oxygen determined by difference.

Table 5-2. Experimental conditions

	Guard bed (GB)	Tar steam reformer (TR)	High-temperature water–gas shift (HTS)	Low-temperature water–gas shift (LTS)
Control temperature (℃)	650	800	380 or 400	200 or 210
Temperature range (℃)	600–670	750–850	350–420	180–240
Space velocity (h^{-1})	900–1600	3000–6000	1500–2300	1000–1600
Catalyst	Calcined dolomite	ICI 46-1	Fe–Cr−based LB	Cu–Zn–Al-based B202
Catalyst volume (mL)	200	60	120	150
Inert material (mL mL^{-1})[a]	0/20	20/20	20/50	25/50

[a] Volume of inert material above and below catalyst layer, respectively.

Table 5-3. Composition of catalysts

Reactor system	Active components	Promoter	Binder	Trace contaminants
Ni-based ICI046-1	NiO	Cao, K_2O/SiO_2, Al_2O_3		
High-temperature shift	Fe_2O_3 78% ±2%	Cr_2O_3 9%±2% CuO 2.0% rare earth 1.5%	Black carbon 0.5%	S < 80 ppm Cl < 100 ppm
Low-temperature shift	CuO > 29%	ZnO 41–47% $Al_2O_3$8.1–10%		S < 1000 ppm Cl < 100 ppm

Table 5-4. Effect of space velocity on performance of HTS reactor (TTR = 800 ℃, THTS = 350 ℃, S/G = 0.9)

Gas constituent (vol%)	Raw gas	Exit of Tar steam reactor[a]	Exit of high-temperature shift reactor		
			1350 h^{-1}	1950 h^{-1}	2300 h^{-1}
H_2	5.8	17.8	28.1	26.6	25.1
CO	15.8	6.7	2.1	2.7	2.7
CO_2	14.4	19.9	26.8	26.4	25.8
CH_4	4.2	3.1	3.3	3.3	3.3
C_2H_4	2.0	0.6	0.3	0.3	0.3

[a] Previous study showed that space velocity (SV) does not substantially affect the performance of the tar steam reaction. Therefore, the measurements on the tar steam reactor were performed at only one SV of 1950 h^{-1} (3.8 L min^{-1}).

Table 5-5. Effect of temperature on performance of HTS reactor (T_{TR} = 800 ℃, S/G = 0.7, SV = 1950 h^{-1})

Gas constituent (vol%)	Raw gas	Exit of tar steam reactor	Exit of high-temperature shift reactor			
			360 ℃	380 ℃	420 ℃	440 ℃
H_2	7.74	19.85	27.78	28.48	28.3	28.14
CO	13.27	8.38	2.58	1.14	1.21	1.38
CO_2	16.69	20.71	27.40	27.80	27.82	27.72
CH_4	3.89	3.19	2.97	2.94	2.95	2.94
C_2H_4	1.71	0.26	0.22	0.22	0.22	0.22

Table 5-6. Effect of steam/gas ratio (S/G) on performance of HTS reactor (T_{TR} = 800 ℃, T_{HTS} = 400 ℃, SV = 1950 h^{-1})

Gas constituent (vol%)	Raw gas	Exit of tar reactor				Exit of high−temperature shift reactor			
		Steam/Gas				Steam/Gas			
		1.09	0.73	0.67	0.6	1.09	0.73	0.67	0.6
H_2	7.74	21.61	20.47	19.85	18.52	29.97	28.78	28.48	27.65
CO	13.27	5.42	7.22	8.38	10.21	1.02	1.22	1.39	2.03
CO_2	16.69	23.14	21.60	20.70	19.30	27.63	27.54	27.56	27.58
CH_4	3.89	3.05	3.17	3.19	3.24	2.94	2.95	2.94	2.95
C_2H_4	1.71	0.19	0.28	0.26	0.30	0.21	0.21	0.21	0.21

Table 5-7. Effect of space velocity on performance of LTS reactor (TTR = 800 ℃, TLTS = 210 ℃, S/G = 0.8)

Gas constituent (vol%)	Raw gas	Exit of tar steam reactor[a]	Exit of low-temperature shift reactor		
			800 h^{-1}	1200 h^{-1}	1600 h^{-1}
H_2	6.53	20.50	36.11	29.68	29.13
CO	14.18	8.04	0.4	0.43	0.49
CO_2	16.30	20.90	28.83	28.63	28.72
CH_4	4.04	3.17	2.97	2.97	2.97
C_2H_4	1.77	0.21	0.28	0.28	0.28

[a] Previous study showed that space velocity (SV) does not substantially affect the performance of the tar steam reaction. Therefore, the measurements on the tar steam reactor were performed at only one SV of 1200 h^{-1} (3.0 L min^{-1}).

Table 5-8. Effect of temperature on performance of LTS reactor (T_{TR} = 800 ℃, S/G = 0.8, SV = 1200 h^{-1})

Gas constituent (vol%)	Raw gas	Exit of tar steam reactor	Exit of low-temperature shift reactor			
			180 ℃	200 ℃	220 ℃	240 ℃
H_2	6.53	20.50	29.68	29.60	29.56	29.44
CO	14.18	8.04	0.20	0.31	0.37	0.46
CO_2	16.30	20.90	28.50	28.45	28.51	28.30
CH_4	4.04	3.17	2.97	2.97	2.98	2.98
C_2H_4	1.77	0.21	0.25	0.25	0.26	0.25

Table 5-9. Effect of steam/gas ratio (S/G) on performance of LTS reactor (TTR = 800 ℃, TLTS = 200 ℃, SV = 1200 h^{-1})

Gas constituent (vol%)	Raw gas	S/G (Exit of tar steam reactor)				S/G (Exit of low-temperature shift reactor)			
		1.2	0.85	0.54	0.32	1.2	0.85	0.54	0.32
H_2	8.81	23.86	23.53	22.80	21.07	27.83	28.1	27.75	27.51
CO	13.23	7.99	9.01	10.33	12.63	0.19	0.16	0.20	0.40
CO_2	17.01	20.85	20.41	19.38	17.37	27.20	27.04	26.90	26.70
CH_4	3.81	3.13	3.34	3.51	3.44	3.05	3.05	3.05	3.05
C_2H_4	1.69	0.30	0.26	0.22	0.20	0.24	0.24	0.24	0.24

Table 5-10. Concentrations of atomic species (mol%) in the catalysts as determined by X-ray photoelectron spectroscopy (XPS) (feedstock seed corn)

	Ni-based catalyst		Fe–Cr-based catalyst		Cu–Zn-based catalyst	
	Fresh	Spent	Fresh	Spent	Fresh	Spent
Carbon C1s	10.16	13.14	18.27	18.76	12.29	22.91
Oxygen O1s	59.78	54.59	49.96	48.96	46.33	48.10
Sulfur S_2p	0.00	0.02	0.03	0.49	0.07	0.12
Chlorine Cl_2p	0.29	1.09	1.00	1.23	2.12	4.49
Aluminum Al_2p	14.50	15.27	–	–	–	–
Nickel Ni_2p	8.51	8.65	–	–	–	–
Iron Fe_2p	–	–	27.25	23.76	–	–
Chromium Cr_2p	–	–	3.48	6.80	–	–
Copper Cu_2p	–	–	–	–	13.26	4.84
Zinc Zn_2p	–	–	–	–	25.93	19.54

Table 5-11. BET analysis of catalysts

	Ni-based catalyst			Fe–Cr-based catalyst		Cu–Zn-based catalyst		
	Fresh	Spent Switch-grass Seed Corn		Fresh	Spent Switch–grass Seed Corn	Fresh	Spent Switch-grass Seed Corn	
Specific surface (m^2 g^{-1})	18.1	5.7	5.3	131	34.3 37.4	108	77.8	88.4
Average diameter (Å)	129	113	110	61.6	192 155	59.9	83.2	37.4

Table 5-12. Gas Composition at various Locations in the Gas Conditioning System

Gas constituent (vol%)	Raw gas	Exit of tar steam reactor[a]	Exit of Low-temp shift	Exit of high-temp Shift
H_2	8.6	19.4	23.7	26.7
CO	14.3	9.0	1.4	0.1
CO_2	18.0	20.5	26.8	27.4
CH_4	4.5	3.4	3.1	1.9
C_2H_4	1.5	0.3	0.1	0.1

[a] Gas composition is dry basis (vol%) measured by gas chromotography

Table 5-13. Concentrations of atomic species (mol%) in the catalysts as determined by X-ray photoelectron spectroscopy (XPS) (feedstock switchgrass)

	Ni-based catalyst catalyst		Fe–Cr-based catalyst		Cu–Zn-based	
	Fresh	Spent	Fresh	Spent	Fresh	Spent
Carbon C1s	9.93	14.18	18.70	12.43	10.37	20.29
Oxygen O1s	60.61	52.44	49.60	46.31	46.49	41.60
Sulfur S_2p	0.00	0.15	0.05	0.14	0.51	0.38
Chlorine Cl_2p	0.23	0.34	0.92	2.55	2.17	2.32
Aluminum Al_2p	13.18	15.67				
Nickel Ni_2p	8.85	9.7				
Iron Fe_2p	–	–	27.30	32.23		
Chromium Cr_2p	–	–	3.43	6.33		
Copper Cu_2p	–	–	–	–	13.41	12.68
Zinc Zn_2p	–	–	–	–	27.06	22.73

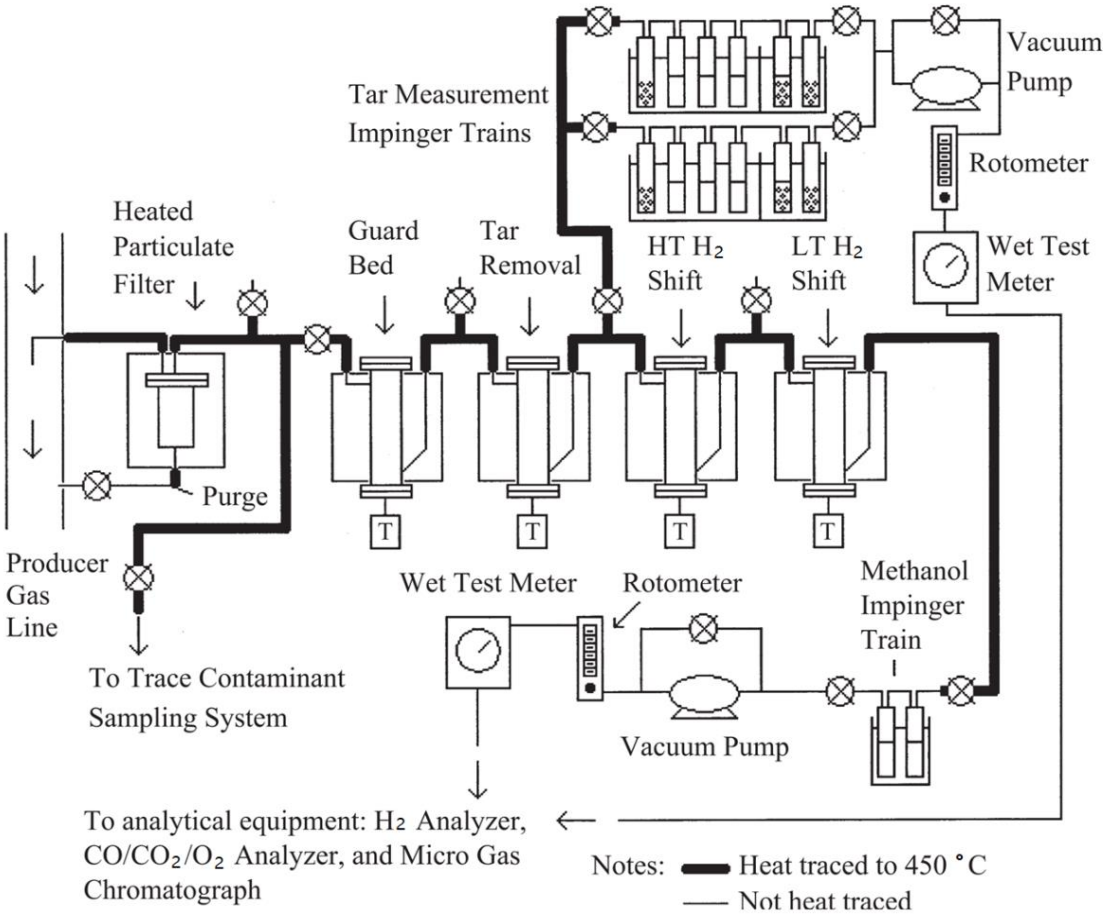

Figure 5-1. Diagram of the catalytic reaction system

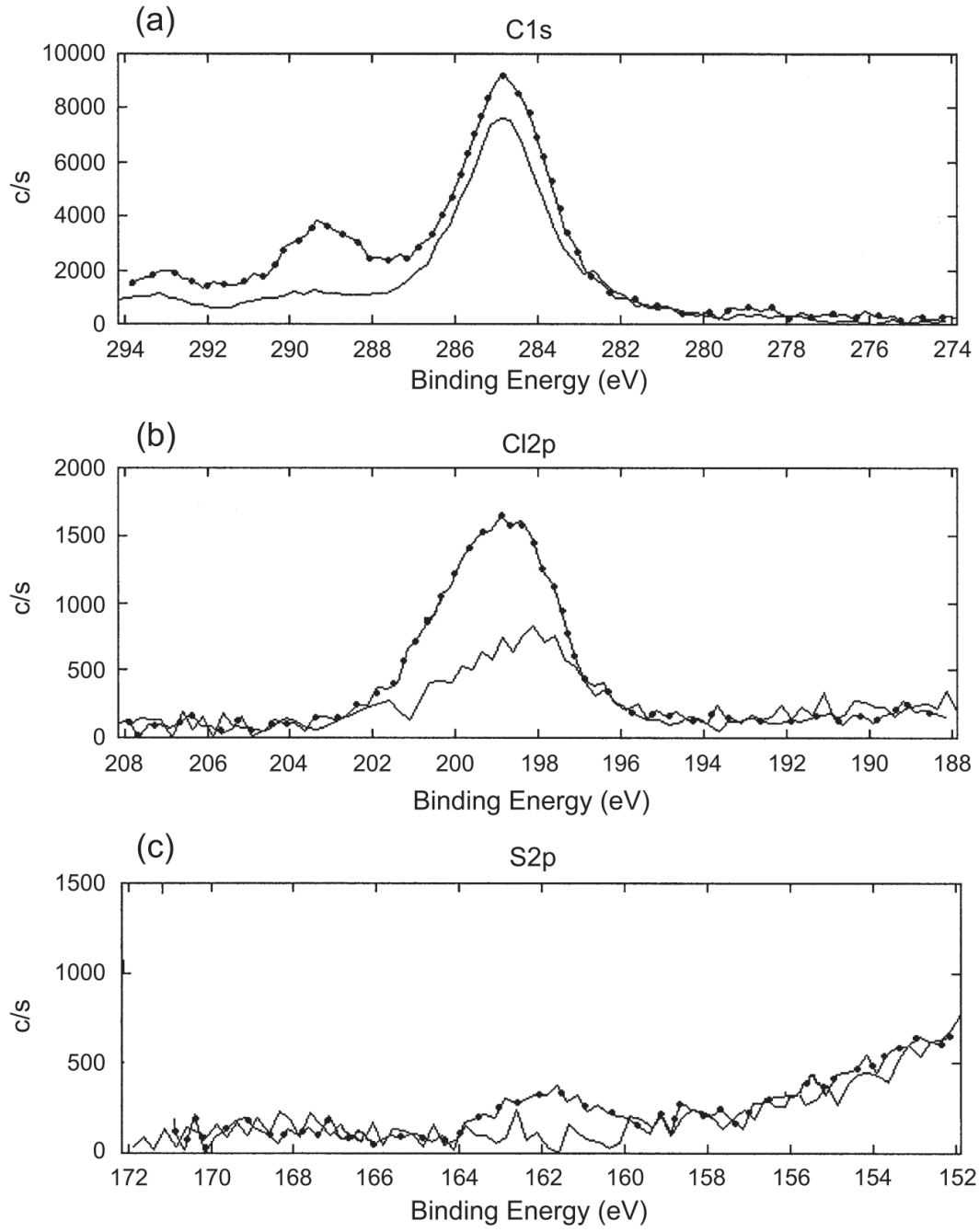

Figure 5-2. X-ray photoelectron spectra (XPS) of Ni-based catalysts using Physical Electronics 5500 equipped with Al Kα source (a) carbon 1s peak, (b) chlorine 2p peak, (c) sulfur 2p peak

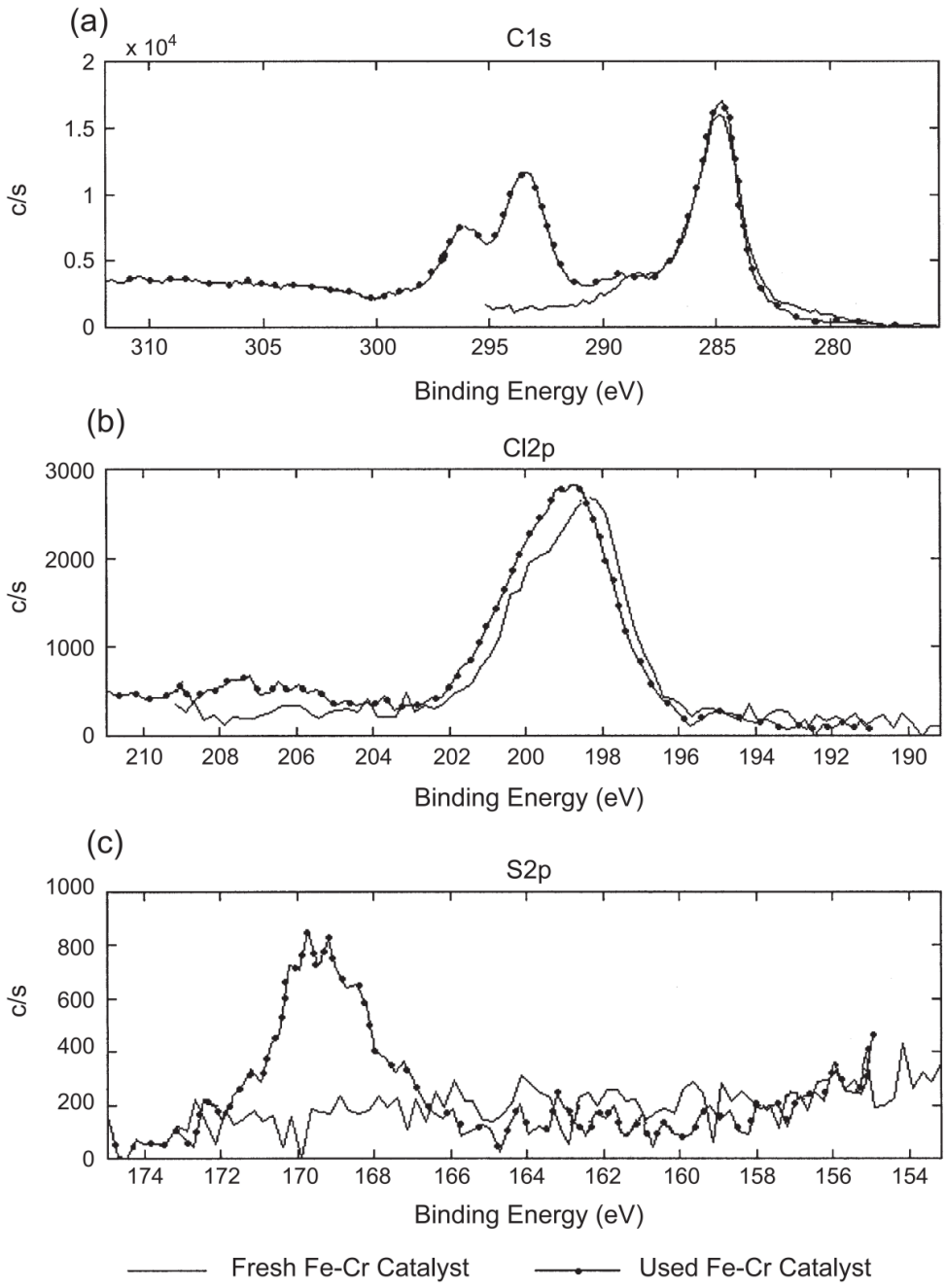

Figure 5-3. X-ray photoelectron spectra (XPS) of Fe–Cr-based catalysts using Physical Electronics 5500 equipped with Al Kα source (a) carbon 1s peak, (b) chlorine 2p peak, (c) sulfur 2p peak

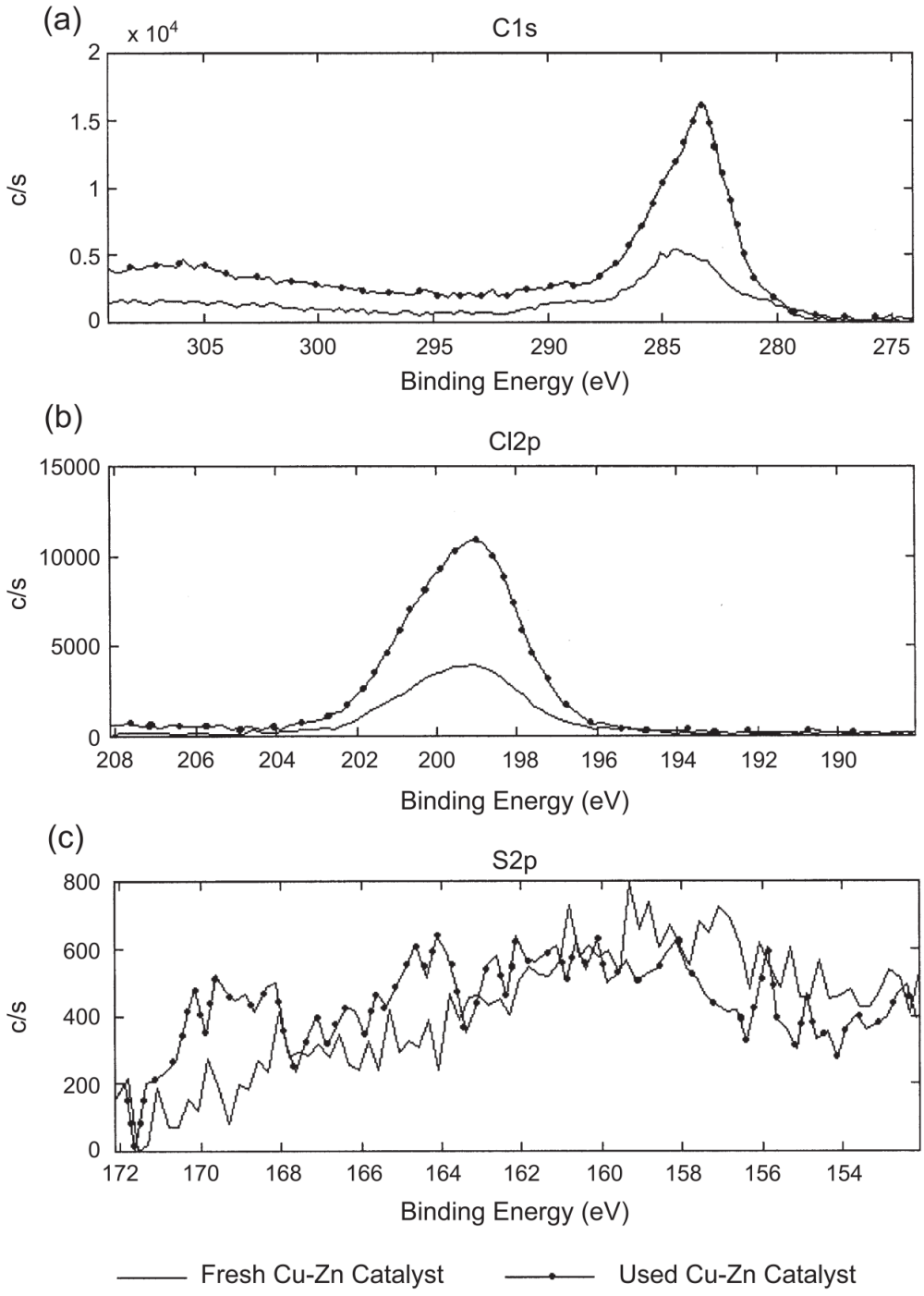

Figure 5-4. X-ray photoelectron spectroscopy (XPS) of Cu–Zn-based catalysts using Physical Electronics 5500 equipped with Al Kα source (a) carbon 1s peak, (b) chlorine 2p peak, (c) sulfur 2p peak

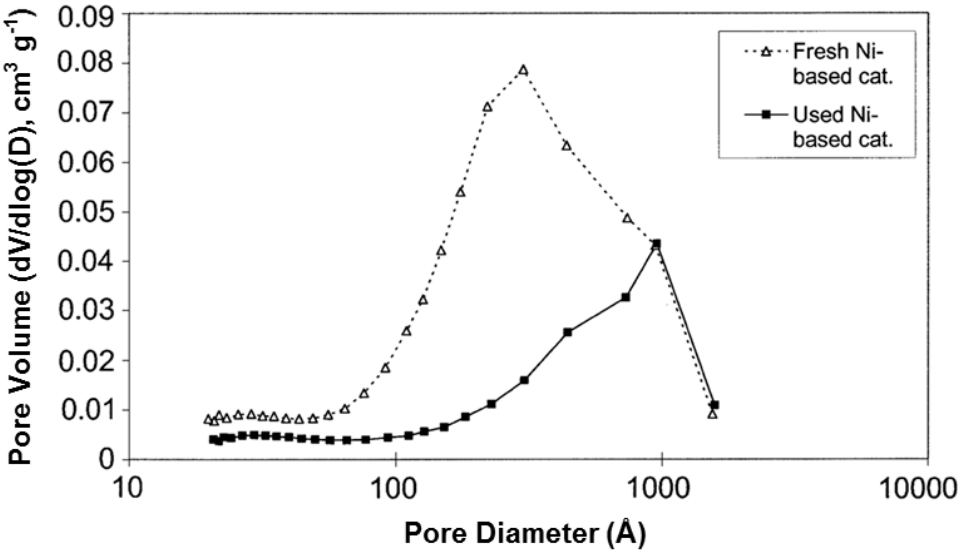

Figure 5-5. BJH pore volume dV/dlog D versus pore diameter of Ni-based catalyst

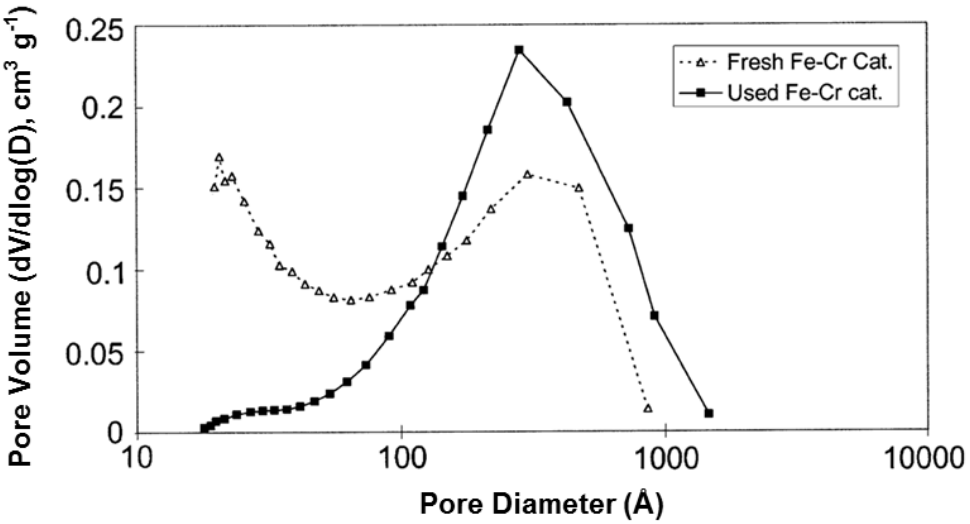

Figure 5-6. BJH pore volume dV/dlog D versus pore diameter of Fe–Cr-based catalyst

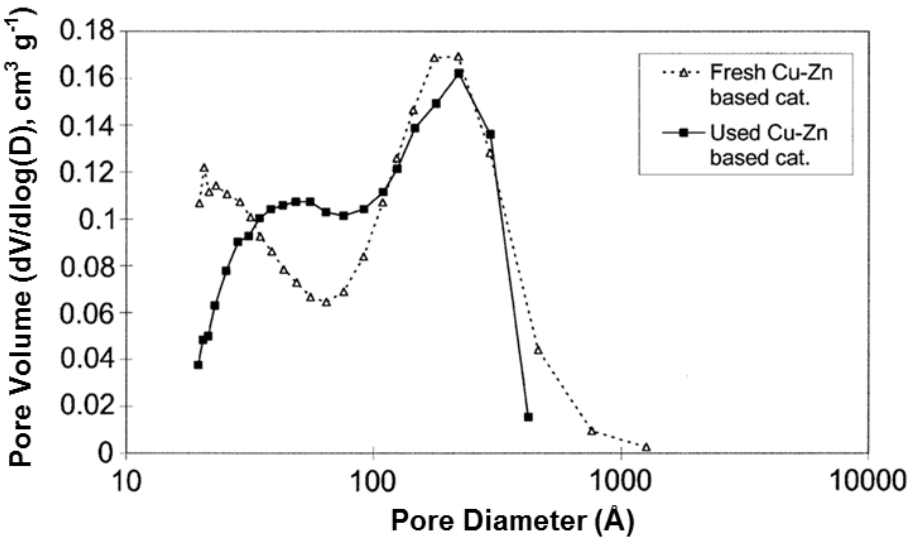

Figure 5-7. BJH pore volume dV/dlog D versus pore diameter of Cu–Zn-based catalyst.

Chapter 6 Conclusions and Future Research

6.1 Conclusions

In this study, catalytic conversion of tar by biomass gasification was conducted through steam reforming of model tar compound with Nickel based catalysts and with promoter of Ce and Mg to improve catalytic activity and coke resistance. The catalytic conversion of tar was also performed through hot cleaning system of two-bed systems to steam reforming of tar along with enhancing H_2 production. High H_2 production by biomass gasification is also realized through combining catalytic hot cleaning system with water-gas shift reactions. Conclusions from the present study can be drawn as follows:

(1) Catalytic conversion of tar is an efficient approach at lower temperatures achieving the most effective removing tars with the benefit of energy saving and better fuel value of producer gas from biomass gasification. The innovative catalytic hot cleaning system along with newly developed catalysts and optimized operating conditions surely enhances H_2 production.

(2) Nickel based catalysts are suitable for steam reforming of tar. Nickel based catalysts were prepared by wet impregnation method using olivine as a substrate for catalytic steam reforming of benzene in a bench scale fixed bed reactor at temperatures between 700 and 830 °C using a molar ratio of steam/carbon equal to 5. The results indicated that for all three catalysts used, the benzene conversions increased with increased temperature. However, benzene conversions by catalyst NiO/olivine doped with CeO_2 were much higher than those by two other catalysts at lower temperature due to that fact that doped CeO_2 increased the crystal oxygen on the surface and hence promoted the catalytic activity of nickel and resisted the deposition of the carbon through a redox mechanism. The mechanism of steam reforming involves the absorption of the target molecules and water vapor on the catalyst surface where they react until all carbon atoms are converted to CO or CO_2.

(3) The performance of Ce and Mg promoted Ni/olivine catalysts was better than that of only Ce promoter and Ni/olivine alone. The addition of 1% Mg to 3% Ni–1%Ce/olivine also increased reaction activity (toluene conversion up to 93%), prevented coke deposition, and was resistant to H_2S poison. Furthermore, Ni–Ce–Mg/olivine was resistant to deactivation due to its resistance to carbon deposition and 10 ppm H_2S poison at 100 mL min^{-1} up to 400 min. It is

suggested that 3% Ni-1%Ce-1% Mg/olivine is the most promising catalyst due to its minimum coke amount and the lower activation energy of coke burning as well as the high durability.

(4) A guard bed and catalytic reactor to treat the producer gas from an air blown, fluidized bed biomass gasifier showed promising results. The guard bed used dolomite to crack the heavy tars. The catalytic reactor was used to evaluate three commercial steam reforming catalysts (ICI46-1, Z409 and RZ409). All three commercial NiO based catalysts proved to be effective in eliminating heavy tars (> 99% destruction efficiency) and in increasing hydrogen concentration by 6–11 vol%. Space velocity had little effect on gas composition while increasing temperature boosted hydrogen yield and reduced light hydrocarbons (CH_4 and C_2H_4), thus suggesting tar destruction is controlled by chemical kinetics.

(5) Air-blown gasification of biomass in fluidized bed reactors produces relatively low concentrations of hydrogen (about 8 vol%). Steam reforming of tars and light hydrocarbons and reacting steam with carbon monoxide via the water–gas shift reaction can increase hydrogen content in the producer gas to 27-30 vol% through the system of catalytic hot cleaning system combining with two water-gas shift reactors. In the tests, the temperature, space velocity, and steam/gas ratio were varied to determine the effect of these variables on hydrogen production.

6.2 Future research perspective

With hundreds, if not thousands, of papers published, in the gasification field, detailed information for understanding the overall process is available. Unfortunately, by the nature of the gasification process as well as the feedstock composition, the formation of tar and other catalyst-fouling causing substances is unavoidable. This leads to catalyst deactivation which hinders full-scale commercial application. The improved technologies include innovative process design and proper operation of gasifiers to reduce tar formation along with newly developed catalysts that resist tar formation and other catalyst-deactivated causing substances; these advances coupled with the high demand for energy worldwide undoubtedly will further spur interest and technology and process development in the gasification field. The innovative gasifiers along with newly developed catalysts and optimized operating conditions surely will enhance H_2 production.

The removal or purification of catalyst-deactivated causing substances in the current "wet/dry scrubber systems" (*end of pipe treatment*) is not sufficient. One needs development of novel catalysts for efficient and cost-effective elimination of these undesirable substances. Still

a better approach is to reduce their presence by reducing impurities from the feedstock (*source control*) and taking advantage of different operational practices and process and reactor designs in gasifiers to reduce these undesirable compounds (*cleaner production*). Also, a better comprehension of deactivation mechanisms at the molecular level is essential for enhancing resistance from catalyst-deactivated causing substances in the development of new catalysts. The catalyst deactivation is unavoidable with regeneration of catalysts a key aspect in prolonging the lifespan and reducing costs associated with gasification. Therefore, the research in the area of regeneration and eventual recovery of precious metals in the spent catalysts needs further investigation – not only from cost consideration, but also from resource conservation and minimization of potential environmental impacts.

One of the main deterrents to the use of biomass in the waste-to-energy industry is the costs associated with it. Improvements in the refining technologies, including both reactor design and catalysts, syngas yield would be improved and the cost of gasification to obtain high energy gases would be significantly reduced. Two important studies are recommended in the future.

(1) It is necessary to build pilot facilities to test the catalytic hot gas cleaning system to achieve the potential for producing syngas and hydrogen from biomass gasification. And the assessment of its feasibility of technology and economy should be done for commercial purpose.

(2) The hybrid of thermal conversion and biochemical method should be evaluated with syngas fermentation to produces cellulosic ethanol or other fuels and chemicals via microbial reactions. Syngas fermentation also has advantages compared to other gasification-based catalytic conversion technologies, including high yield, low operating costs, and tolerance to impurities including a wider range of $CO:H_2$ ratios.

References

Abu El-Rub, Z., Bramer, E.A., Brem, G., 2002. Tar removal in an entrained flow cracker (EFC) with application to biomass gasification. In: Proceedings of Expert Meeting on Pyrolysis and Gasification of Biomass and Waste. p. 337–346.

Abu El-Rub, Z., Bramer, E.A., Brem, G., 2004. Review of catalysts for tar elimination in biomass gasification processes. Ind. Eng. Chem. Res. 43, 6911–6919.

Abu El-Rub, Z., Bramer, E.A., Brem, G., 2008. Experimental comparison of biomass chars with other catalysts for tar reduction. Fuel 87, 2243-2252.

Alden, H., Espenas, B.G., Rensfelt, E., 1988. Conversion of tar in pyrolysis gas from wood using a fixed dolomite bed. In: Bridgwater, A.V., Kuester, J.L. (Eds.), Research in Thermochemical Biomass Conversion, Elsevier Applied Science, London, pp. 987–1001.

Alstrup, I., Rostrup-Nielsen, J.R., Røen, S., 1981. High temperature hydrogen sulfide chemisorption on nickel catalysts. Appl. Catal. 1, 303–314.

Alvin, M.A., 1998. Impact of char and ash fines on porous ceramic filter life. Fuel Process. Technol. 56, 143–168.

Ammendola, P., Cammisa, E., Chirone, R., Lisi, L., Ruoppolo, G., 2012. Effect of sulphur on the performance of Rh–$LaCoO_3$ based catalyst for tar conversion to syngas. Appl. Catal. B-Environ. 113-114, 11-18.

Aneggi, E., Boaro, M., de Leitenburg, C., Dolcetti, G., Trovarelli, A., 2006. Insights into the redox properties of ceria-based oxides and their implications in catalysis. J. Alloys. Compd. 408–412, 1096–1102.

Anis, S., Zainal, Z.A., 2011. Tar reduction in biomass producer gas via mechanical, catalytic and thermal methods: A review. Renew. Sust. Energ. Rev. 15, 2355–2377.

Arauzo, J., Radlein, D., Piskorz, J., Scott, D.S., 1997. Catalytic pyrogasification of biomass. Evaluation of modified nickel catalysts. Ind. Eng. Chem. Res. 36, 67–75.

Asadullah, M., Ito, S., Kunimori, K., Tomishige, K., 2002. Role of catalyst and its fluidization in the catalytic gasification of biomass to syngas at low temperature. Ind. Eng. Chem. Res. 41, 4567-4575.

Asadullah, M., Miyazawa, T., Ito, S., Kunimori, K., Koyama, S., Tomishige, K., 2004. A comparison of $Rh/CeO_2/SiO_2$ catalysts with steam reforming catalysts, dolomite and inert materials as bed materials in low throughput fluidized bed gasification systems. Biomass Bioenerg. 26, 269-279.

Asadullah, M., Miyazawa, T., Ito, S-I., Kunimori, K., Tomishige, K., 2003. Catalyst performance of $Rh/CeO_2/SiO_2$ in the pyrogasification of biomass. Energ. Fuel. 17, 842–849.

Ashok, J. Kawi, S., 2015. Steam reforming of biomass tar model compound at relatively low steam-to-carbon condition over CaO-doped nickel–iron alloysupported over iron–alumina catalysts. Appl. Catal. A-Gen. 490, 24–35.

Ashrafi, M., Pfeifer, C., Pröll, T., Hofbauer, H., 2008. Experimental study of model biogas catalytic steam reforming: 2. Impact of sulfur on the deactivation and regeneration of Ni-based catalysts. Energ. Fuel. 22, 4190–4195.

Atimtay, A.T., 2001. Cleaner energy production with integrated gasification combined cycle systems and use of metal oxide sorbents for H_2S cleanup from coal gas. Clean Technol. Environ. Policy 2, 197-208.

Bachiller-Baeza, B., Rodríguez-Ramos, I., Guerrero-Ruiz, A., 2001. Influence of Mg and Ce addition to ruthenium based catalysts used in the selective hydrogenation of α,β-unsaturated aldehydes. Appl. Catal. A-Gen. 205, 227–237.

Bain, R., Overend, R.P., 1996. New gasification technology offers promise for biomass power plants. Power Eng. 4, 600–606.

Bain, R.L., Dayton, D.C., Carpenter, D.L., 2005. Evaluation of catalyst deactivation during catalytic steam reforming of biomass-derived syngas. Ind. Eng. Chem. Res. 44, 7945-7956.

Baker, E.G., Brown, M.D., Elliott, D.C., Mudge, L.K., 1988. Characterization and treatment of tars from biomass gasifiers. AIChE 1988 Summer National Meeting, Denver, CO, pp. 1–11.

Baker, E.G., Brown, M.D., Robertus, R.J., 1985. Catalytic Gasification of Bagasse for the Production of Methanol. Pacific Northwest Laboratory, prepared for the US Department of Energy under Contract DE-AC06-76RLO 1830. PNL-5100.

Baker, E.G., Mudge, L.K., Brown, M.D., 1987. Steam gasification of biomass with nickel secondary catalysts. Ind. Eng. Chem. Res. 26, 1335-1339.

Bangala, D.N., Abatzoglou, N., Chornet, E., 1998. Steam reforming of naphthalene on Ni-Cr/Al_2O_3 catalysts doped with MgO, TiO2, and La_2O_3. AIChE J. 44, 927-936.

Barisano, D. Freda, C. Nanna, F. Fanelli, E. Villone, A., 2012. Biomass gasification and in-bed contaminants removal: Performance of ironenriched Olivine and bauxite in a process of steam/O_2 gasification. Bioresour. Technol. 118, 187-194.

Barret, E.P., Joyner, L.S., Halenda, P.P., 1951. Determination of pore volume and area distribution in porous substances. J. Am. Chem. Soc. 73, 373–380.

Belgued, M., Pareja, P., Amariglio, A., Amariglio, H., 1991. Conversion of methane into higher hydrocarbons on platinum. Nature 352, 789-790.

Brandt, P., Larsen, E., Henriksen, U., 2000. High tar reduction in a two-stage gasifier. Energ. Fuel. 14, 816-819.

Breysse, M., Afanasiev, P., Geantet, C., Vrinat, M., 2003. Overview of support effects in hydrotreating catalysts. Catal. Today 86, 5–16.

Bridgwater, A.V., 1995. The technical and economic feasibility of biomass gasification for power generation. Fuel 74, 631–653.

Brown, R.C., 2003. Biorenewable Resources: Engineering New Products from Agriculture. Iowa State Press, Ames, IA.

Brown, R.C., Liu, A., Norton, G., 2000. Catalytic effects observed during the co-gasification of coal and switchgrass. Biomass Bioenerg. 18, 499–506.

Bui, T., Loof, R., Bhattacharya, S.C., 1994. Multi-stage reactor for thermal gasification of wood. Energy 19, 397–404.

Bulushev, D.A., Ross, J.R.H., 2011. Catalysis for conversion of biomass to fuels via pyrolysis and gasification: A review. Catal. Today 171, 1-13.

Cao, Y., Wang, Y., Riley. J.Y., Pan, W-P., 2006. A novel biomass air gasification process for producing tar-free higher heating value fuel gas. Fuel Process. Technol. 87, 343-353.

Carlos, E.D., Moreno, S., Molina, R., 2011. Co-precipitated Ni–Mg–Al catalysts containing Ce for CO_2 reforming of methane. Int. J. Hydrogen Energy 36, 3886–3894.

Chaiprasert, P., Vitidsant, T., 2009. Effects of promoters on biomass gasification using nickel/dolomite catalyst. Korean J. Chem. Eng. 26, 1545-1549.

Chang, J-S., Park, S-E., Chon, H., 1996. Catalytic activity and coke resistance in the carbon dioxide reforming of methane to synthesis gas over zeolite-supported Ni catalysts. Appl. Catal. A-Gen. 145, 111–124.

Che, M., Bonneviot, L., 1988. Role of oxide surface in coordination chemistry of transition metal ions in catalytic systems. Pure Appl. Chem. 60, 1369–1378.

Cheah, S., Gaston, K.R., Parent, Y.O., Jarvis. M.W., Vinzant, T.B., Smith. K.M., Thornburg. N.E., Nimlos, M.R., Magrini-Bair, K.A., 2013. Nickel cerium olivine catalyst for catalytic gasification of biomass. Appl. Catal. B-Environ. 134-135, 34-45.

Chen, I., Shiue, D.W., 1988. Resistivity to sulfur poisoning of nickel-alumina catalysts. Ind. Eng. Chem. Res. 27, 1391–1396.

Chen, J., Wang, R., Zhang, J., He, F., Han, S., 2005a. Effects of preparation methods on properties of $Ni/CeO_2–Al_2O_3$ catalysts for methane reforming with carbon dioxide. J. Mol. Catal. A-Chem. 235, 302–310.

Chen, L., Lu, Y., Hong, Q., Lin. J., Dautzenberg, F.M., 2005b. Catalytic partial oxidation of methane to syngas over Ca-decorated- Al_2O_3-supported Ni and NiB catalysts. Appl. Catal. A-Gen. 292, 295–304.

Chen, Y., Xie, C., Li, Y., Song, C., Bolin, T.N., 2010. Sulfur poisoning mechanism of steam reforming catalysts: an X-ray absorption near edge structure (XANES) spectroscopic study. Phy. Chem. Chem. Phys. 12, 5707-5711.

Choi, Y., Stenger, H., 2003. Water gas shift reaction kinetics and reactor modeling for fuel cell grade hydrogen. J. Power Sources 124, 432–439.

Choudhary, V.R., Uphade, B.S., Mamman, A.S., 1997. Oxidative conversion of methane to syngas over nickel supported on commercial low surface area porous catalyst carriers precoated with alkaline and rare earth oxides. J. Catal. 172, 281-293.

Christodoulou, C., Grimekis, D., Panopoulos, K.D., Pachatouridou, E.P., Iliopoulou, E.F, Kakaras, E., 2014. Comparing calcined and un-treated olivine as bed materials for tar reduction in fluidized bed gasification. Fuel Process. Technol. 124, 275–285.

Church, J.S., Cant, N.W., Trimm, D.L., 1994. Surface area stability and characterisation of a novel sulfate-based alumina modified by rare earth and alkaline earth ions. Appl. Catal. A-Gen. 107, 267–276.

Coll, R., Salvadó, J., Farriol, V., Montané, D., 2001. Steam reforming model compounds of biomass gasification tars: Conversion at different operating conditions and tendency towards coke formation. Fuel Process. Technol. 74, 19-31.

Corella, J. 1996. Thermochemical Biomass Conversion: Upgrading of the Crude Gasification Product Gas. Final Synthesis Report, Agro-Industrial Research, EC/AIR, project: AIR2-CT93-1436.

Corella, J., 1988. Fluidized bed steam gasification of biomass with dolomite and a commercial FCC catalyst. In: Bridgwater, A.V., Kuester, J.L. (Eds.), Research in Thermochemical Biomass Conversion, Elsevier Applied Science, London, pp. 754–765

Corella, J., Aznar, M-P., Javier Gil, J., Caballero, M.A., 1999a. Biomass gasification in fluidized bed: Where to locate the dolomite to improve gasification? Energ. Fuel. 13, 1122-1127.

Corella, J., Narvaez, I., Orio, A., 1996. Biomass gasification in fluidized bed: hot and catalytic raw gas cleaning. New developments. In: Chartier, P., Ferrero, G.L., Henius, U.M., Hultberg, S., Sachau, J., Wiimblad, M., (Eds). Proceedings of 9th European Bioenergy Conference, Copenhagen, 24–27 June, 1996. p. 1814–1818.

Corella, J., Orío, A., Toledo, J-M., 1999b. Biomass gasification with air in a fluidized bed: Exhaustive tar elimination with commercial steam reforming catalysts. Energ. Fuel. 13, 702–709.

Corella, J., Orý'o, A., Aznar, M.P., 1998. Biomass gasification with air in fluidized bed: Reforming of the gas composition with commercial steam reforming catalysts. Ind. Eng. Chem. Res. 37, 4617–4624.

Corella, J., Toledo, J.M., Molina, G., 2007. A review on dual fluidized-bed biomass gasifiers. Ind. Eng. Chem. Res. 46, 6831–6839.

Corella, J., Toledo, J.M., Padilla., R., 2004a. Olivine or dolomite as in-bed additive in biomass gasification with air in a fluidized bed: Which Is better? Energ. Fuel. 18, 713-720

Corella, J., Toledo, J.M., Padilla, R.P., 2004b. Catalytic hot gas cleaning with monoliths in biomass gasification in fluidized beds. 1. Their effectiveness for tar elimination. Ind. Eng. Chem. Res. 43, 2433-2445.

Courson, C., Makaga, E., Petit, C., Kiennemann, A., 2000. Development of Ni catalysts for gas production from biomass gasification. Reactivity in steam- and dry-reforming. Catal. Today 63, 427–437.

Courson, C., Udron, L., Swierczy'nski, D., Petit, C., Kiennemann, A., 2002. Hydrogen production from biomass gasification on nickel catalysts tests for dry reforming of methane. Catal. Today 76, 75–86.

Dalai, A.K., Majumdar, A., Chowdhury, A., Tollefson, E.L., 1993. The effects of pressure and temperature on the catalytic oxidation of hydrogen sulfide in natural gas and regeneration of the catalyst to recover the sulfur produced. Canadian J. Chem. Eng. 71, 75–82.

DDG, 2012: Dried Distillers Grain, Biomass Burn Characteristics. http://www.omafra.gov.on.ca/english/engineer/facts/11-033.htm (accessed on Nov 2012)

de Andrés, J.M., Narros, A., Rodríguez, M.E., 2011. Behaviour of dolomite, olivine and alumina as primary catalysts in air–steam gasification of sewage sludge. Fuel 90, 521–527.

Delgado, J., Aznar, M.P., Corella, J., 1996. Calcined dolomite, magnesite, and calcite for cleaning hot gas from a. fluidized bed biomass gasifier with steam: Life and usefulness. Ind. Eng. Chem. Res. 35, 3637–3643.

Demirbas, A., 2001. Biomass resource facilities and biomass conversion processing for fuels and chemicals. Energ. Convers. Manage. 42, 1357-1378.

Devi, L., Ptasinski, K.J., Janssen, F.J.J.G., 2003. A review of the primary measures for tar elimination in biomass gasification processes. Biomass Bioenerg. 24, 125-140.

Devi, L., Ptasinski, K.J., Janssen, F.J.J.G., van Paasen, S.V.B., Bergman, P.C.A., Kiel, J.H.A., 2005b. Catalytic decomposition of biomass tars: Use of dolomite and untreated olivine. Renew. Energy 30, 565–587.

Devi, M., Craje, L., Thüne, P., Ptasinski, K.J., 2005a. Olivine as tar removal catalyst for biomass gasifiers: catalyst characterization. Appl. Catal. A-Gen. 294, 68-79.

Di Carlo, A., Borello, D., Sisinni, M., Savuto, E., Venturini, P., Bocci, E., Kuramoto, K., 2015. Reforming of tar contained in a raw fuel gas from biomass gasification using nickel-mayenite catalyst. Int. J. Hydrogen Energ. 40, 9088-9095.

Dou, B., Zhang, M., Gao, J., Shen, W., Sha, X., 2002. High-temperature removal of NH_3, organic sulfur, HCl, and tar component from coal-derived gas. Ind. Eng. Chem. Res. 41, 4195–4200.

Draelants, D.J., Zhao, H.-B., Baron, G.V., 2001. Preparation of catalytic filters by the urea method and its application for benzene cracking in H_2S-containing biomass gasification gas. Ind. Eng. Chem. Res. 40, 3309–3316.

Draelants, D.J., Zhao, H-B., Baron, G.V., 2000. Catalytic conversion of tars in biomass gasification fuel gases with nickel-activated ceramic filters. Stud. Surf. Sci. Catal. 130, 1595-1600.

Du, V.A., Sidorenko, A., Bethge, O., Paschen, S., Bertagnolli, E., Schubert, U., 2011. Iron silicide nanoparticles in a SiC/C matrix from organometallic polymers: Characterization and magnetic properties. J. Mater. Chem. 21, 12232-12238.

Duman, G., Watanabe, T., Uddin, M.A., Yanik J., 2014. Steam gasification of safflower seed cake and catalytic tar decomposition over ceria modified iron oxide catalysts. Fuel Process. Technol. 126, 276–283.

ECN, 2004. Tar Removal in Fluidized Gasifier: Impact of Fuel Properties and Operating Conditions. Energy Research Centre of the Netherlands, ECN-C-04-013, March 2004.

Efryushina, N.P., Shamshurin, A.V., Zhikhareva, E.A., 1998. Crystal-field parameters of Mn^{2+} in Mg_2SiO_4: Mn^{2+}, $Mg_5(SiO_4)_2F_2$: Mn^{2+}, and $Mg_2SiO_4 \cdot MgF_2$: Mn^{2+}. Inorg. Mater 34, 514–516.

Einvall, J., Albertazzi, S., Hulteberg, C., Malik, A., Basile, F., Larsson, A-C., Brandin, J., Sanati, M., 2007. Investigation of reforming catalyst deactivation by exposure to fly ash from biomass gasification in laboratory scale. Energ. Fuel. 21, 2481-2488.

Ekstrom, C., Lindman, N., Pettersson, R., 1985. Catalytic conversion of tars, carbon black and methane from pyrolysis and gasification of biomass. In: Overend, A.T. Milne, K.L. Mudge (Eds.), Fundamentals of Thermochemical Biomass Conversion, Elsevier Applied Science Publishers, London, 601–618.

Elliot, D.C., Baker, E.G., 1986. The effect of catalysis on wood gasification tar composition. Biomass 9, 195–203.

Elliott, D.C., Neuenschwander, G.G., Hart, T.R., Butner, R.S., Zacher, A.H., Engelhard, M.H., Young, J.S., McCready, D.E., 2004. Chemical processing in high-pressure aqueous environments. 7. Process development for catalytic gasification of wet biomass feedstocks. Ind. Eng. Chem. Res. 43, 1999-2004.

Elliott, D.C., Sealock, Jr. L.J., Baker, E.G., 1993. Chemical processing in high-pressure aqueous environments. 2. Development of catalysts for gasification. Ind. Eng. Chem. Res. 32, 1542-1548.

Engelen, K, Zhang, Y.H., Draelants, D.J., Baron, G.V., 2003. A novel catalytic filter for tar removal from biomass gasification gas: Improvement of the catalytic activity in presence of H_2S. Chem. Eng. Sci. 58, 665-670.

Espenas, B.G., Lammers, G., Huijnen, H., Beenackers, A.A.C.M., Simell, P.A., 1998. Round test on measurement of model tar compound decomposition kinetics. In: Kopetz, H., Weber, T, Palz, W., Chartier, P., Ferrero, G.L. (Eds). Proceedings of 10th European Conference and Technology Exhibition/Biomass for Energy and Industry, Wurzburg, 8–11 June 1998.

European Commission, 2003. Reference Document on Best Available Techniques in the Large Volume Organic Chemical Industry. European IPPC Bureau at the Institute for Prospective Technological Studies, Seville, Spain.

Fenouil, L.A., Lynn, S., 1995. Study of calcium-based sorbents for high-temperature H_2S removal. 1. Kinetics of H_2S sorption by uncalcined limestone. Ind. Eng. Chem. Res. 34, 2324–2333.

Ferella, F., Stoehr, J., De Michelis, L., Hornung, A., 2013. Zirconia and alumina based catalysts for steam reforming of naphthalene. Fuel 105, 614–629.

Figueiredo, J.L., 1982. Carbon formation and gasification on nickel. In: Figueiredo, J.L. (Ed.), Progress in Catalyst Deactivation, Martinus Nijhoff Publishers, The Hague

Furusawa, T., Saito, K., Kori, Y., Miura, Y., Sato, M., Suzuki, N., 2013. Steam reforming of naphthalene/benzene with various types of Pt- and Ni-based catalysts for hydrogen production. Fuel 103, 111–121.

Furusawa, T., Tsutsumi, A. 2005. Comparison of Co/MgO and Ni/MgO catalysts for the steam reforming of naphthalene as a model compound of tar derived from biomass gasification. Appl. Catal. A-Gen. 278, 207-212.

Gabra, M., Nordin, A., Öhman, M., Kjellström, B., 2001. Alkali retention/separation during bagasse gasification: a comparison between a fluidised bed and a cyclone gasifier. Biomass Bioenerg. 21, 461–476.

Galindo, A.L., Giraldo, S.Y., Lesme-Jaén, R., Cobas, V.M., Andrade, R.V., Loraf, E.S., 2012. Experimental study of tar and particles content of the produced gas in a double stage downdraft gasifier. The 25th International Conference on Efficiency, Cost, Optimization, Simulation, and Environmental Impact of Energy Systems, June, 2012. Perugia, Italy.

Garcia, L., Benedicto, A., Romeo, E., Salvador, M.L., Arauzo, J., Bilbao, R., 2002. Hydrogen production by steam gasification of biomass using Ni−Al coprecipitated catalysts promoted with magnesium. Energ. Fuel. 16, 1222–1230.

Garcia, L., Salvador, M.L., Arauzo, J., Bilbao, R., 1999. Catalytic steam gasification of pine sawdust.Effect of catalyst weight/biomass flow rate and steam/biomass ratios on gas production and composition. Energ. Fuel. 13, 851–859.

Gates, B.C., Huber, G.W., Marshall, C.L., Ross, P.N., Siirola, J., Wang, Y., 2008. Catalysts for emerging energy applications. MRS Bulletin 33, 429–435.

Gebhard, S., 1995. Evaluation of Battelle Columbus Laboratory modified method #5 tar sampling procedure and performance of catalysts tested with the 9 tons/day indirectly heated gasifier. Thermochemical Conversion: Process Research Branch C-Milestone Completion Report,

Gil, J., Caballero, M.A, Martin, J.A., Aznar, M.P., Corella, J., 1999. Biomass gasification with air in a fluidized bed: Effect of the in-bed use of dolomite under different operation conditions. Ind. Eng. Chem. Res. 38, 4226–4235.

Glazer, M.P., Khan, N.S., de Jong, W., Spliethoff, H., Schu¨rmann, H., Monkhouse, P., 2005. Alkali metals in circulating fluidized bed combustion of biomass and coal: Measurements and chemical equilibrium analysis. Energ. Fuel. 19, 1889-1897.

Göransson, K., Söderlind, U., He. J., Zhang, W., 2011. Review of syngas production via biomass DFBGs. Renew. Sust. Energ. Rev. 15, 482–492.

Grieco, E.M., Gervasio, C., Baldi, G., 2013. Lanthanum–chromium–nickel perovskites for the catalytic cracking of tar model compounds. Fuel 103, 393–397.

Gröbl, T., Walter, H., Haider, M., 2012. Biomass steam gasification for production of SNG – Process design and sensitivity analysis. Appl. Energ. 97, 451–461.

Gustam, E., Dalaim, A.K., Uddin, M.A., Sasaoka, E., 2009. Catalytic decomposition of biomass tars with dolomites. Energ. Fuel. 23, 2264–2272.

Haber, J., 1999. Manual on catalyst characterization. Pure Appl. Chem. 63, 1227-1246.

Han, J., Kim, H., 2008. The reduction and control technology of tar during biomass gasification/pyrolysis: An overview. Renew. Sust. Energ. Rev. 12, 397-416.

He, M., Hu, Z., Xiao, B., Li, J., Guo, X., Luo, S., Yang, F., Feng, Y., Yang, G., Liu, S., 2009. Hydrogen-rich gas from catalytic steam gasification of municipal solid waste (MSW): Influence of catalyst and temperature on yield and product composition. Int. J. Hydrogen Energ. 34, 195-203.

Henriksen, U., Ahrenfeldta, J., Jensen, Y.K., Gøbel, B., Bentzen, J.D., Hindsgaul, C., Sørensen, L.H., 2006. The design, construction and operation of a 75 kW two-stage gasifier. Energy 31, 1542–1553.

Hepola, J., 1993. Usability of Catalytic Gas Cleaning in a Simplified IGCC Power System. Deactivation of Ni/Al_2O_3 catalysts. Literature Review, Finland. VTT Publication 1445

Hepola, J., Simell, P., 1997a. Sulphur poisoning of nickel-based hot gas cleaning catalysts in synthetic gasification gas: I. Effect of different process parameters. Appl. Catal. B-Environ. 14, 287-303.

Hepola, J., Simell, P., 1997b. Sulphur poisoning of nickel-based hot gas cleaning catalysts in synthetic gasification gas. II. Chemisorption of hydrogen sulphide. Appl. Catal. B-Environ. 14, 305-321.

Hepola, J., Simell, P., Ståhlberg, P., 1994. Sulphur poisoning of nickel catalysts in catalytic hot gas cleaning conditions of biomass gasification. Stud. Surf. Sci. Catal. 88, 499–506.

Hu, X., Hanaoka, T., Sakanishi, K., Shinagawa, T., Matsui, S., Tada, M., Iwasaki, T., 2007. Removal of tar model compounds produced from biomass gasification using activated carbons. J. Jap. Inst. Energ. 86, 707-711.

Huang, B.S., Chen, H.Y., Chuang, K.H., Yang, R.X., Wey, M.Y., 2012. Hydrogen production by biomass gasification in a fluidizedbed reactor promoted by an Fe/CaO catalyst. Int. J. Hydrogen Energ. 37, 6511–6518.

Huang, J., Schmidt, K.G., Bian, Z., 2011. Removal and conversion of tar in Syngas from woody biomass gasification for power utilization using catalytic hydrocracking. Energies 4, 1163–1177.

Huang, L., Xie, J., Chen, R., Chu, D., Hsu, A.T., 2009. Fe promoted Ni–Ce/Al_2O_3 in auto-thermal reforming of ethanol for hydrogen production. Catal. Lett. 130, 432–439.

Huber, G.W., Iborra, S., Corma, A., 2006. Synthesis of transportation fuels from biomass: Chemistry, catalysts, and engineering. Chem. Rev. 106, 4044–4098.

Hulteberg, C., 2012. Sulphur-tolerant catalysts in small-scale hydrogen production, a review. Int. J. Hydrogen Energ. 37, 3978–3992.

Inaba, M., Murata, K., Saito, M., Takahara, I., 2006. Hydrogen production by gasification of cellulose over Ni catalysts supported on Zeolites. Energ. Fuel. 20, 432–438.

JCPDS, 1984. Joint Committee of Powder Diffraction Standards. Magnesium Silicate/Forsterite Synthesis. Nattonal Bureau of Standards, US Monograph 25, 20, 71, JCPDS34-0189.

Kawamoto, K., Kuramochi, H., Go, I., 2005. Hydrogen production from catalytic gasification-reforming of waste wood. Nippon Kikai Gakkai Kankyo Kogaku 15, 194–197.

Kawamoto, K., Wu, W., Kuramochi, H., 2009. Development of gasification and reforming technology using catalyst at lower temperature for effective energy recovery: Hydrogen recovery using waste wood. J. Environ. Eng. 4, 409–421.

Kepinski, L., Stasinskab, B., Borowiecki, Y., 2000. Carbon deposition on Ni/Al_2O_3 catalysts doped with small amounts of molybdenum. Carbon 38, 1845–1856.

Kim, K., Jevon, S.K., Vo, C., Park, C.S., Norbeck, J.M., 2007. Removal of hydrogen sulfide from a steam-hydrogasifier product gas by Zinc Oxide sorbent. Ind. Chem. Res. 46, 5848–5854.

Kimura, T., Miyazawam, T., Nishikawa, J., Kado, S., Okumura, K., Miyao, T., Naito, S., Kunimori, K., Tomishige, K., 2006. Development of Ni catalysts for tar removal by steam gasification of biomass. Appl. Catal. B-Environ. 68, 160–170.

Kinoshita, C.M., Wang, Y., Zhou, J.C., 1994. Tar formation under different biomass gasification conditions. J. Anal. Appl. Pyrol. 29, 169–181.

Klimova, T., Calderón, M., Ramırez, J., 2003. Ni and Mo interaction with Al-containing MCM-41 support and its effect on the catalytic behavior in DBT hydrodesulfurization. Appl. Catal. A-Gen. 240, 29–40.

Ko, T.H., Chu, H., Chaung, L.K., Tseng, T.K., 2004. High temperature removal of hydrogen sulfide using an N-150 sorbent. J. Hazard. Mater. 114, 145–152.

Ko, T-H., Chu, H., Liou, Y-J., 2007. A study of Zn–Mn based sorbent for the high-temperature removal of H_2S from coal-derived gas. J. Hazard. Mater. 147, 334–341.

Kobayashi, M., Shirai, H., Nunokawa, M., 1997. Investigation on desulfurization performance and pore structure of sorbents containing zinc ferrite. Energ. Fuel. 11, 887-896.

Koike, K., Ishikawa, C., Li, D., Wang, L., Nakagawa, Y., 2013. Catalytic performance of manganese-promoted nickel catalysts for the steam reforming of tar from biomass pyrolysis to synthesis gas. Fuel 103, 122–129.

Kong, M., Fei, J., Wang, S., Lu, W., Zheng, W., 2011. Influence of supports on catalytic behavior of nickel catalysts in carbon dioxide reforming of toluene as a model compound of tar from biomass gasification. Bioresour. Technol. 102, 2004-2008.

Kong, M., Yang, Q., Fei, J.H., Zheng, X.M., 2012. Experimental study of Ni/MgO catalyst in carbon dioxide reforming of toluene, a model compound of tar from biomass gasification. Int. J. Hydrogen Energ. 37, 13355-13364.

Koningen, J., Sjöström, K., 1998. Sulfur-deactivated steam reforming of gasified biomass. Ind. Eng. Chem. Res. 37, 341–346.

Kumar, A., Jones, D.D., Hanna, N.A., 2009. Thermochemical biomass gasification: A review of the current status of the technology. Energies 2, 556-581.

Kurkela, E., Stahlberg, J., Laatikainan, J., Simell, P., 1993. Development of simplified IGCC-processes for biofuels: supporting gasification research at VTT. Bioresour. Technol. 46, 37–47.

Kurkela, E., Sthalberg, P., 1992. Air gasification of peat, wood and brown coal in a pressurized fluidized-bed reactor. I. Carbon conversion, gas yields and tar formation. Fuel Process. Technol. 3, 1–21.

Kwon, K.C., Park, Y., Gangwal, S.K., Das, K., 2003. Reactivity of sorbents with hot hydrogen sulfide in the presence of moisture and hydrogen. Sep. Sci. Technol. 38, 3289–3311.

Lakhapatri, S.L., Abraham, M.A., 2011. Analysis of catalyst deactivation during steam reforming of jet fuel on Ni-(PdRh)/gamma-Al_2O_3 catalyst.Appl. Catal. A-Gen. 405, 149–159.

Leach, B.E., 1984. Applied Industrial Catalysis. Vol 3, Academic Press, New York

Li, C., Hirabayashi, D., Suzuki, K., 2009a. Development of new nickel based catalyst for biomass tar steam reforming producing H_2-rich syngas. Fuel Process. Technol. 90, 790–796.

Li, C., Suzuki, K., 2009. Tar property, analysis, reforming mechanism and model for biomass gasification—An overview. Renew. Sust. Energ. Rev. 13, 594–604.

Li, C.S., Hirabayashi, D., Suzuki, K., 2010. Steam reforming of biomass tar producing H_2-rich gases over Ni/MgOx /CaO_{1-x} catalyst. Bioresour. Technol. 101, 97–100.

Li, D.L., Nakagawa, Y., Tomishige, K., 2012. Development of Ni-Based catalysts for steam reforming of tar derived from biomass pyrolysis. Chin. J. Catal. 33, 583–594.

Li, D.L., Tamura, M., Nakagawa, Y., Tom, K., 2015. Metal catalysts for steam reforming of tar derived from the gasification. Bioresour. Technol. 178, 53–64.

Li, H., Monnell, J.D., Alvin, M., Vidic, R.D., 2008. Factors affecting activated carbon-based catalysts for selective hydrogen sulfide oxidation. Main Group Chem. 7, 239-250.

Li, J., Xiao, B., Yan, R., Xu, X., 2009b. Development of a supported tri-metallic catalyst and evaluation of the catalytic activity in biomass steam gasification. Bioresour. Technol. 100, 5295–5300.

Li, X.K., Ji, W.J., Zhao, J., Wang, S.J., Au, C.T., 2005. Ammonia decomposition over Ru and Ni catalysts supported on fumed SiO_2, MCM-41, and SBA-15. J. Catal. 236, 181-189.

Lin, Y-C., Huber, G.W., 2009. The critical role of heterogeneous catalysis in lignocellulosic biomass conversion. Energ. Environ. Sci. 3, 69-80.

Lucas, C., Szewczyk, D., Blasiak, W., Mochida, S., 2004. High-temperatureair and steam gasification of densified biofuels. Biomass Bioenerg. 27, 563–575.

Lv, P., Chang, J., Wang, Y., Fu, Y., Chen, Y., 2004. Hydrogen-rich gas production from biomass catalytic gasification. Energ. Fuel. 18, 228–233.

Ma, L., Baron, G.V., 2008. Mixed zirconia–alumina supports for Ni/MgO based catalytic filters for biomass fuel gas cleaning. Powder Technol. 180, 21-29.

Ma, L., Parharso, Trimm, D.L., 1999. Rare earth oxides promoted Nickel based catalysts for steaming reforming. Mater. Sci. Forum 135-136, 187-193.

Mann, M.K., 1995. Technical and Economic Assessment of Producing Hydrogen by Reforming Syngas from the Battelle Indirectly Heated Biomass Gasifier, National Renewable Energy Laboratory, Task No. TP-431-8143, August 1995.

Mashapa, T.N., Rademan, J.D., van Vuuren, M.J.J., 2007. Catalytic performance and deactivation of precipitated iron catalyst for selective oxidation of hydrogen sulfide to elemental sulfur in the waste gas streams from coal gasification. Ind. Eng. Chem. Res. 46, 6338-6344.

McKendry, P., 2002a. Energy production from biomass (part 1): Overview of biomass. Bioresour. Technol. 83, 37–46.

McKendry, P., 2002b. Energy production from biomass (part 2): Conversion technologies. Bioresour. Technol. 83, 47–54.

McKendry, P., 2002c. Energy production from biomass (part 3): Gasification technologies. Bioresour. Technol. 83, 55–63.

McMinn, T.E., Moates, F.C., Richardson, J.T., 2001. Catalytic steam reforming of chlorocarbons: Catalyst deactivation. Appl. Catal. B-Environ. 31, 93–105.

Michel, R., Łamacz, A., Krzton, A., Djega-Mariadassou, G., Burg, P., Courson, C., Gruber, R., 2013. Steam reforming of a-methylnaphthalene as a model tar compound over olivine and olivine supported nickel. Fuel 109, 653–660.

Milne, T.A., Abatzoglou, N., Evans, R.J., 1998. Biomass Gasifier Tars: Their Nature, Formation and Conversion. National Renewal Energy Laboratory, NREL/TP-570-25357, Golden, Colorado.

Milne, T.A., Elam, C.C., Evans, R.J., 2002. Hydrogen from Biomass: State of the Art and Research Challenges. International Energy Agency Report IEA/H2/TR-02/001.

Min, Z.H., Yimsiri, P., Zhang, S., Wang, Y., Asadullah, M., Li, C.Z., 2013. Catalytic reforming of tar during gasification. Part III. Effects of feedstock on tar reforming using ilmenite as a catalyst. Fuel 103, 950–955.

Miyazawa, T., Kimura, T., Nishikawa, J., Kado, S., 2006. Catalytic performance of supported Ni catalysts in partial oxidation and steam reforming of tar derived from the pyrolysis of wood biomass. Catal. Today 115, 254-262.

Mun, T.Y., Cho, M.H., Kim, J.S., 2014. Air gasification of dried sewage sludge in a twostage gasifier. Part 3: Application of olivine as a bed a bed material and nickel coated distributor for the production of a clean hydrogen-rich producer gas. Int. J. Hydrogen Energ. 39, 5634-5643.

Mun, T-Y., Kang, B-S., Kim, J-S., 2009. Production of a producer gas with high heating values and less tar from dried sewage sludge through air gasification using a two-stage gasifier and activated carbon. Energ. Fuel. 23, 3268-3276.

Narváez, I., Corella, J., Orío A., 1997. Fresh tar (from a biomass gasifier) elimination over a commercial steam-reforming catalyst.Kinetic and effect of different variables of operation. Ind. Eng. Chem. Res. 36, 317–327.

Ni, M., Dennis Y.C. Leung, D.Y.C., Leung, M.K.H., Sumathy, K., 2006. An overview of hydrogen production from biomass. Fuel Process.Technol. 87, 461–472.

Nishikawa, J., Miyazawa, T., Nakamura, K., Asadullah, M., Kunimori, K., Tomishige, K., 2008. Promoting effect of Pt addition to $Ni/CeO_2/Al_2O_3$ catalyst for steam gasification of biomass. Catal. Commun. 9, 195–201.

Orío, A., Corella, J., Narváez, I., 1997. Performance of different dolomites on hot raw gas cleaning from biomass gasification with air. Ind. Eng. Chem. Res. 36, 3800–3808.

Ozaki, J.I., Takei, M., Takakusagi, K., Takahashi, N., 2012. Carbon deposition on a Ni/Al_2O_3 catalyst in low-temperature gasification using C6-hydrocarbons as surrogate biomass tar. Fuel Process. Technol. 102, 30-34

Paisley, M.A., 1997. Catalytic hot gas conditioning of biomass derived product gas. In: Bridgwater, A.V., Boocock, D.G.B. (Eds.), Developments in Thermochemical Biomass Conversion, vol. 2, Blackie Academic & Professional, London, pp. 1209–1223

Park, H.J., Park, S.H., Sohn, J.M., Park, J., Jeon, J-K., Kim, D-S., Park, Y.K., 2010. Steam reforming of biomass gasification tar using benzene as a model compound over various Ni supported metal oxide catalysts. Bioresour. Technol. 101, S101–S103.

Pecho, J., Schildhauer, T.J., Sturzenegger, M., Biollaz, S., Wokaun, A., 2008. Reactive bed materials for improved biomass gasification in a circulating fluidised bed reactor. Chem. Eng. Sci. 63, 2465–2476.

Perlack, R.D., Wright, L.L., Turhollow, A.F., Graham, R.L., Stokes, B.J., Erbach, D.C., 2005. Biomass as Feedstock for a Bioenergy and Bioproducts Industry: The Technical Feasibility of a Billion-Ton Annual Supply. DOE/G0-102005-2135, Oak Ridge National Lab, Oak Ridge, TN

Petit, C., Kiennemann, A., Chaumette, P., Clause, O., 1995. Oxidation Catalyst and Process for the Partial Oxidation of Methane, US Patent No. 5,447,705,

Pfeifer, C., Hofbauer, H., 2008. Development of catalytic tar decomposition downstream from a dual fluidized bed biomass steam gasifier. Powder Technol. 180, 9–16.

Pfeifer, C., Koppatz, S., Hofbauer, H., 2011. Steam gasification of various feedstocks at a dual fluidised bed gasifier: Impacts of operation conditions and bed materials. Biomass Convers. Biorefinery. 1, 39-53.

Pfeifer, C., Rauch, R., Hofbauer, H., 2004. In-bed catalytic tar reduction in a dual fluidized bed biomass steam gasifier. Ind. Eng. Chem. Res. 43, 1634–1640.

Polychronopoulou, K., Giannakopoulos, K., Efstathiou, A.M., 2012. Tailoring MgO-based supported Rh catalysts for purification of gas streams from phenol. Appl. Catal. B-Environ. 111-112, 360-375.

Provendier, H., Petit, C., Estournès, C., Libs, S., Kiennemann, A., 1999. Stabilisation of active nickel catalysts in partial oxidation of methane to synthesis gas by iron addition. Appl. Catal. A 180, 163–173.

Qian, K., Kumar, A., 2017. Catalytic reforming of toluene and naphthalene (model tar) by char supported nickel catalyst. Fuel 187, 128–136.

Qiu, M., Li, Y., Wang, T., Zhang, Q., Wang, C., Zhang, X., Wu, C., Ma, L., Li, K., 2012. Upgrading biomass fuel gas by reforming over Ni-MgO/gamma-Al_2O_3 cordierite monolithic catalysts in the lab-scale reactor and pilot-scale multi-tube reformer. Appl. Energ. 90, 3-10.

Rabou, L.P.L.M., Zwart, R.W.R., Vreugdenhil, B.J., Bos, L., 2009. Tar in biomass producer gas, the energy research centre of The Netherlands (ECN) experience: an enduring challenge. Energ. Fuel. 23, 6189-6198.

Rangan, M., Yung, M.M., Medlin, J.W., 2012. NiW and NiRu bimetallic catalysts for ethylene steam reforming: Alternative mechanisms for sulfur resistance. Catal. Lett. 142, 718-727.

Rapagnà, S., Gallucci, K., Di Marcello, M., Foscolo, P.U., Nacken, M., Heidenreich, S., 2009. Particulate abatement in a fluidized-bed biomass gasifier. Energ. Fuel. 23, 3804–3809.

Rapagnà, S., Jand, N., Foscolo, P.U., 1998. Catalytic gasification of biomass to produce hydrogen rich gas. Int. J. Hydrogen Energ. 23, 551–557.

Rapagna, S., Jand, N., Foscolo, P.U., 1998. Utilisation of suitable catalyst for the gasification of biomass. Proceedings of 10th European Conference and Technology Exhibition/Biomass for Energy and Industry. Wurzburg, 8–11 June 1998, pp 1720–1723.

Rapagna, S., Jand, N., Kiennemann, A., Foscolo, P.U., 2000. Steam-gasification of biomass in a fluidized-bed of olivine particles. Biomass Bioenerg. 19, 187–197.

Rapagná, S., Provendier, H., Petit, C., Kiennemann, A., Foscolo, P.U., 2002. Development of catalysts suitable for hydrogen or syngas production from biomass gasification. Biomass Bioenerg. 22, 377–388.

Rapagnà, S., Virginie, M., Gallucci, K., Courson, C., Di Marcello, M., Kiennemann, A., Foscolo, P.U., 2011. Fe/olivine catalyst for biomass steam gasification: Preparation, characterization and testing at real process conditions. Catal. Today 176, 163–168.

Roberts, G.W., Brown, D.M., Hsiung, T.H., Lewnard, J.J., 1993. Deactivation of methanol synthesis catalysts. Ind. Eng. Chem. Res. 32, 1610-1621.

Ronkkonen, H., Simell, P., Reinikainen, M., Krause, O., 2009. The Effect of sulfur on ZrO2-based biomass gasification.gas clean-up catalysts. Top. Catal., 52, 1070-1078.

Ronkkonen, H., Simell, P., Reinikainen, M.. Niemela, M., Krause, O., 2011a. Precious metal catalysts in the clean-up of biomass gasification gas Part 1: Monometallic catalysts and their impact on gasification gas composition. Fuel Process. Technol. 92, 1457–1465.

Ronkkonen, H., Simell, P., Niemela, M., Krause, O., 2011b. Precious metal catalysts in the clean-up of biomass gasification gas part 2: Performance and sulfur tolerance of rhodium based catalysts. Fuel Process Technol., 92, 1881-1889.

Rose'n, C., Björnbom, E., Yu, Q., Sjöström, K., 1997. Fundamentals of pressurized gasification of biomass. In: Bridgwater, A.V., Boocock, D.G.B. (Eds.), Developments in Thermochemical Biomass Conversion, Blackie, London, 817–827.

Ross, J., 1975. Surface and Defect Properties of Solids, vol. 4, The Chemical Society, London

Rostrup-Nielsen, J., Trimm, D.L., 1977. Mechanisms of carbon formation on nickel-containing catalysts. J. Catal. 48, 155-165.

Rostrup-Nielsen, J.R., 1984. in: J.R. Anderson, M. Boudart (Eds.), Catalytic Steam Reforming Catalysis, Science & Technology, Vol. 5, Springer, Berlin.

Sarvaramini, A., Larachi, F., 2012. Catalytic oxygenless steam cracking of syngas-containing benzene model tar compound over natural Fe-bearing silicate minerals. Fuel 97.741–750.

Sato, K., Fujimoto, K., 2007. Development of new nickel based catalyst for tar reforming with superior resistance to sulfur poisoning and coking in biomass gasification. Catal. Commun. 8, 1697–1701.

Sato, K., Shinoda, T., Fujimoto, K., 2007. New nickel-based catalyst for tar reforming, with superior resistance to coking and sulfur poisoning in biomass gasification processes. J. Chem. Eng. Jap. 40, 860-868.

Seo, J.G., Youn, M.H., Jung, J.C., Song, I.L., 2009. Effect of preparation method of mesoporous Ni–Al_2O_3 catalysts on their catalytic activity for hydrogen production by steam reforming of liquefied natural gas (LNG). Int. J. Hydrogen Energ. 34, 5409-5416.

Shen, Y., 2015. Chars as carbonaceous adsorbents/catalysts for tar elimination during biomass pyrolysis or gasification. Renew. Sust. Energ. Rev. 43, 281–295.

Shen, Y., Chen, M.D., Sun, T.H., Jia, J.P., 2015. Catalytic reforming of pyrolysis tar over metallic nickel nanoparticles embedded in pyrochar. Fuel 159, 570–579.

Shen, Y., Zhao, P., Shao, Q., Ma, D., Takahashi, F., Yoshikawa, K., 2015. In-situ catalytic conversion of tar using rice husk char-supported nickel-iron catalysts for biomass pyrolysis/gasification. Appl. Catal. B-Environ. 152–153, 140–150.

Simell, P., Bredenburg, J.B., 1990. Catalytic purification of tarry fuel gas. Fuel 69, 1219–1225.

Simell, P., Kurkela, E., Ståhlberg, P., Hepola, J., 1996. Catalytic hot gas cleaning of gasification gas. Catal. Today 27, 65-72.

Simell, P., Stahlberg, P., Kurkela, E., Albrecht, J., Deutsch, S., Sjostrom, K., 2000. Provisional protocol for the sampling and analysis of tar and particulates in the gas from large-scale biomass gasifiers. Biomass Bioenerg. 18, 19–28.

Simell, P.A., Hakala, N.A.K., Haario, H.E., Krause, A.O.I., 1997. Catalytic decomposition of gasification gas tar with benzene as the model compound. Ind. Eng. Chem. Res. 36, 42–51.

Smeenk, J., Brown, R.C., 1998. Experience with atmospheric fluidized bed gasification of switchgrass. In: BioEnergy ’98 Conference, Madison, WI, October 4–8, 1998.

Srinakruang, J., Sato, K., Vitidsant, T., Fujimoto, K., 2006a. A highly efficient catalyst for tar gasification with steam. Catal. Commun. 6, 437–440.

Srinakruang, J., Sato, K., Vitidsant, T., Fujimoto, K., 2006b. Highly efficient sulfur and coking resistance catalysts for tar gasification with steam. Fuel 85, 2419-2426.

Strohm, J.J., Zheng, J., Song, C.S., 2006. Low-temperature steam reforming of jet fuel in the absence and presence of sulfur over Rh and Rh-Ni catalysts for fuel cells. J. Catal. 238, 309-320.

Susanto, H., Beenackers, A.A.C.M., 1996. A moving-bed gasifier with internal recycle of pyrolysis gas. Fuel 75, 1339-1347.

Sutton, D., Kelleher, B., Julian R.H., 2001. Review of literature on catalysts for biomass gasification. Fuel Process. Technol. 73, 155–173.

Świerczyński, D., Courson, C., Bedel, L., Kiennemann, A., Guille, J., 2006. Characterization of Ni−Fe/MgO/Olivine catalyst for fluidized bed steam gasification of biomass. Chem. Matter 18, 4025–4032.

Świerczyński, D., Courson, C., Kiennemann, A., 2008. Study of steam reforming of toluene used as model compound of tar produced by biomass gasification. Chem. Eng. Process. Process Inten. 47, 508-513.

Świerczyński, D., Libs, S., Courson, C., Kiennemann, A., 2007. Steam reforming of tar from a biomass gasification process over Ni/olivine catalyst using toluene as a model compound. Appl. Catal. B-Environ.74, 211-222.

Tanksale, A., Beltramini, J.N., Lu, Q.M., 2010. A review of catalytic hydrogen production processes from biomass. Renew. Sust. Energ. Rev. 14, 166–182.

Taralas, G., Kontominas, M.G., 2004. Kinetic modelling of VOC catalytic steam pyrolysis for tar abatement phenomena in gasification/pyrolysis technologies. Fuel 83, 1235–1245.

Taufiq-Yap, Y.H., Sivasangar, S., Salmiaton, A., 2012. Enhancement of hydrogen production by secondary metal oxide dopants on NiO/CaO material for catalytic gasification of empty palm fruit bunches. Energy 47, 158-165.

Tohji, K., Udagawa, Y., Tanabe, S., Ida, T., Ueno, A., 1984. Catalyst preparation procedure probed by EXAFS spectroscopy. 2. Cobalt on titania. J. Am. Chem. Soc. 106, 5172–5178.

Tomishige, K., Asadullah, M., Kunimori, K., 2004.Syngas production by biomass gasification using $Rh/CeO_2/SiO_2$ catalysts and fluidized bed reactor. Catal. Today 89, 389-403.

Tomishige, K., Kimura, T., Nishikawa,J., Miyazawa, T., Kunimori, K., 2007. Promoting effect of the interaction between Ni and CeO_2 on steam gasification of biomass. Catal. Commun. 8, 1074–1079.

Tomishige, K., Miyazawa, T., Kimura, T., Kunimori, K., Koizumi, N., Yamada, M., 2005. Resistance to sulfur poisoning of hot gas cleaning catalysts for the removal of tar from the pyrolysis of cedar wood. Appl. Catal. B-Environ. 60, 299-307.

Turn, S.Q., Kinoshita, C.M., Ishimura, D.M., Hiraki, T.T., Zhou. J., Masutani, S.M., 2001. An experimental investigation of alkali removal from biomass producer gas using a fixed bed of solid sorbent. Ind. Eng. Chem. Res. 40, 1960–1967.

Turn, S.Q., Kinoshita, C.M., Ishimura, D.M., Zhou, J., 1998. The fate of inorganic constituents of biomass in fluidized bed gasification. Fuel 77, 135–146.

Twigg, M.V., 1996. Catalyst Handbook. 2nd ed., Wolfe Publishing Ltd., pp 284−290.

Umeki, K., Yamamoto, K., Namioka, T., Yoshikawa, K., 2010. High temperature steam-only gasification of woody biomass. Appl. Energ. 87, 791–798.

UNIQUE, 2012. Integration of Particulate Abatement, Removal of Trace Elements and Tar Reforming in One Biomass Steam Gasification Reactor Yielding High Purity Syngas for Efficient CHP and Power Plants. web site: www.uniqueproject.eu (accessed on Nov 2012)

Vassilev, S.V., Baxter, D., Andersen, L.K., Vassileva, C.G., 2010. An overview of the chemical composition of biomass. Fuel 89, 913–933.

Viinikainen, T., Kauppi, I., Korhonen, S., Lefferts, L., Kanervo, L., Lehtonen, J., 2013. Molecular level insights to the interaction of toluene with ZrO_2-based biomass gasification gas clean-up catalysts. Appl. Catal. B- Environ. 142– 143, 769– 779.

Virginie, M., Adanezb, J., Courson, C., de Diego, L.F., Garcia-Labiano, F., Niznansky, D., Kiennemann, A., Gayan, P., Abad, A., 2012. Effect of Fe–olivine on the tar content during biomass gasification in a dual fluidized bed. Appl. Catal. B-Environ. 121–122, 214– 222.

Virginie, M., Courson, C., Niznansky, D., Chaoui, N., Kiennemann, A., 2010. Characterization and reactivity in toluene reforming of a Fe/olivine catalyst designed for gas cleanup in biomass gasification. Appl. Catal. B-Environ. 101, 90-100.

Vogt, E.T.C., Van Dillen, A.J., Geus, T.W., 1987. Catalyst deactivation. In: Delmon, B., Froment, G.F. (Eds). Studies in Surface Science and Catalysis, 34, 221–226.

Vreugdenhil, B.J., Zwart, R.W.R., 2009. Tar Formation in Pyrolysis and Gasification. Energy Research Center of the Netherlands, Amsterdam.

Waldner, M.H., Krumeich, F., Vogel, F., 2007. Synthetic natural gas by hydrothermal gasification of biomass: Selection procedure towards a stable catalyst and its sodium sulfate tolerance. J. Supercrit. Fluid. 43, 91–105.

Wambach, J., Schubert, M., Doebeli, M., Vogel, F., 2012. Characterization of a spent Ru/C catalyst after gasification of biomass in supercritical water. Chimia 66, 706–711,

Wang, J.B., Cheng, G., You, Y.L., Xiao, B., Liu, S.M., He, P.W., Guo, D.B., Guo, X.J., Zhang, G.J., 2012. Hydrogen-rich gas production by steam gasification of municipal solid waste (MSW) using NiO supported on modified dolomite. Int. J. Hydrogen Energ. 37, 6503-6510.

Wang, L., Murata, K., Inaba, M., 2009. Highly efficient conversion of gasoline into hydrogen on Al2O3-supported Ni-based catalysts: Catalyst stability enhancement by modification with W. Appl. Catal. A-Gen. 358, 264-268.

Wang, L., Weller, C.L., Jones, D.D., Hanna, M.A., 2008. Contemporary issues in thermal gasification of biomass and its application to electricity and fuel production. Biomass Bioenerg. 32, 573–581.

Wang, S., Lu, G.Q.M., 1998. CO_2 reforming of methane on Ni catalysts: Effects of the support phase and preparation technique. Appl. Catal. B-Environ. 16, 269–277.

Wang, T., Chang, J., Lv, P., Zhu, J., 2005a. Novel catalyst for cracking of biomass tar. Energ. Fuel. 19, 22–27.

Wang, T., Li, Y., Wang, C., Zhang, X., Ma, L., Wu, C., 2011a. Synthesis gas production with Nio-Mgo/γ-Al_2O_3/cordierite monolithic catalysts in a pilot-scale biomass-gasification-reforming system. Energ. Fuel. 25, 1221–1228.

Wang, W., Padban, N., Ye, Z., Andersson, A., Bjerle, I., 1999. Kinetics of ammonia decomposition in hot gas cleaning. Ind. Eng. Chem. Res. 38, 4175–4182.

Wang, W., Padban, N., Ye, Z., Olofsson, G., Andersson, A., Bjerle, I., 2000. Catalytic hot gas cleaning of fuel gas from an air-blown pressurized fluidized-bed gasifier. Ind. Eng. Chem. Res. 39, 4075-4081.

Wang, W., Padban, N., Ye, Z., Olofsson, G., Andersson, A., Bjerle, I., 2000. Catalytic hot gas cleaning of fuel gas from an air-blown pressurized fluidized-bed gasifier. Ind. Eng. Chem. Res. 39, 4075–4081.

Wang, X., Robbins, C., Hoekman, S.K., Chow, J.C., Watson, J.G., Schuetzle, D., 2011b. Dilution sampling and analysis of particulate matter in biomass-derived syngas. Frontiers Environ. Sci. Eng. China 5, 320-330.

Weerachanchai, P., Horio, M., Tangsathitkulchai, C., 2009. Effects of gasifying conditions and bed materials on fluidized bed steam gasification of wood biomass. Bioresour. Technol. 100, 1419–1427.

Wu, X., Zhang, J., Chang, L., 1987. Catalyst deactivation. In: Delmon, B., Froment, G.F. (Eds), Studies in Surface Science and Catalysis, 34, 209.

Xie, C., Chen, Y., Engelhard, M.H., Song, C., 2012. Comparative study on the sulfur tolerance and carbon resistance of supported noble metal catalysts in steam reforming of liquid hydrocarbon fuel. Catalysis 2, 1127-1137.

Xie, C., Chen, Y., Li, Y., Wang, X., Song, C., 2011. Influence of sulfur on the carbon deposition in steam reforming of liquid hydrocarbons over CeO_2-Al_2O_3 supported Ni and Rh catalysts. Appl. Catal. A-Gen. 394, 32-40.

Xu, C., Donald, J., Byambajav, E., Ohtsuka, Y., 2010. Recent advances in catalysts for hot-gas removal of tar and NH_3 from biomass gasification. Fuel 89, 1784–1795.

Xu, J., Saeys, M., 2006. Improving the coking resistance of Ni-based catalysts by promotion with subsurface boron. J. Catal. 242, 217–226.

Yang, J., Wang, X., Li, L., Shen, K., Lu, X., Ding, W., 2010a. Catalytic conversion of tar from hot coke oven gas using 1-methylnaphthalene as a tar model compound. Appl. Catal. B-Environ. 96, 232–237.

Yang, J.C., Shul, N.G., Louis, C., Che, M., 1998. In situ EXAFS study of the nucleation and crystal growth of Ni particles on SiO_2 support. Catal. Today 44, 315–325.

Yang, X., Xu, S., Xu, H., Liu, X., Liu, C., 2010b. Nickel supported on modified olivine catalysts for steam reforming of biomass gasification tar. Catal. Commun. 11, 383–386.

Yoon, S-J., Choi,Y-C, Lee, J.G., 2010. Hydrogen production from biomass tar by catalytic steam reforming. Energ. Convers. Manage. 51, 42–47.

Yue, B., Wang, X., Ai, X,, Yang, J., Li, L., Lu, X., Ding, W., 2010. Catalytic reforming of model tar compounds from hot coke oven gas with low steam/carbon ratio over Ni/MgO–Al_2O_3 catalysts. Fuel Process. Technol. 91, 1098–1104.

Yumura, M., Furimsky, E., 1985. Comparison of calcium oxide, zinc oxide, and iron(III) oxide hydrogen sulfide adsorbents at high temperatures. Ind. Eng. Chem. Process Des. Develop. 24, 1165–1168.

Yung, M.M., Kuhn, J.N., 2010. Deactivation mechanisms of ni-based tar reforming catalysts as monitored by x-ray absorption spectroscopy. Langmuir 26, 16589-16594.

Zeng, S., Zhang, L., Zhang, X., Wang, Y., Pan, H., Su, H., 2012. Modification effect of natural mixed rare earths on Co/γ-Al_2O_3 catalysts for CH_4/CO_2 reforming to synthesis gas. Int. J. Hydrogen Energ. 37, 9994–10001.

Zhang, R.Q., Ma, W.Z., 2000. Preparation and Method of High-Temperature Shift Catalyst for Low Steam to Gas Ratio. China National Patent: No. ZL 96102477.1, April 2000.

Zhang, Y., Cheng, H., Lu, A., Ding, W., Zhou, G., 2009. Influence of rare earth promoters on the performance of Ni/Mg(Al)O catalysts for hydrogenation and steam reforming of toluene. Rare Metals 28, 582-589.

Zhang, Y., Draelants, D.J., Engelen, K., Baron, G.V., 2003. Development of nickel-activated catalytic filters for tar removal in H_2S-containing biomass gasification gas. J. Chem. Technol. Biotechnol. 78, 265-268.

Zhao, Z., Lakshminarayanan, N., Kuhn, J.N., Senefeld-Naber, A., Felix, L.G., Slimane, R.B., Choi, C.W., Ozkan, U.S., 2009. Optimization of thermally impregnated Ni-olivine catalysts for tar removal. Appl. Catal. A-Gen. 363, 64-72.

Zhao, Z.K., Lakshminarayanan, M., Swartz, S.L., Arkenberg, G.B., Felix, L.G., Slimane, R.B., Choi, C.C., Ozkan, U.S., 2015. Characterization of olivine-supported nickel silicate as

potential catalysts for tar removal from biomass gasification. Appl. Catal. A- Gen. 489, 42–50.

Zhou, J., Ishimura, D.M., Kinoshita, C.M., 1999. Effects of injecting steam on catalytic reforming of gasified biomass. Proceedings of the Fourth Biomass Conference of the Americas, Oakland, CA, 1999. p. 991–7

Zou, W., Gonzalez, R.D., 1992. The chemical anchoring of noble metal amine precursors to silica. Catal. Today 15, 443–453.

Acknowledgments

Professor Zhenya Zhang's guidance and encouragement are greatly appreciated. He provides me the opportunity to study for my doctorate degree at the University of Tsukuba. My thesis could not be finished without his instructive advice and professional guidance. I'd also like to thank Professor Yabar Helmut for his co-supervising my doctoral study.

The assistance from both Professor Zhongfang Lei and Professor Kazuya Shimizu is also appreciated for their patient and carefully instructions during my doctoral study. And many thanks should give to Professor Xiaoyan Tang from Peking University and my colleagues, Mr. Andy Suby, Mr. Huajian Wang, Mr. Yanchang Wang and et al., from Zhengzhou University in China and Iowa State University in the United States where I undertook most of my research works.

Professor Robert Brown, the Anson Marston Distinguished Professor of Engineering, was my mentor who introduced me into the biomass-energy field while I was a visiting scholar at Iowa State University in 2001. I appreciated the guidance from Prof Brown.

Special gratitude should give to my thesis committee members, Professor Zhengya Zhang, Professor Zhongfang Lei, Professor Kazuya Shimizu, Professor Yabar Helmut and Professor Motoo Utsumi, for their valuable and helpful suggestions and comments on my thesis.

Last, but not the least, my gratitude to my beloved family for their support to me through all these years.

Publications

1. **Ruiqin Zhang,** Huajian Wang, Xiaoxue Hou, 2014. Catalytic reforming of toluene as tar model compound: Effect of Ce and Ce-Mg promoter using Ni/Olivine catalyst. Chemosphere 97, 40-46.
2. **Ruiqin Zhang,** Yanchang Wang, Robert, C. Brown, 2007. Steam reforming of tar compounds over Ni/Olivine catalysts doped with CeO_2. Energy Conversion and Management 48, 68-77.
3. **Ruiqin Zhang,** Robert C. Brown, Andy Suby, Keith Cummer, 2004. Catalytic destruction of tar in biomass derived producer gas. Energy Conversion and Management 45, 995-1014.
4. **Ruiqin Zhang,** Robert C. Brown, Andy Suby, 2004. Thermochemical generation of hydrogen from switchgrass. Energy & Fuels 18, 251-256.